



NRL/MR/6114--20-10,056

CO₂ Radiocarbon Analysis to Quantify Organic Contaminant Degradation MNA and Engineered Remediation Approaches

THOMAS J. BOYD

MICHAEL T. MONTGOMERY

*Chemical Dynamics and Diagnostics Branch
Chemistry Division*

RICHARD H. CUENCA

YUTAKA HAGIMOTO

*Hydrologic Engineering, Inc.
Corvallis, OR*

MARIA VERNET

JENNIFER GONZALEZ

*IOD, Scripps Institution of Oceanography
La Jolla, CA*

June 1, 2020

DISTRIBUTION STATEMENT A: Approved for public release; distribution is unlimited.

REPORT DOCUMENTATION PAGE				Form Approved OMB No. 0704-0188	
Public reporting burden for this collection of information is estimated to average 1 hour per response, including the time for reviewing instructions, searching existing data sources, gathering and maintaining the data needed, and completing and reviewing this collection of information. Send comments regarding this burden estimate or any other aspect of this collection of information, including suggestions for reducing this burden to Department of Defense, Washington Headquarters Services, Directorate for Information Operations and Reports (0704-0188), 1215 Jefferson Davis Highway, Suite 1204, Arlington, VA 22202-4302. Respondents should be aware that notwithstanding any other provision of law, no person shall be subject to any penalty for failing to comply with a collection of information if it does not display a currently valid OMB control number. PLEASE DO NOT RETURN YOUR FORM TO THE ABOVE ADDRESS.					
1. REPORT DATE (DD-MM-YYYY) 01-06-2020		2. REPORT TYPE NRL Memorandum Report		3. DATES COVERED (From - To) 1 Oct 2015 – 30 Sept 2019	
4. TITLE AND SUBTITLE CO ₂ Radiocarbon Analysis to Quantify Organic Contaminant Degradation MNA and Engineered Remediation Approaches				5a. CONTRACT NUMBER	
				5b. GRANT NUMBER	
				5c. PROGRAM ELEMENT NUMBER	
6. AUTHOR(S) Thomas J. Boyd, Michael T. Montgomery, Richard H. Cuenca*, Yutaka Hagimoto*, Maria Vernet**, and Jennifer Gonzalez**				5d. PROJECT NUMBER	
				5e. TASK NUMBER	
				5f. WORK UNIT NUMBER 5557	
7. PERFORMING ORGANIZATION NAME(S) AND ADDRESS(ES) Naval Research Laboratory 4555 Overlook Avenue, SW Washington, DC 20375-5320				8. PERFORMING ORGANIZATION REPORT NUMBER NRL/MR/6114--20-10,056	
9. SPONSORING / MONITORING AGENCY NAME(S) AND ADDRESS(ES) SERDP 4800 Mark Center Drive, Suite 17D08 Alexandria, VA 22350-3605				10. SPONSOR / MONITOR'S ACRONYM(S) SERDP	
				11. SPONSOR / MONITOR'S REPORT NUMBER(S)	
12. DISTRIBUTION / AVAILABILITY STATEMENT DISTRIBUTION STATEMENT A: Approved for public release; distribution is unlimited.					
13. SUPPLEMENTARY NOTES *Hydrologic Engineering, Inc., P.O. Box 948, Corvallis, OR 97339-0948 **IOD, Scripps Institution of Oceanography, UC San Diego, 9500 Gilman Drive, Suite 0218, La Jolla, CA 92093-0218					
14. ABSTRACT This report summarizes SERDP ER2338 efforts at the Naval Air Station North Island (NASNI) IR-5 Unit 2 and OU-19/20 study sites with preliminary information on recent deployments at Indian Head Naval Surface Warfare Center IR-17 and IR-57. This report includes equipment and sampler design(s), deployment and long-term monitoring activities at field sites to determine in situ chlorinated volatile organic compound (cVOC) degradation. Samples from one-year collections at IR-5U2 and OU-19/20 were analyzed for overall respiration (CO ₂ production), CO ₂ radiocarbon content, and ancillary measurements (cations, contaminant concentrations, well casing methane). CO ₂ collection rate measurements were used to create and refine zone of influence (ZOI) simulations. A two end-member isotope mixing model was used to determine the respiration attributable to fossil (contaminant) source(s) during each one-month CO ₂ trap deployment. A background well (no contamination) was used at each site to represent contemporary CO ₂ age (from natural root and soil respiration). All data were converted to rates per unit volume and interpolated over the site for each ~1-month trap deployment. These data were then compiled to determine an overall cVOC degradation over the site over the one-year period. CO ₂ traps were deployed at two sites Indian Head NSWC in February 2017, IR-17 and IR-57. Both sites have TCE contamination. Over one year of 1-2 month samplings have been collected and analyzed for respiration rate. ZOI simulations have been performed to provide a volumetric basis. Radiocarbon analysis has been delayed. An ad hoc effort has been initiated to assemble a CO ₂ cryogenic distillation line to purify CO ₂ for gas-source inlet AMS at Woods Hole Oceanographic Institution's NOSAMS lab. This would reduce analytical costs almost 10-fold and allow greater spatial and temporal resolution for the radiocarbon method. Results from IR-5 U2 have been published in peer-reviewed journal articles and 3 additional manuscripts are being finalized for publication. Two additional sites with fuel contamination were studied using co-funding by RPMs and presented to regulators. A template QAPP (Tier-II SAP) was developed for deploying the described methods. Linking results at IR-5 U2 with a commercial soil: atmosphere trap helped transition to a funded ESTCP project to cross validate radiocarbon-based methods and provide usage guidance to RPMs.					
15. SUBJECT TERMS					
16. SECURITY CLASSIFICATION OF:			17. LIMITATION OF ABSTRACT	18. NUMBER OF PAGES	19a. NAME OF RESPONSIBLE PERSON
a. REPORT	b. ABSTRACT	c. THIS PAGE			Thomas J. Boyd
Unclassified Unlimited	Unclassified Unlimited	Unclassified Unlimited	Unclassified Unlimited	73	19b. TELEPHONE NUMBER (include area code) (202) 404-6424

This page intentionally left blank.

Table of Contents

Table of Contents	iii
List of Figures	iv
List of Tables	v
List of Acronyms and Abbreviations and Keywords.....	vii
Acknowledgements.....	vii
Abstract.....	ix
Executive Summary.....	x
Introduction	x
Objectives.....	x
Technical Approach.....	xi
Results and Discussion	xii
Implications for Future Research and Benefits.....	xiv
Objective	1
Background	2
Site Descriptions	5
IR-5 Unit 2, NASNI	5
OU-19/20, NASNI	8
IR-17, Indian Head NSWC.....	9
IR-57, Indian Head NSWC.....	10
Materials and Methods.....	11
IR-5 U2 Hardware and Field Sampling.	11
OU19/20, IR-17/IR-57 Hardware and Field Sampling	12
Water Quality Analyses.....	13
Soil Gas Methane Concentrations	13
Radiocarbon analysis	14
CO ₂ Production Rate Analysis	14
Zone of Influence Model/Simulation	14
Determining the Contaminant Respired.....	15
Results and Discussion	16
IR-5 Unit 2	16
ZOI simulations	16
Water quality measurements	18
Respiration	19
Radiocarbon analysis	19
Conversion from radiocarbon and respiration to cVOC degradation.....	20
Site-Wide TCE degradation and long-term remediation	33
OU-19/20 NASNI	35
ZOI simulations	35
Water quality measurements	35
Respiration	36

Radiocarbon analysis	36
Conversion from radiocarbon and respiration to cVOC degradation.....	36
Site-Wide TCE degradation and long-term remediation	46
IR-17 Indian Head.....	48
ZOI simulations	48
Water quality measurements	49
Respiration	49
IR-57 Indian Head.....	49
ZOI simulations	50
Water quality measurements	50
Respiration	51
Radiocarbon – IR-17 and IR-57.....	51
Conclusions and Implications for Future Research / Implementation	54
Literature Cited	56
Appendix A. Supporting Data.....	59
Appendix B. List of Scientific / Technical Publications.....	lx

List of Figures

Figure 1. CO ₂ radiocarbon age upgradient, above, and downgradient of petroleum-based chemical plume.	2
Figure 2. ¹⁴ C analysis in a "Natural Lab"	3
Figure 3. IR Site 5 (all units).....	5
Figure 4. IR Site 5 Unit 2 (Shaw 2013).....	7
Figure 5. OU-19/20 NASNI (Noreas, 2014)	8
Figure 6. IR-17 NSWC Indian Head (CH2MHill)	9
Figure 7. IR-57 NSWC Indian Head showing upper and mid-plumes (Osage)	10
Figure 8. Well headspace gas recirculating pumps, sealed	11
Figure 9. Solar power distribution system in place.....	12
Figure 10. Well headspace CO ₂ collection system	12
Figure 11. NaOH trap showing support and reservoir	13
Figure 12. Well cap sealed in place with sparge line and check valve.....	13
Figure 13. Calibrated CO ₂ distribution.	17
Figure 14. Historical cVOC contamination IR-5 U2	20
Figure 15. TCE degradation 11/06/14-11/24/14	22
Figure 16. TCE degradation 11/24/14-12/05/14	22
Figure 17. TCE degradation 12/05/14-12/18/14	23
Figure 18. TCE degradation 12/19/14-01/05/15	23
Figure 19. TCE degradation 01/18/15-01/27/15	24
Figure 20. TCE degradation 02/02/15-02/16/15	24
Figure 21. TCE degradation 02/16/15-03/09/15	25
Figure 22. TCE degradation 03/10/15-04/10/15	25
Figure 23. TCE degradation 04/10/15-04/30/15	26

Figure 24. TCE degradation 04/30/15-05/20/15	26
Figure 25. TCE degradation 05/20/15-06/01/15	27
Figure 26. TCE degradation 06/01/15-06/15/15	27
Figure 27. TCE degradation 06/15/15-06/28/15	28
Figure 28. TCE degradation 06/28/15-07/20/15	28
Figure 29. TCE degradation 07/20/15-08/18/15	29
Figure 30. TCE degradation 08/18/15-08/27/15	29
Figure 31. TCE degradation 08/27/15-09/13/15	30
Figure 32. TCE degradation 09/13/15-10/06/15	30
Figure 33. TCE degradation 10/06/15-11/03/15	31
Figure 34. TCE degradation 11/03/15-11/30/15	31
Figure 35. TCE degradation 11/30/15-12/17/15	32
Figure 36. Total site-wide TCE degradation and rainfall over the entire sampling period	34
Figure 37. OU-19/20 at NASNI, San Diego, CA.....	36
Figure 38. OU-19 TCE degradation 12/17/15-02/02/16	37
Figure 39. OU-19 TCE degradation 02/02/16-03/19/16	38
Figure 40. OU-19 TCE degradation 03/19/16-05/19/16	38
Figure 41. OU-19 TCE degradation 05/19/16-07/18/16	39
Figure 42. OU-19 TCE degradation 07/18/16-08/29/16	39
Figure 43. OU-19 TCE degradation 08/29/16-10/13/16	40
Figure 44. OU-19 TCE degradation 10/13/16-02/23/17	40
Figure 45. OU-20 TCE degradation 07/21/15-08/29/15	41
Figure 46. OU-20 TCE degradation 08/29/15-11/02/15	41
Figure 47. OU-20 TCE degradation 11/02/15-12/17/15	42
Figure 48. OU-20 TCE degradation 12/17/15-02/02/16	42
Figure 49. OU-20 TCE degradation 02/02/16-03/18/16	43
Figure 50. OU-20 TCE degradation 03/19/16-05/19/16	43
Figure 51. OU-20 TCE degradation 05/19/16-07/18/16	44
Figure 52. OU-20 TCE degradation 07/18/16-08/29/16	44
Figure 53. OU-20 TCE degradation 08/29/16-10/13/16	45
Figure 54. OU-20 TCE degradation 10/13/16-02/23/17	45
Figure 55. cVOC degradation and rainfall at OU-19/20	47
Figure 56. CaCO ₃ and organic acid concentrations, IR-17.....	49
Figure 57. CaCO ₃ relation to pH, alkalinity and organic acids, IR-57	51
Figure 58. New distillation line (early 2019)	52
Figure 59. TCE degradation 11/03/15-11/30/15	54

List of Tables

Table 1. Hydrogeologic parameters used in IR-5 U2 ZOI model(s)	16
Table 2. Selected cation concentrations and pH for IR-5 U2	19
Table 3. TCE degradation over IR-5 U2 by time bin	33
Table 4. Hydrogeologic parameters used for OU-19/20 ZOI models	35

Table 5. Selected cation and pH measurements for OU-19/20.....	35
Table 6. TCE degradation over OU-19 by time bin	46
Table 7. TCE degradation over OU-20 by time bin	46
Table 8. IR-17 analyses by sample time bins	48
Table 9. Hydrogeologic parameters used for IR-17 ZOI models	48
Table 10. IR-57 analyses by sample time bins	50
Table 11. Mean hydrogeologic parameters used for IR-57 ZOI models	50

List of Acronyms and Abbreviations and Keywords

bgs	below ground surface
CH	chlorinated hydrocarbons
COI	contaminants of interest
COC	contaminants of concern
cVOC	chlorinated volatile organic compound
$\delta^{13}\text{C}$	Delta C-13 (stable isotope ratio)
$\Delta^{14}\text{C}$	Delta C-14 (radiocarbon isotope ratio)
DIC	dissolved inorganic carbon (dissolved CO_2)
DNAPL	dense non-aqueous phase liquid
DO	dissolved oxygen
DoD	U.S. Department of Defense
EPA	U.S. Environmental Protection Agency
EVO	emulsified vegetable oil
IR	Installation Restoration
LNAPL	light non-aqueous phase liquid
LTM	long-term monitoring
MNA	monitored natural attenuation
NAVBASE	Naval Base
NAVFAC LANT	Naval Facilities Engineering Command Atlantic
NAVFAC Northwest	Naval Facilities Engineering Command Northwest
NAVFAC Southwest	Naval Facilities Engineering Command Southwest
Navy	U.S. Navy
NRL	Naval Research Laboratory
OU	Operable Unit
QA	quality assurance
QC	quality control
ROD	Record of Decision
RPM	Remedial Project Manager
SAP	Sampling and Analysis Plan
SOP	standard operating procedure
TCA	trichloroethane
TCE	trichloroethylene
VOC	volatile organic compound
ZOI	Zone of Influence

Keywords: biodegradation, petroleum-source, fossil end-member, radiocarbon, radiocarbon-depleted, monitoring well, headspace.

Acknowledgements

This project was made possible by funding through SERDP and co-funding by RPMs at NAVFAC Southwest, Northwest and LANT. Site logistics were aided by RPMs (access, historical documents, storage space, shipping/receiving, and site discussions). The project team would like to thank Michael Pound, Alex Scott, Phil Nenninger and Malcolm Gander for additional site access and seed funding. The project was also supported by on-base contractors who provided critical information on site conditions and helped steer efforts toward the most fruitful outcomes. We wish to thank Todd Wiedemeier (which sadly can no longer be done personally), Vitthal Hosangadi (Noreas), Glen Wyatt (Tetrattech), Brian White (Shaw), Erika Thompson (Shaw), Andrew Louder (NAVFAC) and Gunarti Coghlan (NAVFAC) for site-specific information and logistic support. We also wish to thank co-participants in a limited field study which led to ESTCP transition comparing and cross-validating methods; Julio Zimbron (E-Flux, LLC), Chuck Newell (GSI), and John T. Wilson (Scissortail Environmental).

Executive Summary

Introduction

The Department of Defense (DoD) faces billion-dollar expenditures for environmental cleanup in the United States. Prohibitive cleanup costs make treatment strategies such as monitored natural attenuation (MNA), enhanced passive remediation (EPR) or low-cost engineered solutions attractive remediation alternatives for reaching Response Complete (RC) status. Several lines of converging evidence are seen as necessary to establish reasonable evidence for in situ bioremediation or natural attenuation. It is generally accepted that no single analysis or combination of ex situ or laboratory tests provides an accurate confirmation or rate for biodegradation under in situ conditions (1). Similarly, reports sponsored by DoD, the DOE and the Environmental Protection Agency (EPA) advocate collection of a wide array of data in order to attempt confirmation of contaminant attenuation and predict timescale(s) for remediation (2, 3). SERDP/ESTCP priorities include:

- Quantifying natural attenuation capacities;
- Reducing uncertainty;
- Assessing and managing spatial variability;
- Determining side-effects of remediation;
- Optimizing existing technologies;
- Understanding emerging contaminants;
- Improving long-term monitoring;
- Source delineation and characterization and source zone characterization and flux analysis;
- Bioaugmentation and source zone bioremediation; and
- Effects of treatment amendments (SERDP/ESTCP 2002; Leeson and Stroo 2011).

The ultimate end-product for organic contaminant degradation is CO₂— representing a complete conversion to a relatively harmless product. A methodological limitation for current technologies is the inability to conclusively link contaminants, daughter products, electron acceptors, hydrogeological parameters, and in some cases, biological activities to actual contaminant removal (*e.g.*, conversion to CO₂). This study combines CO₂ radiocarbon measurements with CO₂ flux measurements to quantify contaminant carbon conversion to CO₂— and thus complete degradation.

Objectives

This project's objective is to combine CO₂ respiration, CO₂ radiocarbon content and a Zone of Influence (ZOI) model to calculate chlorinated hydrocarbon degradation occurring at real DoD contaminated sites. Radiocarbon analysis will measure the fraction of petroleum-source in the CO₂ pool. To determine COI degradation rate, we will measure the CO₂ production rate by circulating groundwater well headspace through a CO₂ trap over time or use a passive trap suspended in the wells' headspace. A well zone of influence (ZOI) can be calculated using process-based simulation models of gas transport in porous media (4). The ZOI model and CO₂ production rate will be used to determine the overall CO₂ production rate per soil unit. Given the fraction of

CO₂ derived from a petroleum-source and CO₂ produced per soil unit (cubic meter for example), the contaminant degradation rate can be determined over both time and space. This will support all research needs outlined in the SERDP needs section (5, 6) – enhancing management, assessing efficacy or fully quantifying natural attenuation capacities. This technology is straightforward and commercially-available, and will provide two key answers for site management and remediation efficacy (both active and passive) that have not been available:

- Is remediation occurring? We will be able to track the amount (percentage basis) of the degradation end product (CO₂). On the basis of this one measurement, a site manager will be able to definitively state whether (*bio*)degradation is occurring or not.
- At what rate is the remediation occurring? By measuring the proportion of fossil fuel-derived CO₂ and the CO₂ production rate over time, we will be able to calculate the rate of (*bio*)degradation occurring on-site. Using groundwater transport models and given an estimated size or volume of source material and plume dimensions, a much more accurate estimation of the time for remediation can be predicted:

$$\left(\frac{\text{unit time (i.e. days)}}{g \text{ CO}_2 \text{ from contaminant}} \right) (g \text{ source contaminant}) \cong \text{time to remediate}$$

Technical Approach

The technical approach for the project is relatively well defined. It involves measuring the CO₂ production over unit time (respiration) and determining a radiocarbon age for that respired product. If the CO₂ is radiocarbon-depleted relative to a background site where natural organic matter is the only respiratory substrate, the radiocarbon-depleted CO₂ must be derived from the petroleum-sourced contaminant. By coupling the respiration rate and the differential respiration product derived from the contaminant, a contaminant degradation rate can be determined. Developing a model based on site hydrogeologic parameters which determines the volume sampled during each respiration measurement allows scaling contaminant degradation rate spatially and interpolation between wells sampled as above allows site-wide contaminant degradation estimates.

Respiration was measured using CO₂ traps deployed either adjacent to or within the casing of groundwater monitoring wells. The external traps were supplied with gas lines so that in-well headspace gas could be continuously cycled over the trap material. Due to the nature of many sites (operable units), actively cycled traps and the associated power support equipment were not practical. Passive traps were developed that were not as efficient (slower timeframe to equilibrium) but effective at trapping CO₂ evolved from groundwater and liberated into well headspaces over deployment time. In all cases, trap material was recovered after 2-10 weeks, dissolved in a known amount of CO₂-free water, and analyzed for CO₂ content. Collection rate was determined as the amount of CO₂ collected per unit time (hours or days). Respiration was

calculated as the collection rate minus the lowest collection rate value determined for the entire field site deployment with the assumption that the lowest value could represent equilibrium trapping alone (meaning no respiration, but the in-ground residual CO₂ pool would be trapped due to equilibrium forces).

The final component was to develop ZOI models for each well and time-point using hydrogeologic parameters measured on-site (*c.f.* Tables, 4, 9 and 11) and CO₂ collection rates. ZOI models were developed using MODFLOW-2005 and front-ends tailored to contaminant and CO₂ diffusion (MT3DMS). Parameterized simulations for each well and time-point had volumetric outputs (*e.g.* m³) which represented the volume sampled to obtain the given CO₂ collection rate.

With a respiration rate (mg cVOC degraded per day) and a parameterized estimate for the sample volume (m³), a straightforward calculation for the degradation rate at each well was made (*e.g.* mg cVOC carbon degraded m⁻³ d⁻¹). The rates were then interpolated over the entire sampled area using estimates for plume dimensions to calculate the cVOC mass degraded over the entire site in time.

Results and Discussion

At each site, time-point and well, respiration and ¹⁴CO₂ data were compiled and analyzed to determine cVOC degradation (as TCE carbon degraded m⁻³ d⁻¹). cVOC degradation rates were calculated for IR-5 U2, OU-19 and OU-20 at NASNI over the course of one year (each site). Respiration values along with site hydrogeologic parameters were used to create ZOI simulations for each well and time-point sampled. Ancillary measurements (cations, pH, organic acids) were used to ensure limestone (calcium carbonate) deposits did not interfere with radiocarbon analysis. Collected CO₂ was combined according to well and respiration values for radiocarbon analyses due to the cost per sample.

TCE degradation ranged from 0 to 400 mg TCE C m⁻³ d⁻¹ at IR-5 U2. At IR-5 U2, the highest TCE degradation occurred at the plume fringes (up and side-gradient primarily) with lower degradation rates observed within the central plume with highest cVOC concentrations. At downgradient wells (*e.g.* MW-32, MW-35, MW-41), respiration was in line with other fringe wells (*e.g.* MW-21, MW-42, MW-38) but CO₂ radiocarbon content often did not indicate high cVOC degradation. This was likely due to either lack of cVOC substrate(s) due to attenuation upgradient, or perhaps lack of suitable co-metabolic precursors needed for complete cVOC respiration. Site-wide cVOC degradation was computed using interpolation between sampled wells and published plume dimensions. Site-wide degradation ranged from ~4 to 112 g TCE C d⁻¹ over the greater than one-year sampling period. Although a significant correlation did not exist, highest cVOC degradation occurred after steady rain events (Fig. i) which we hypothesize may be responsible for replenishing limiting resources and liberating pools of DNAPL from soils within the vadose zone. Time-averaged degradation over the course of the one-year collection period amounted to ~ 7 kg cVOC degraded per year.

TCE degradation ranged from 0 to 63 mg TCE C m⁻³ d⁻¹ at OU-19 and 0 to 31 mg TCE C m⁻³ d⁻¹ at OU-20. Overall, OU-19 had a higher cVOC degradation average (36 ± 2.3 S.E.) than OU-20 (1.7 ± 0.59 S.E.) Data for OU-19 and OU-20 reflect ZOI estimates which require additional QA/QC before final publication due to widespread heterogeneity in hydrogeologic parameters. cVOC degradation rates were highest at OU-

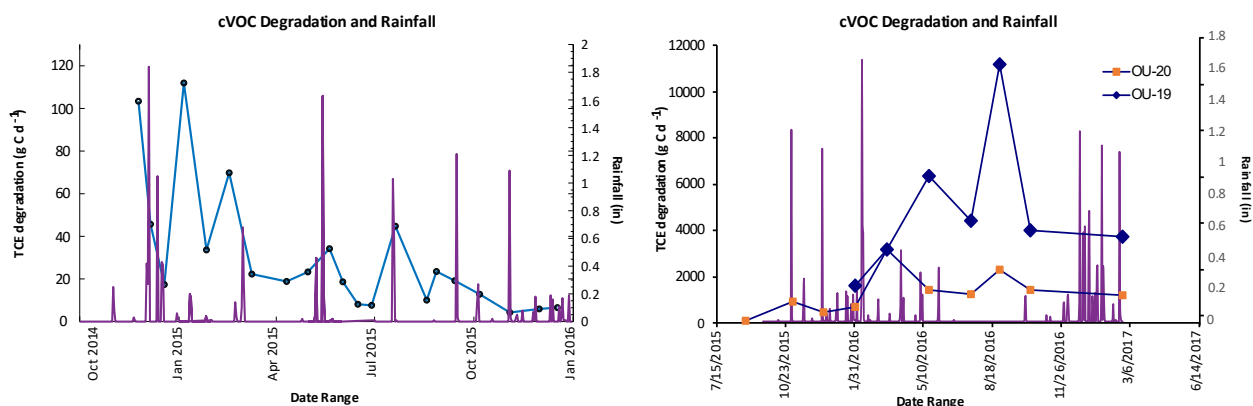


Figure i. cVOC degradation (IR-5 U2 – left; OU-19, OU-20 – right) over study periods

19 in a region where steam pipes underlay the pavement (MW-04, PZ-04, MW-04, MW-08, MW-11). Rates determined at downgradient wells (MW-102, MW-79C, MW-87C and MW-100C) were usually an order of magnitude lower. We hypothesize that increased groundwater temperatures are largely responsible for the higher cVOC degradation rates observed at OU-19. At OU-20, cVOC degradation rates were usually highest at fringe regions (MW-14C, MW-90C, and sometimes PRZ-91 and RMW-1A). Wells PRZ-91, RMW-1A and HP-17 were in a region treated by EVO injection in SEP-OCT 2015. The highest cVOC degradation rates were observed in these wells before the EVO injection event. CO₂ radiocarbon values became more modern following the EVO injection. We noted exceptional gas evolution from the wells (assumed to be CH₄ – and confirmed with well headspace methane analysis). It is unclear if the radiocarbon signal from cVOC degradation was “masked” by increased CO₂ evolution due to EVO degradation or that the EVO injection did not lead to cVOC conversion to CO₂.

cVOC degradation was integrated between wells at each site and using published plume dimensions (1000 m long, ~500 m wide and 10-20 m depth), yielded a site-wide estimate for total cVOC degraded during each time-bin from the year-long study period. At OU-19, we estimate that as much as 11 kg cVOC could be degraded per day over the 0.05 km² site. At OU-20, as much as 3.3 kg cVOC could be degraded over the 0.1 km² site (Fig. i). As with IR-5 U2, although a correlation did not exist between rainfall and cVOC degradation, higher cVOC rates seemed to occur after relatively sustained rain events (Fig. i).

At the RPM’s request, two additional sites (IR-17 and IR-57) at Indian Head NSWC, MD were sampled during this project. At both sites, respiration rates and ZOI calculations have been completed. Due to funding constraints and the desire to obtain higher-resolution measurements, collected CO₂ has not been analyzed for radiocarbon content. A cryogenic distillation line for purifying CO₂ has been built but has had leaking issues. The goal is to distill and purify CO₂ so that it can be analyzed by direct gas-source AMS which is one almost one seventh the cost (\$60 vs \$400) per sample. Work continues to bring the distillation system online and conversion to cVOC degraded will be relatively straightforward once the radiocarbon

values are obtained. Logistics for completing the datasets for these sites and eventual publication of results have been secured.

Implications for Future Research and Benefits

With costs far outpacing resources available for site assessment and cleanup, robust tools to evaluate MNA and engineered solutions are necessary. We have developed technologies which target the contaminant carbon backbone and thus are able to measure contaminant degradation with certainty (radiocarbon-depleted CO₂ must come from a petroleum-sourced material). The technologies can be deployed using several modes each having different suitability based on site characteristics (active trapping, passive trapping and even short-term incubations – see publications section). Well-studied sites may have ample data such that models (BioChlor and/or REMChlor) may provide adequate site management information with minimal CO₂ radiocarbon evidence. For instance, it may be enough just to measure groundwater CO₂ for ¹⁴C-depletion and thus irrefutably confirm a contaminant source. Sites with varying characteristics and needs will require varying degrees of coupled flux-radiocarbon evidence based on physical layout, existing data, ROD requirements, RPM needs, *etc.* In all cases, radiocarbon-based technologies provide concrete evidence (should ¹⁴C-depleted CO₂ be associated with a contaminant plume) that contaminants are being converted to CO₂ – a harmless end-product. While costly in terms of analysis costs, radiocarbon-based measurements are definitive and if well-administered can be used in place of many indirect measurements whose costs add up – and that only provide lines of evidence for contaminant respiration.

During this SERDP project, several ancillary studies were performed using commercially-available soil:atmosphere CO₂ traps and using short-term respiration measurements (incubations) coupled to radiocarbon measurements to estimate cVOC degradation rates. In addition, a REMChlor model was developed for one site and methods were directly compared. This cross-validation study is in final editing for publication but very briefly, we found reasonable agreement between soil:atmosphere CO₂ traps and in-well traps for a shallow cVOC DNAPL plume within a short-term deployment (~2 weeks). A long-term REMChlor model showed lower degradation rates, but results from a year-long radiocarbon-based collection demonstrated an almost 1 order of magnitude variation in rates over the course of one year. Essentially, at lower resolution (yearly timeframes), a REMChlor-type model may predict long-term cVOC attenuation. Radiocarbon-based technologies are able to provide short-term, high-resolution (seasonal) and spatial information to better refine remediation management.

Results from this SERDP project have been transitioned to ESTCP in which we will deploy various radiocarbon-based technologies at the same sites over the same timescales in order to cross validate radiocarbon techniques and assess their strengths and weaknesses given different site conditions, deployed remediation technologies and remedial management goals. The goal is to create a decision support tool (DST) encompassing these disparate but related characteristics

with the ultimate goal to decrease overall uncertainty and increase cost effectiveness and cost avoidance.

Objective

This project's objective is to sample existing groundwater wells to combine CO₂ respiration, CO₂ radiocarbon content and a Zone of Influence (ZOI) model to calculate chlorinated hydrocarbon degradation. Radiocarbon content is used to determine the fraction of petroleum-derived carbon in respired CO₂. To determine cVOC degradation rate, CO₂ production rate is measured by circulating groundwater well headspace through a CO₂ trap over time or by passive traps deployed within a well's headspace. A well zone of influence (ZOI) will be calculated using process-based gas transport simulation models for porous media (4). CO₂ production rates and ZOI volume outputs will be used to determine CO₂ respiration in a given volume associated with each groundwater monitoring well. Collected respiration CO₂ will be analyzed for radiocarbon content with the understanding that ¹⁴C-depleted CO₂ must arise from a fossil source (*e.g.* petroleum-derived fuels or industrial chemicals). The fraction CO₂ derived from petroleum-source can be calculated using a two end-member model with a background sample as an index for the radiocarbon age of natural organic matter on-site. Armed with these data, the contaminant degradation rate can be determined in both temporal and spatial scales.

Ultimately, the objective is to determine

- Is remediation occurring? We will be able to track the amount (percentage basis) of the degradation end product (CO₂). On the basis of this one measurement, a site manager will be able to definitively state whether (*bio*)degradation is occurring or not.
- At what rate is the remediation occurring? By measuring the proportion of fossil fuel-derived CO₂ and the CO₂ production rate over time, we will be able to calculate the rate of (*bio*)degradation occurring on-site. Using groundwater transport models and given an estimated size or volume of source material and plume dimensions, a much more accurate estimation of the time for remediation can be predicted:

The objective will be met by a series of field samplings at cVOC-contaminated DoD sites. Sites will be selected based on cVOC contamination, historical data already available for cVOC distribution and concentrations, hydrogeologic parameters for creating ZOI models, and RPM need/desire to host the project. Additionally, sites with existing groundwater monitoring well networks will be selected so that CO₂ traps can be immediately deployed. cVOC degradation data will be scaled over the site and over the nominal one-year site collection to estimate the site-wide degradation over scalable time periods.

Background

Environmental management and cleanup from historical contamination amounts to billions of dollars in costs. Treatment strategies such as monitored natural attenuation (MNA), enhanced passive remediation (EPR) or low cost engineered solutions can be attractive to reach Response Complete (RC) status in the United States. Many common contaminants (e.g. fuels, solvents, chlorinated compounds, munitions, etc.) are persistent and degraded slowly in the environment. Some contaminants, while readily degraded, are present in quantities too high to be degraded within reasonable time-frames. In the U.S. the Department of Defense (DoD), Department of Energy (DOE) and the Environmental Protection Agency (EPA) suggest collecting data from multiple lines of evidence to confirm contaminant attenuation and improve our estimates for remediation time-frames (2, 3). Generally, no single analysis or *ex situ* laboratory test provides ample evidence for in situ contaminant attenuation - and rarely can an accurate contaminant turnover rate be calculated with confidence using lines of evidence approaches (1, 7-9).

Because site managers must balance risk, costs and outcomes that satisfy regulators and stakeholders, there is a persistent need for methodological improvements to provide contaminant degradation rates with increased veracity which reduces the need and expense for measuring multiple indirect lines of evidence. Recently, SERDP-funded research on radiocarbon isotope measurements has quantified organic contaminant turnover in chlorinated solvent sites. CO₂ radiocarbon analysis (e.g., chlorinated hydrocarbon degradation end-product) targets the actual contaminant carbon backbone thus reducing uncertainty inherent in indirect measurements.

Radiocarbon is produced in the atmosphere via cosmic radiation - converting ¹⁴N to ¹⁴C. Plants assimilate radiocarbon by photosynthesis into their tissues. When plant material becomes buried and removed from contemporary carbon cycling (e.g. during diagenesis into petroleum reserves), the ¹⁴C will decay away (~6,000-year half-life) without replacement leaving a carbon pool

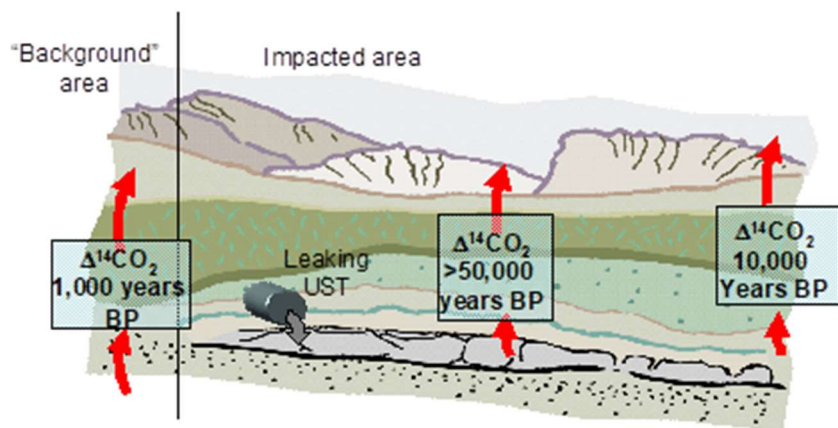


Figure 1. CO₂ radiocarbon age upgradient, above, and downgradient of petroleum-based chemical plume.

(petroleum) completely devoid of any ¹⁴C. If the petroleum-based chemical leaks into the environment - and is degraded to CO₂, one might expect the CO₂ age upgradient of the spill to represent the natural organic matter radiocarbon age, while above an actively-degrading plume, the CO₂ age would represent the fossil

petroleum source. Downgradient, one might expect to find a mix of natural and petroleum-derived CO₂ (Fig. 1).

Using natural abundance ¹⁴C in the field is analogous to a laboratory microcosm with the labeled tracer "reversed": a typical microcosm has un-labeled natural organic matter (NOM) from the water sample for instance - and ¹⁴C - labeled contaminant tracer (*e.g.*, TCE). A natural on-site "lab" has ¹⁴C -labeled NOM (modern), and un-labeled (fossil) contaminant tracer (Fig. 2). Radiocarbon analysis can provide definitive *in situ* chlorinated solvent degradation evidence (or any fossil fuel-derived contaminant of interest - COI) in an accurate and cost-effective manner. Several well-chosen samples may be sufficient to confirm contaminant degradation. ¹⁴C measurements are sensitive and high resolution and able to apportion the original contaminant source, putative daughter products, and degradation end products such as CO₂ and CH₄ to either the natural or fossil end-member.

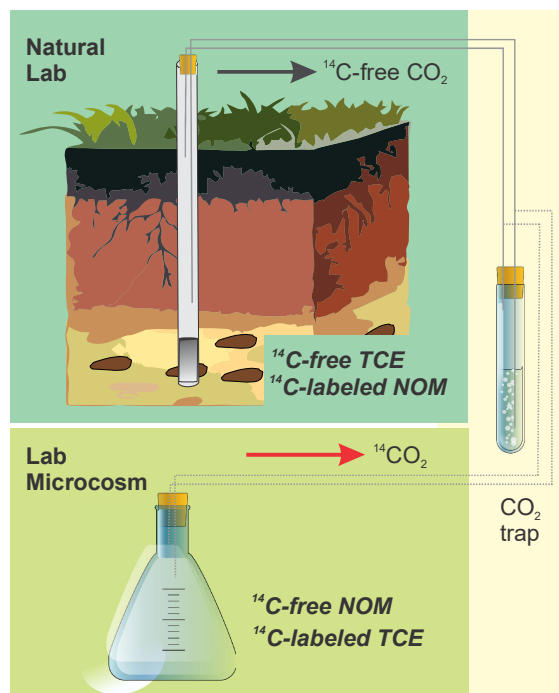


Figure 2. ¹⁴C analysis in a "Natural Lab"

Groundwater CO₂ radiocarbon measurements have traditionally been used to assess aquifer water residence times. In the mid-1980s, highly ¹⁴C-depleted CO₂ led to the discovery of subsurface contamination and offered insight into using radiocarbon to track contaminant degradation (10). Additional studies validated this observation (11). Relying on the fact that fuels and industrial chemicals made from petroleum feedstocks are devoid of ¹⁴C, sites with subsurface fuel and chlorinated solvent contamination were systematically assessed for ¹⁴C -depleted CO₂. This information was used to confirm *in situ* contaminant degradation rates (12-20). Most recently, CO₂ radiocarbon measurements have been combined with CO₂ flux estimates to determine the *in situ* contaminant biodegradation rate using in-well CO₂ trapping, soil:atmosphere flux traps and short-term respiration incubations (16, 17, 21-25). Most applications are for LNAPL, for which the technologies are used to determine natural source-zone depletion. Application of this technology to chlorinated DNAPL sites is relatively new. Radiocarbon analysis measures the petroleum-sourced fraction in the CO₂ pool. To determine COI degradation rate, CO₂ production rate can be measured by atmosphere:soil traps (22), in-well CO₂ traps (16, 17), or by short-term respiration incubations (21). For in-well traps, a well zone of influence (ZOI) can be calculated using process-based simulation models of gas transport in porous media (16, 17). The ZOI model and CO₂ production rate are used to determine the overall CO₂ production rate per soil volume. For atmosphere:soils traps, a plume depth can be assumed for converting flux per unit area to flux per unit volume. With short-term incubations,

a volumetric estimate is inherent as respiration rates are measured in a given volume under in situ conditions (21). Under all method variants, the contaminant degradation rate can be determined over both time and space.

Note that biodegradation pathways of chlorinated solvents are more complicated than those at fuel hydrocarbon sites. The radiocarbon analysis approach using CO₂ as a dead-end product addresses the source of the carbon (*i.e.*, from the fossil fuel contaminant, differentiating it from modern carbon, relatively rich in ¹⁴C). However, information about the degradation pathways is not provided by this analysis. At petroleum sites, all of the ¹⁴C-depleted CO₂ comes from the biodegradation of LNAPL and its dissolution products. At chlorinated solvent sites, another electron donor is biodegraded to form dissolved hydrogen which is then utilized by dechlorinating bacteria to reductively dechlorinate the solvents. At many or perhaps most of these sites, the electron donor is another anthropogenic hydrocarbon such as mineral oils or fuel compounds. These hydrocarbons also produce ¹⁴C-depleted CO₂ that will be measured by the field methods implemented by this project. To account for this possible reaction, additional field parameters such as volatile fatty acids, total organic carbon, and total petroleum hydrocarbons will be measured at strategic locations to help understand the relative contribution of any anthropogenic hydrocarbon electron donor and the biodegradation of the chlorinated solvents themselves.

As stated, the power of these measurements is that one analysis provides direct evidence, more straightforward and less uncertain than using an analysis suite providing indirect lines of evidence. The methods to be validated here collect respired CO₂ over time and use the collected CO₂ for radiocarbon analysis (providing both flux and percent of contaminant carbon) as the basis to estimate contaminant mass losses per volume. The techniques have demonstrated biodegradation in the field with analytical certainty (13-15, 17, 19, 23, 26). For the CO₂ traps, using a capture diameter of 4" and a deployment time of 2 weeks, a sensitivity of 0.1% g CO₂ g⁻¹ sorbent translates into a flux detection limit of 0.025 micromoles CO₂ m⁻² sec⁻¹. This can be increased by increasing capture area and deployment time, if necessary.

To tie discreet lines of evidence together, an industry-standard model is often used to estimate contaminant removal. For chlorinated hydrocarbon-contaminated sites one such method is the REMChlor model. REMChlor relies on hydrogeologic data, long-term contaminant and contaminant daughter product monitoring, and other indirect data to predict contaminant degradation rate (27). REMChlor applicability may be limited if the site is relatively "new" without a full or long-term monitoring dataset. REMChlor is integrative, offering a site-wide estimate for contaminant fate and transport. It makes a good framework for evaluating radiocarbon method efficacy and cross-validation. It will be used at test sites as a foundation for inter-comparing radiocarbon methods.

Isotope techniques have been applied to contaminated sites since the early 1990s. Although stable carbon isotope analysis has proven useful for discreet spills where a pool of starting material with known isotopic composition can be tracked (*c.f.*, (9, 28, 29)), radiocarbon techniques track the radioactive isotope (^{14}C) which is essentially unimpacted by physical and chemical processes (half-life is an accepted standard). Several variations on combining radiocarbon and CO_2 flux studies have been developed relying on measuring CO_2 flux and radiocarbon from the same subsample(s). One technology involves passive CO_2 flux traps (22). Although recently commercialized (E-Flux, LLC), this is a mature technology that relies on open cartridges containing CO_2 adsorbent material deployed across the soil:atmosphere interface. The trap design eliminates ambient CO_2 interference. The traps are deployed for multiple days (typically several weeks), recovered, the CO_2 quantified, then subjected to radiocarbon analysis. ^{14}C -depleted CO_2 (relative to uncontaminated background sites) can be related to contaminant degradation over the sampled area ($\text{mg contaminant CO}_2 \text{ m}^{-2} \text{ d}^{-1}$). This technology has been used at hundreds of LNAPL contaminated sites, having achieved significant regulatory acceptance. This is the only mature technology to measure natural source-zone depletion rates that routinely accounts for carbon isotopic correction (30).

Site Descriptions

IR-5 Unit 2, NASNI. Groundwater from pre-existing monitoring wells at a site with on-going

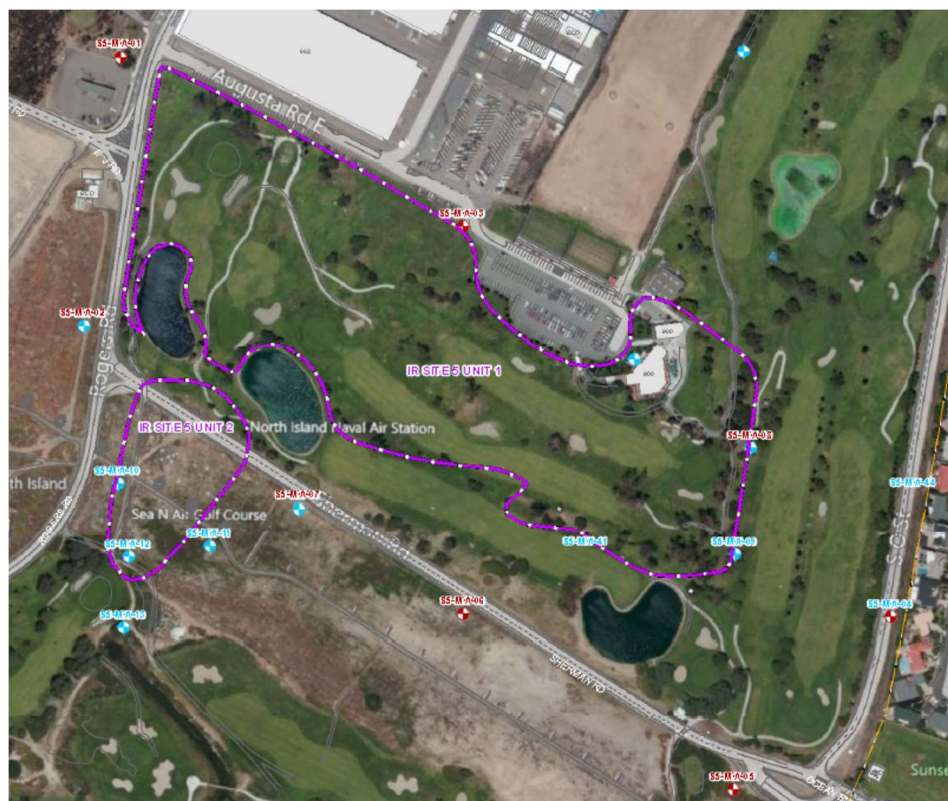


Figure 3. IR Site 5 (all units)

remediation and investigation efforts was the target for this study (31). IR Site 5 at North Island, Coronado, CA was identified as a prime candidate due to a rich archive of existing data on contaminant levels, hydrogeology and the need for site closure information. The site is a former landfill. An estimated 1-2,000 tons of hazardous wastes were

disposed at the site before 1970. Waste was then transferred off-site using the area before it was converted to a golf course in 1983. Two pits were associated with Unit 2 (Eastern and Western). Only the Eastern pit was excavated (2001). Waste deposited at IR-5 included trash, solvents, oils, caustics, hydraulic fluid, contaminated solid waste, sludge and paints. The current site maintenance includes monitoring, inspection and maintenance of the landfill cover. Groundwater well monitoring has shown that groundwater adjacent to IR 5 Unit 2 has virtually no residual organic contamination (TCE, *cis*-DCE, and VC were detected in one well adjacent to IR-5, Unit 2). Monitoring has been conducted semi-annually and the plume of chlorinated solvent material appears to be stable, but receding over time. The presumed attenuation mechanism is biological degradation. The site is heavily vegetated (for the region) within Unit 1 (the golf course

region, while Unit 2 consists of more natural vegetation (Fig. 3). Wells within Unit 1 were sampled for dissolved CO₂ radiocarbon when searching for a suitable background site during the fuel farm project outlined in the Background section above. We found ¹⁴C depleted CO₂ within the two wells sampled (only ~42% modern) indicating a potential fossil organic matter source in the region. Wells sampled for this project are labeled in blue (Fig. 4).

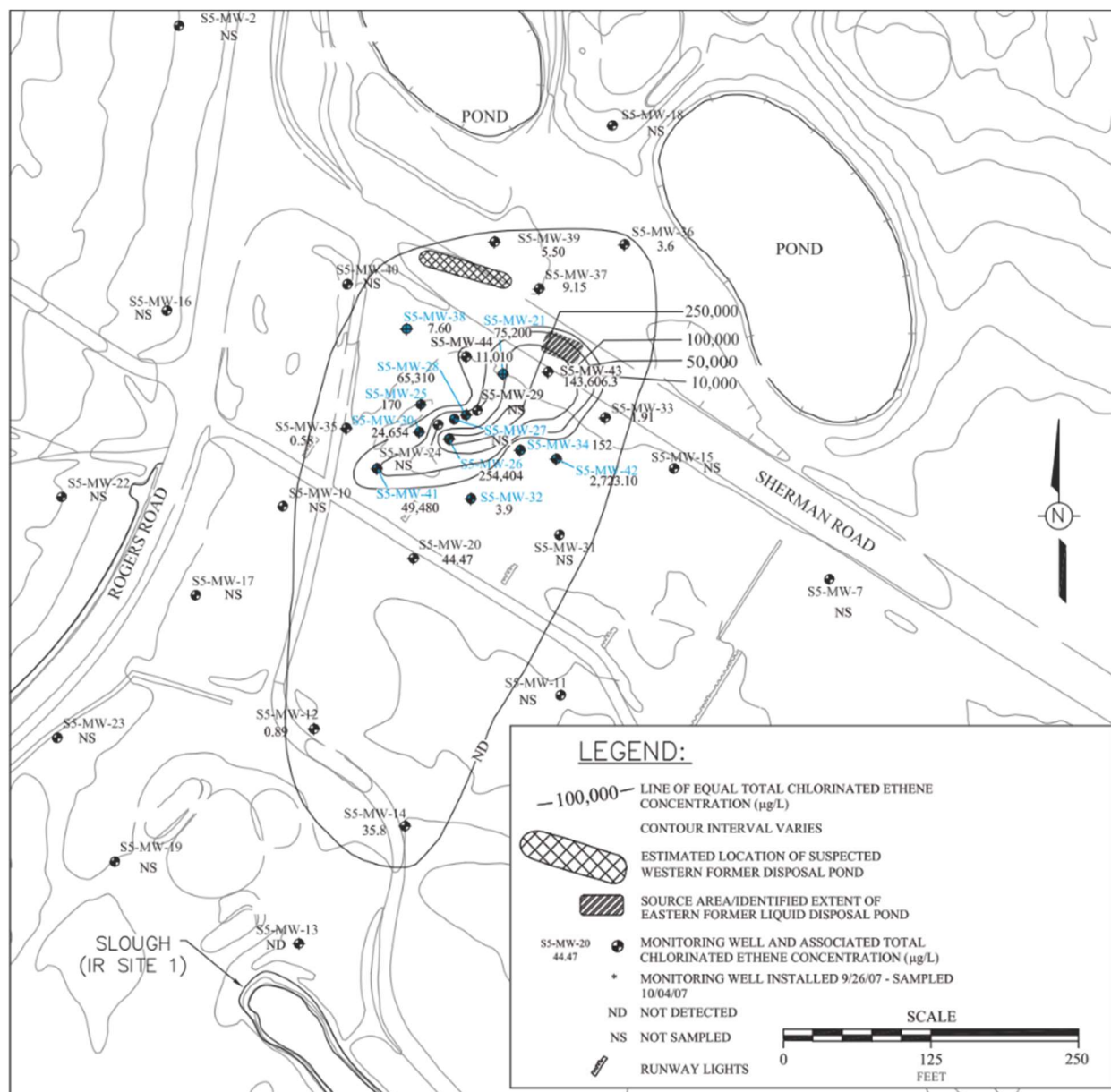


Figure 4. IR Site 5 Unit 2 (Shaw 2013)

LEGEND

- FREE PRODUCT PLUME
- TCE CONCENTRATION ($\mu\text{g/L}$)
- SEALASKA MONITORING WELL
- NORAS INSTALLED MONITORING WELL
- HISTORIC MONITORING WELLS; PMW
- PIEZOMETER
- HYDROPUNCH LOCATION
- OU 1820 BOUNDARY
- IR SITE
- NASNI BOUNDARY

Figure 5-5A: Map of the Naval Air Station, North Island, California, showing monitoring wells, product plume, and boundaries.

contamination exist with a potential source at OU-19 (SW) and OU-20 (NE) (Fig. 5). OU-19/20 has numerous historical sources for potential contamination spanning years and a wide breadth of military maintenance operations. Numerous leaks and breaches in containment systems and waste pipelines as well as overflows and surface discharges were documented over the years. Inferred, undocumented releases are also probable throughout the site. Underground and above ground storage tanks containing solvents were also prevalent on-site and were documented sources for cVOC and other contamination. Releases for cVOCs have been estimated as high as 350,000 gallons (32).

8

information for various zones on site. Vary small gradients exist across the site (0.001 to 0.002 ft ft⁻¹). However, due to variations in soil types (natural vs fill), a very large range in aquifer transmissivity values is found (0.5 up to ~1,000 ft² min⁻¹). Tidal influence is relatively small (up to 30%) at shallow groundwater wells, but may be over 50% at deeper wells. Most influence is below ~20 meters where salinity has been recorded at 30 (32).

Due to remedial investigations begun in the 1990s, LNAPL (consisting of mostly JP-5 and Stoddard solvent) and DNAPL (cVOC) plumes were delineated. CERCLA activities began in the 1990s with LNAPL recovery. Various LNAPL recovery efforts led to removal of ~17,000 gallons LNAL brining dissolved concentrations down to remediation goals. DNAPL has been persistent and several pilot studies using zero valent iron (ZVI), persulfate, and EVO injection were used to evaluate remedial alternatives. Current values for fuel-related LNAPL components are low across OU-19/20 with benzene concentrations lower than 20 µg L⁻¹ (Noreas, Inc, personal communication). Due to the geographical discontinuity in the cVOC plume, each OU within the OU-19/20 “cluster” was evaluated separately during the study (OU-19 and OU-20). One background well (MW-84C) was used for both site (this well showed little to no historical contamination).

IR-17, Indian Head NSWC. Site IR-17 is a low-lying vegetated area adjacent to Mattawoman Creek

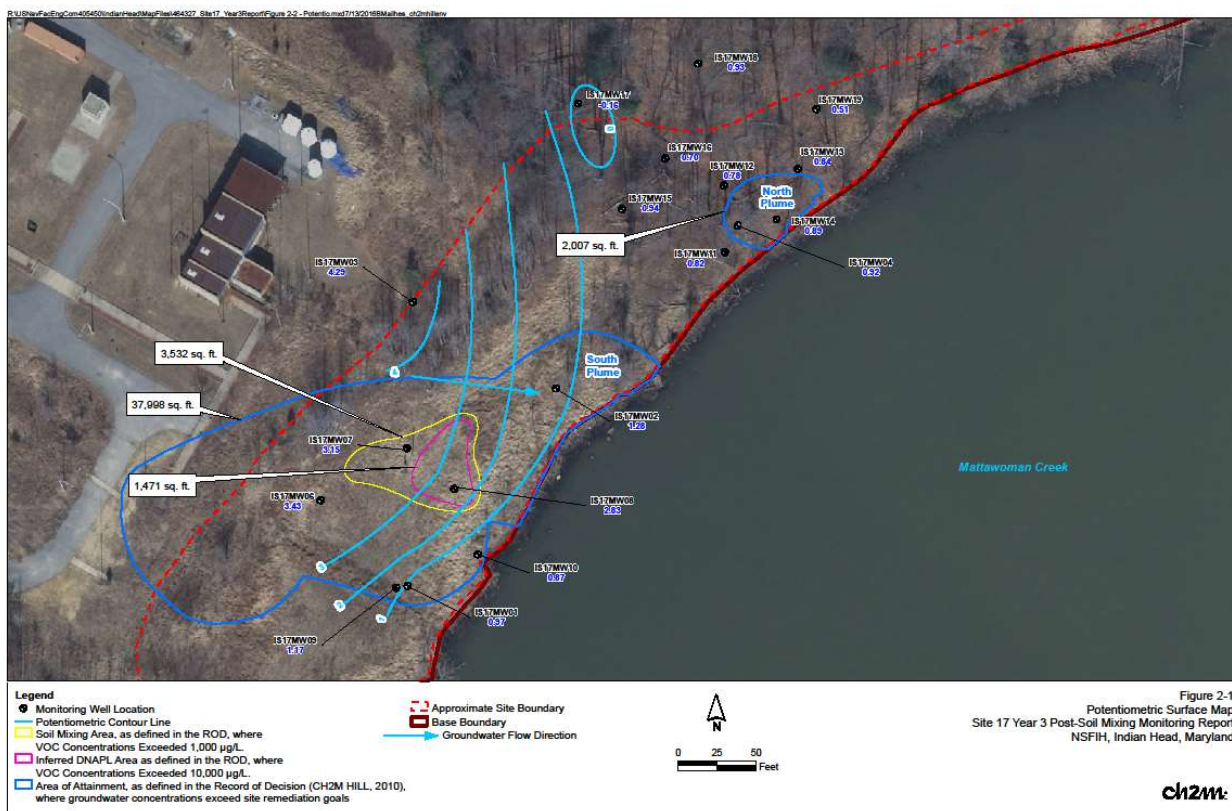


Figure 6. IR-17 NSWC Indian Head (CH2MHill)

at the Naval Surface Warfare Center in Indian Head, MD. Discarded barrels were discovered on-

site in the 1980s (Fig. 6). Starting in 2000, an assessment was undertaken to determine the magnitude and scope of any residual contamination. Small-scale initial sampling found TCE, VC and DCE on-site. Concentrations indicated a potential DNAPL source. No contaminants were detected in Mattawoman Creek waters. Several feasibility studies have been completed within the past 15 years. This site is relatively undisturbed and has on-going remediation efforts in place (including ESTCP projects). Engineered solutions have proven elusive given site hydrology and soil characteristics.

IR-57, Indian Head NSWC. Site IR-57 covers a relatively large area having around 100 m of vertical relief. The upper reaches (Bldg. 292) housed maintenance activities with cleaning and degreasing

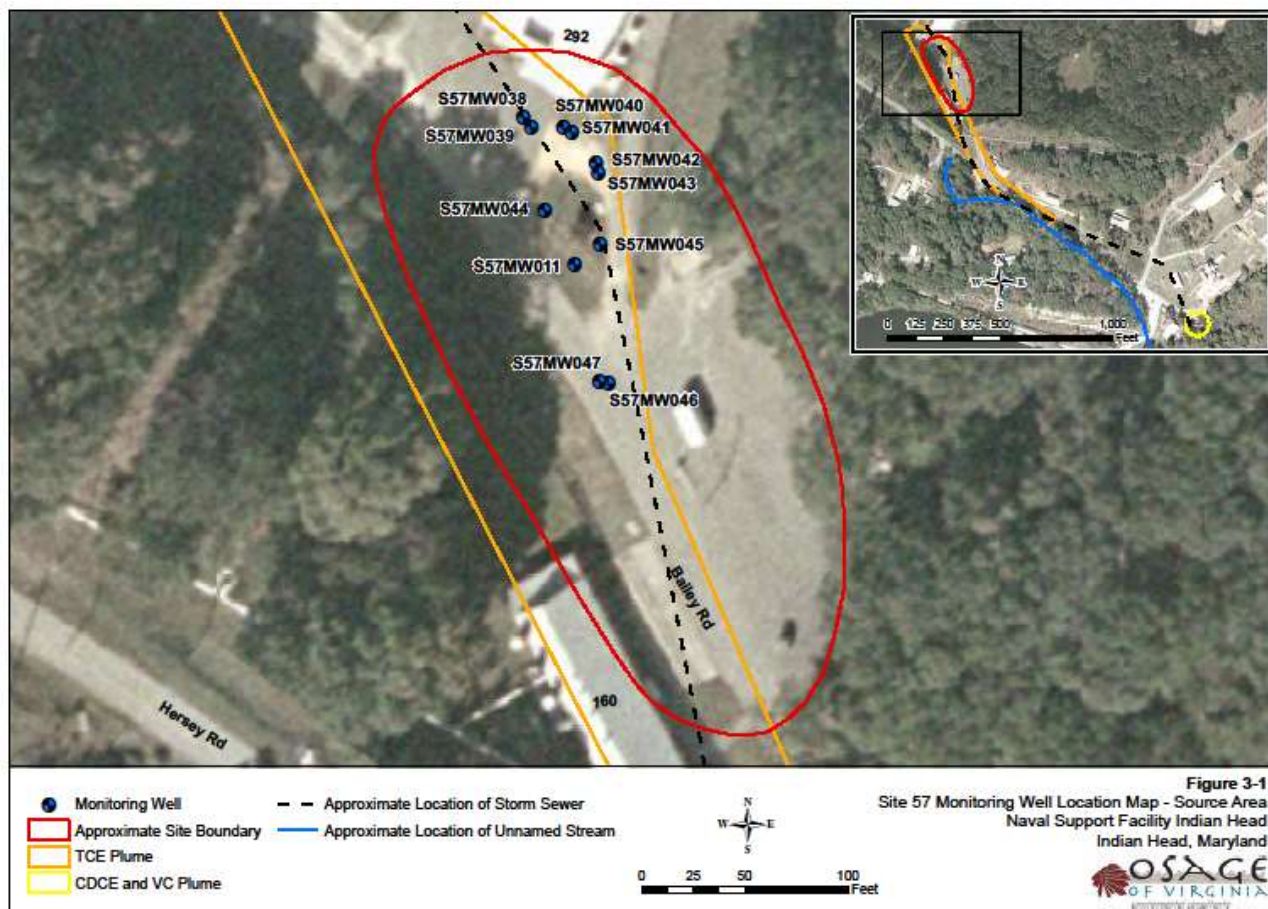


Figure 7. IR-57 NSWC Indian Head showing upper and mid-plumes (Osage)

operations during the 1970s and 1980s. Operations ceased in 1989. TCE was used, stored and reclaimed using barrels on-site. Leaking during operations is thought responsible for TCE, VC and DCE contamination in soils and groundwater on-site. The site was treated with a proton reduction technology (PRT) consisting of electrodes designed to create reducing conditions on-site for reductive dechlorination. In a 2013 report, the initial test demonstrated reducing conditions at selected wells - but no concomitant decrease in TCE concentrations.

Materials and Methods

Similar methods were used at all sites (with variation). Three main analytical objectives were attempted at each site; 1) determine the CO₂ flux at each well and ascribe the correct proportion to microbial respiration, 2) determine the radiocarbon age for CO₂ collected during flux measurements, and 3) develop a ZOI based on site hydrogeologic data to estimate the *in situ* volume sampled during each collection. In general, ~ one-month collection periods were used with in-well CO₂ traps to gather respiration product. Trapping was carried out based on site conditions. Ancillary measurements (historical and contemporary) were used to provide context.

IR-5 U2 Hardware and Field Sampling. At IR-5, pumps with vibrating assemblies (no motorized parts) were sourced and sealed in order to only recirculate gas in the well headspace. We identified serious shortcomings in the pumps procured for the initial limited scope deployment. Motorized pumps were not robust enough to handle field deployment for weeks on end.



Figure 8. Well headspace gas recirculating pumps, sealed

Different pumps having only vibrating assemblies were sourced and sealed in order to only recirculate gas in the well headspace (Fig. 8). "Power distribution" systems were also modified for the new pumps. Potentiometers were used to adjust pump voltage (at the wells) and monitored using a voltage logging system (Hobo data logger). The power distribution center was deployed along with solar panels to provide appropriately ~4V from a solar:battery system to each pump (Fig. 9).

A closed-system sampling system was used at IR-5. Briefly, each well headspace was sealed with a modified well cap - fitted with two gas lines: one long enough to pull gas samples in the vicinity of the groundwater head; the other fitted near the cap. Gas lines were sealed with vacuum grease along with the cap threads and sealing flange. Gas was drawn from the lower gas line, bubbled through a sodium hydroxide trap (pellet NaOH) to collect CO₂. The scrubbed gas was recirculated into the top of the well casing to minimize any pressure

differential. A "cluster" of wells was so outfitted in the region around the highest historical contamination. One background well (identified and used in an earlier study, S5-MW-01) was sampled to obtain the respiration rate and radiocarbon age for natural organic matter (19). Pumps were turned on and an initial 24-hour period to purge out any atmospheric CO₂ was initiated (Nov 14). Expended traps were discarded and replaced with fresh ones and temporal sampling was initiated.



Figure 9. Solar power distribution system in place

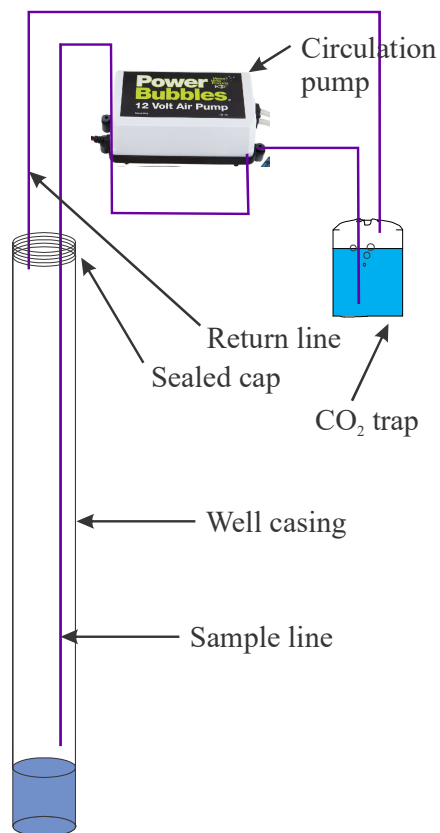


Figure 10. Well headspace CO₂ collection system

OU19/20, IR-17/IR-57 Hardware and Field Sampling. At OU-19/20, it was not possible to have "actively" sampled wells (Operable Units). Therefore, a passive in-well trap was developed. In-well traps consisted of plastic screen material to which tethers were glued. Threaded end fittings allowed a NaOH-filled cap to be added and suspended into the well headspace. Well caps were modified by drilling two holes which allowed gas-tight tubing to be inserted into the well headspace. The "inflow" tubing was pulled through roughly 1/2 m through the cap and the "outflow" tubing was pulled just out of the cap bottom. Gas-tight valves were fitted on the outside terminals of each gas tube. During deployment, the well was opened, traps replaced and the well caps reseated and sealed. Argon gas was then flowed into the headspace (scrubbed with ascarite) allowing the headspace gas to be purged out (from the bottom as Argon is denser than air) (Fig. 12). Traps were deployed for 1-3 months at a time. At each trap recovery, NaOH was transferred from the reservoir to a volumetric container and dissolved with CO₂-free water (sparged with He or Ar). The amount of water used was annotated on each container. In-well traps were deployed as described at OU-19/20, IR-17 and IR-57. The passive design advantages include a) no need to provide a

power source, b) no exposed wires and power infrastructure and c) no clogged lines or needles (which has occurred with the current system on occasion, and d) no issues with catastrophic events (a lightning strike in all likelihood caused a power outage on the current system).

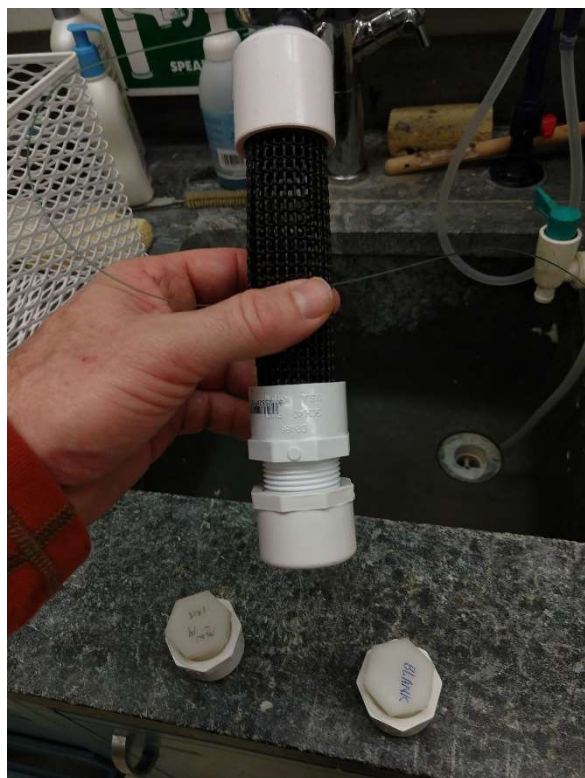


Figure 11. NaOH trap showing support and reservoir

There are different equilibrium kinetics using passive traps relative to active pumping traps. The CO₂ collection rate is lower based due to a passive diffusion gradient instead of active. ZOI model simulations take into account the CO₂ collection rate at each well (16, 17). A concomitant decrease in the ZOI for each well was proportionally simulated – thus the final degradation per unit area and time is appropriately scaled to trap design.

Water Quality Analyses. To ensure soils with carbonates (limestone) are not impacting measurements, water samples were taken in pre-cleaned 40 mL vials for pH and cations and any additional chemical analyses. The samples were

assayed for K⁺, Ca⁺⁺, Mg⁺⁺ and Na⁺ ions using a Dionex DX120 or ICS3000 ion chromatograph with a CS12A cation column. Cation analysis and soil characterization data from borehole studies at all sites indicate no limestone soil lenses so we conclude carbonates will not impact measurements at this site. However, if this method is to be increasingly applied to contaminated sites, this best practice check should be done.

Soil Gas Methane Concentrations. Soil gas samples were taken for methane concentrations were sampled at various time-points since November 2014. Samples were taken from NaOH gas trap lines (Fig. 12) during trap replacement (while pumps were not operational) or before well headspace was compromised prior to trap removal and replacement. Headspace gas was sampled by 60 mL syringe fitted with a three-way valve. Two samples were pulled and discarded. The third sample was reserved. The sample was transferred underwater



Figure 12. Well cap sealed in place with sparge line and check valve

to a water-filled inverted serum bottle (displacing the water). A gas-impermeable septum was inserted and the bottle was crimp-sealed. Serum bottles were returned to NRL. A subsample from the bottle headspace (3 mL) was injected into a Shimadzu GC-14A gas chromatograph fitted with a Hayesep 0.80/100 column. Column flow was $\sim 10 \text{ mL min}^{-1}$ and concentrations were determined against certified reference standards (Scott Gas, Plumbsteadville, PA).

Radiocarbon analysis. Water samples with ample dissolved inorganic carbon (*e.g.* CO_2) were sent to the University of Georgia Center for Applied Isotope Studies (CIAS). CAIS sparges, cryogenically distills, and purifies CO_2 then produces graphite targets for accelerator mass spectrometry (AMS). The high-sensitivity analysis allows radiocarbon age dating in samples back to $\sim 50,000$ years. Due to the high per-sample costs, samples were combined quantitatively to decrease the number of total analyses. Details are given in the supplementary materials. Data are reported in percent modern carbon (pmc) which can be converted to $\Delta^{14}\text{C}$ (per mil – ‰) for modeling (see below) using standard conversions (33).

CO_2 Production Rate Analysis. Collected CO_2 samples (from traps) were diluted in a known amount of Ar- or He-sparged water until all residual solid NaOH was dissolved. Samples were appropriately diluted and analyzed by acidifying the CO_2 out of solution and measuring by coulometry (34). CO_2 was quantified relative to a certified reference material (35). CO_2 production rate was calculated by the total recovered CO_2 divided by the time of collection. Respiration was determined for each well by subtracting the lowest collection rate measurement (assumed to be equilibrium CO_2 collection only).

Zone of Influence Model/Simulation. ZOI models were created for each well based on the well hydrogeology and local soil characteristics (obtained from boring records, slug tests, conductivity tests, etc.). Input variables included well construction (casing dimensions, depth to water) temperature, atmospheric pressure and soil permeability values. Analysis of well logs and prior well tests in the project area were used to develop a hydrogeologic model of the site. This information was coupled with CO_2 equilibrium simulation models to create the ZOI models. The ZOI model was developed using MT3DMS (36) and MODFLOW-2005 (37). MT3DMS is the biodegradation model capable of simulating multi-solute transport and reaction, and used to simulate CO_2 solute transport as a part of the ZOI model. MODFLOW-2005 is the hydrogeological model considered as the reference code to simulate groundwater dynamics and is used to simulate groundwater flow in the unconfined aquifer at the study site. The two models have been used together as the standard package for multi-species contaminant transport simulations (38). In this study, ModelMuse was used to link and interface the two models (39).

The target for this study was CO_2 produced from chlorinated solvent degradation (*e.g.* TCE, DCE and VC). Among different biodegradation models studied (*e.g.* MT3DMS, RT3D, Bioscreen, Biochlor, and SEAM3D), there is no model that is capable of coupling a groundwater simulation model and simulating this complex CO_2 system while tracking individual CO_2 solutes. This project

treats all CO₂ with different origins together - and the radiocarbon content was used to uniquely distinguish CO₂ derived from chlorinated solvents.

Determining the Contaminant Respired. The isotopic mixing model was applied to each sample using the radiocarbon value for CO₂ collected at the background wells (MW-01 for IR-5 U2 and MW-84C for OU-19/20) as the appropriate site-wide background value ($\Delta^{14}\text{C}_{\text{natural organic matter}}$). The $\Delta^{14}\text{C}_{\text{petroleum}}$ was assigned the value -999 ‰. The *fraction*_{petroleum} was solved for each well via a two end-member mixing model:

$$\Delta^{14}\text{CO}_2 = (\Delta^{14}\text{C}_{\text{petroleum}} \times \text{fraction}_{\text{petroleum}}) + [\Delta^{14}\text{C}_{\text{natural organic matter}} \times (1 - \text{fraction}_{\text{petroleum}})]$$

¹⁴C-content measurements could then be used to determine the proportion of vadose zone CO₂ derived from the cVOC (15). Using respiration values (g CO₂ produced per unit time) and ZOI simulations for each time-point and well (volume sampled), contaminant degraded per unit time and volume can be computed in a straightforward manner (*e.g.* CO₂ respired per unit time times the fraction derived from fossil sources divided by the volume sampled).

Results and Discussion

Roughly one year of measurements were completed at each of two sites during the course of the project. At the RPM's request, we initiated measurements at two sites local to NRL (IR-17 and IR-57, Indian Head NSWC). These sites were sampled for all parameters but radiocarbon analysis has not been completed due to time and funding constraints. Site-specific results and discussion follow:

IR-5 Unit 2. Traps were deployed starting in November 2014 and cycled every 2-4 weeks until November 2015. Trap material was analyzed for CO₂ concentration and radiocarbon. Selected concurrent samples for cations, well casing CH₄ concentrations and water quality measurements were taken. Results are summarized by analysis.

ZOI simulations. Groundwater hydraulic and CO₂ solute properties for the study site were obtained from previous reports (40, 41). Three years of weather data (2007, 2011 and 2012) were obtained from the CIMIS San Diego station (Station ID 184) to estimate the recharge rate of the aquifer. Tidal data for the same three years were obtained from the NOAA San Diego Station (Station ID: 9410170) to define boundary conditions. From the aerial photo, surface water pools (e.g. ponds and creeks) were identified on the Northeastern side of the area (in the golf course and park). A constant head equal to the elevation of these surface water bodies was assigned to the boundary. The following shows results for one collection time period (in detail). Each collection time period was simulated accordingly.

The areal model indicated that the effects of short term (e.g. daily and weekly periods) changes in sea level around the peninsula on groundwater flow at the study site were not significant. This result agrees with the previous report from Wiedemeier and Associates (personal communication, April, 2013). The ground-water hydrology at the study site is usually steady

Table 1. Hydrogeologic parameters used in IR-5 U2 ZOI model(s)

Parameter	Units	Value
Hydrology		
Hydraulic Conductivity	(m hr ⁻¹)	0.44 (aquifer), 10 (well)
Porosity (aquifer)		0.48 (aquifer), 0.99 (well)
Bulk Density	(g cm ⁻³)	1.4
Specific Yield	(cm ³ cm ⁻³)	0.2
Hydraulic Gradient	(m m ⁻¹)	0.015
CO₂ Solute Transport		
Diffusion Coefficient (CO ₂)	(m ² hr ⁻¹)	6.77 X 10 ⁻⁶
Longitudinal Dispersivity	(m)	6.1
Horizontal Transverse Dispersivity	(m)	0.61
Vertical Transverse Dispersivity	(m)	0.061
Soil Gas CO ₂	(%)	0.56

between late summer and fall. Therefore, the groundwater flow during the CO₂ collection periods was assumed steady (i.e. constant hydraulic gradient). The hydraulic gradient estimated by the areal model was 0.009 m m⁻¹, which was reasonably close to the value estimated

from the groundwater elevation map in June 2011 (40). Parameters obtained from literature sources are outlined in Table 1.

Prior to the CO₂ sampling, the initial distribution of solute CO₂ in the aquifer around the sampling well was assumed in equilibrium with the CO₂ supplied from the overlying soil gas and mineralization; therefore, the CO₂ distribution was assumed uniform. Any CO₂ gradient observed at the end of the simulation period (given by the time between trap cycling) was assumed to be attributable to CO₂ collection in the well. With uniform CO₂ distribution, the ZOI associated with the CO₂ collection was defined as the volume of aquifer that has a CO₂ concentration of 95% or less of the initial concentration. Using Henry's law, the CO₂ equilibrium concentration at the groundwater table with the CO₂-rich soil gas was estimated as 8.4 g CO₂ m⁻³. Because biochemical conditions in the unconfined aquifer at the time of the CO₂ collection was unknown, the ZOI model assumed constant and conservative mineralization rates for the chlorinated solvents (*e.g.* half-life of DCE and VC = 3.8 and 9.5 years, respectively). The CO₂ production rate from the chlorinated solvents was estimated using this assumption, and appeared to be negligibly small (< 0.001 g m⁻³ d⁻¹) compared to the observed CO₂ collection rate at the site which ranged from 0.01 - 0.31 g d⁻¹. The ZOI model was thus simplified by not accounting for mineralization during the CO₂ collection period. However, mineralization has certainly accumulated CO₂ in the aquifer over time as CO₂ radiocarbon ages were older than the background value.

The calibrated ZOI model was run with the estimated hydraulic gradient (0.015 m m⁻¹) and hypothetical background CO₂ concentration (8.4 g CO₂ m⁻³). The entire model domain for this scenario was 9.0 m x 4.5 m x 10.0 m deep. The horizontal spatial resolution is set to 0.09 m x 0.09 m, which makes one grid area equal to 0.0081 m², the same as the well area. The vertical spatial resolution varied from 0.05 m at the surface to 1.7 m at the bottom. The hydraulic gradient was applied to the ZOI model by setting the constant head condition along the two boundaries, which allowed groundwater to flow in the left to right direction (Fig. 13).

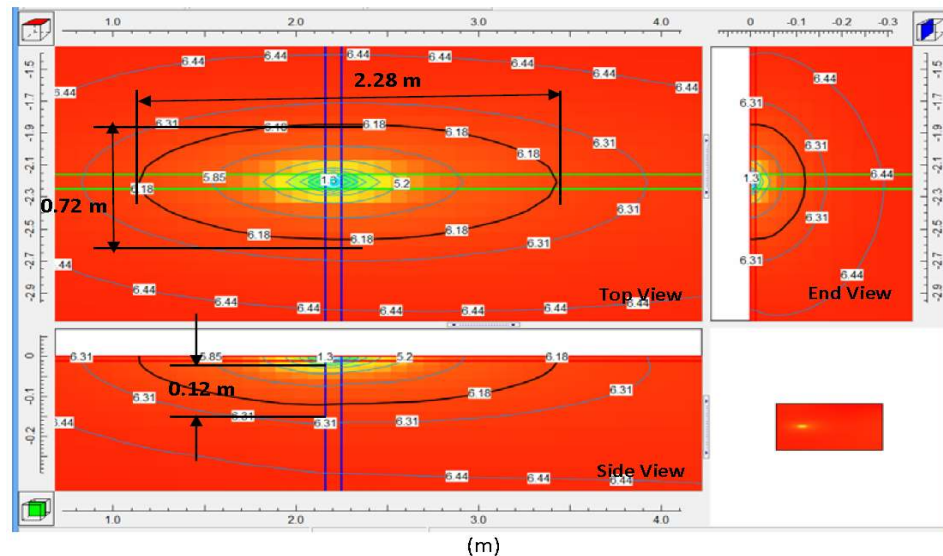


Figure 13. Calibrated CO₂ distribution.

Each well and time-point ZOI model was then coupled with the observed CO₂ collocation rates. The calibration assumed that the collection rate was constant during the collection period. The calibration also assumed the equilibrium between the CO₂ output (*i.e.* collection) and supply (*i.e.* diffusion) at the water table in the well at the end of the collection period. In other words, the CO₂ concentration of the water surface in the well was assumed to be decreased to 0.0 g CO₂ m⁻³ by the end of the simulation.

Taking the CO₂ collection rate into account, ZOI calibrations varied (see Appendix A for data from all simulations). The calibration result indicated strong linear correlations between the observed collection rate and the calibrated background CO₂ concentration. Also, estimated ZOI volumes indicated a strong linear correlation with background CO₂ concentrations and thus CO₂ collection rates. Assuming the partial pressure of the atmospheric CO₂ of 0.04 %, the equilibrium CO₂ concentration of non-contaminated aquifer exposed to the atmosphere would be 0.60 g m⁻³. The estimated background CO₂ concentration for all collection rates was higher than this value which suggests groundwater contamination with chlorinated solvents (*e.g.* DCE and VC) and their active mineralization. However, the estimated background CO₂ concentrations were routinely below solubility of CO₂ (1,450 g m⁻³ at 25 °C) so CO₂ does not appear to be saturated in the aquifer.

The calibrations assumed a steady hydraulic gradient and constant collection rates. A supplemental simulation for the average CO₂ collection rate indicated approximately 50 % increase in the estimated background CO₂ concentration (*i.e.* increased from 6.5 to 9.7 g m⁻³) with 10 % increase in hydraulic gradient (*i.e.* increased from 0.0150 to 0.0165 m m⁻¹). Another supplemental simulation for the average CO₂ collection rate indicated approximately 46 % increase in the estimate background CO₂ concentration (*i.e.* increased 6.5 to 9.5 g m⁻³) if the collection rate changed from 0.00530 (+10 %) to 0.00434 g h⁻¹ (-10 %) over the 2-week collection period. Furthermore, the ZOI model assumed constant and conservative reaction rate for the chlorinated solvents. After accounting for the small difference in the first and second CO₂ collection rates, the reaction rate appeared to be underestimated for the study site. Therefore, it is important for ZOI estimation to collect and account for these aquifer and operation parameters for better accuracy and reliability.

Water quality measurements. Samples for cation and pH were analyzed in March and July 2013 before trap deployment to assess site suitability. The primary concern is that low pH might promote carbonate dissolution which could bias radiocarbon analysis (see M&M section). Due to the nature of soils at NASNI, this analysis was probably not necessary (no significant source of carbonates in dredge fill), however, shell deposits could be of concern. pH was near neutral for all wells sampled (Table 2). Wells on the site's Southern side generally had a higher Na⁺ content, but were not in a range which indicated significant seawater intrusion. Calcium ion concentrations ranged from 8.0 to 58 mg L⁻¹ (Tables 1 and 2) but did not inversely correlate with pH to indicate significant carbonate dissolution during either sampling ($r^2 < 0.3$). We performed a trend analysis with the water quality data using principal components analysis (PCA). Bi-plots showed no strong loadings with any water quality variable.

Respiration. Respiration was measured during each time period as the amount of CO₂ collected per unit time per unit volume (using ZOI simulations). The lowest CO₂ collection rate (95 μmol

Table 2. Selected cation concentrations and pH for IR-5 U2

Well	Na ⁺ (mg L ⁻¹)	K ⁺ (mg L ⁻¹)	Mg ²⁺ (mg L ⁻¹)	Ca ²⁺ (mg L ⁻¹)	pH
MW-01	131	18	32	58	7.34
MW-10	320	104	54	45	6.71
MW-11	430	24	62	32	7.84
MW-12	774	45	109	50	7.76
MW-14	212	19	53	53	7.72
MW-17	427	30	54	27	8.00
MW-20	535	50	56	26	7.69
MW-21	168	41	40	44	7.76
MW-24	385	73	48	29	7.74
MW-26	404	101	39	14	7.46
MW-28	299	44	43	18	7.75
MW-30	492	87	47	17	7.67
MW-31	269	22	43	32	7.92
MW-32	258	76	40	32	7.42
MW-33	128	14	40	62	7.92
MW-34	377	48	47	30	7.35
MW-35	80	26	21	30	7.58
MW-38	178	23	40	51	7.82
MW-40	77	10	18	38	7.78
MW-41	165	88	25	14	7.81
MW-42	487	30	56	17	7.58
MW-43	136	18	37	74	7.60
MW-44	130	19	32	48	7.61

CO₂ d⁻¹) during the year-long collection period was used as the value due to equilibrium trapping alone (a conservative assumption) and subtracted from the all other CO₂ rate measurements. The resultant values were considered to be respiratory CO₂ production rates. A total of 224 measurement were made over the 13-well sampling grid. MW-01 (~200 meters from the main well cluster) was considered to be background (no historical contamination).

Respiration ranged from 0 to 31 mmol CO₂ day⁻¹ and converted to volumetric basis (divide by the ZOI), ranged from 0 to 196 mg CO₂ m⁻³ d⁻¹. The highest respiration rates occurred at MW-01 (background well), MW-21 (at the upgradient plume fringe) and other plume fringe wells (MW-38, MW-41, MW-

42). Although not universal, respiration was generally lower in the central well cluster where historical cVOC contamination was highest (Fig. 14).

Radiocarbon analysis. Because radiocarbon analysis is very expensive (\$350-\$500 per sample), in order to obtain representative data for each well and each time-series, samples were combined so that a value could be applied to each calculation. Combining samples was done by analyzing the respiration and adjacent time points. In general, sub-samples with similar respiration rates were combined. Adjacent sub-samples with similar respiration rates were combined but usually not with others with similar respiration rates if the latter were separated by several inter-samplings. Low relative respiration rate sub-samples were often combined even if they were non-sequential. The reasoning was that very low respiration rates were likely limited by similar site conditions and thus would likely have similar radiocarbon signatures. The act of combining samples likely led to more overall uncertainty as mistakenly combining a highly ¹⁴C-depleted and a highly ¹⁴C-enriched sample would imply that both were similarly apportioned with ¹⁴C when the opposite was true. Sub-sample combinations are identified by colors in the master sheet

(column W) found in Appendix A for IR-5 U2. Equal amounts from each sub-sample were combined based on the dissolved CO₂ concentration and diluted amount.

CO₂ Radiocarbon ranged from 23% to 100% modern ($\Delta^{14}\text{C}$ ranged from -771 to 0 ‰). The background well (MW-01) was 85 ± 1 pmc for all samplings. Sub-samples having radiocarbon values greater than 85 pmc were assumed to be either compromised by atmospheric CO₂ (some leaking and plugging occurred during time-series). The most radiocarbon depleted wells were those on the fringe (MW-21, MW-30, MW-34, MW-35, MW-38, and MW-42). Interestingly, well MW-41 which is the furthest downgradient showed only modern respired CO₂. This could indicate the plume material is attenuated ~10 meters downgradient of the highest

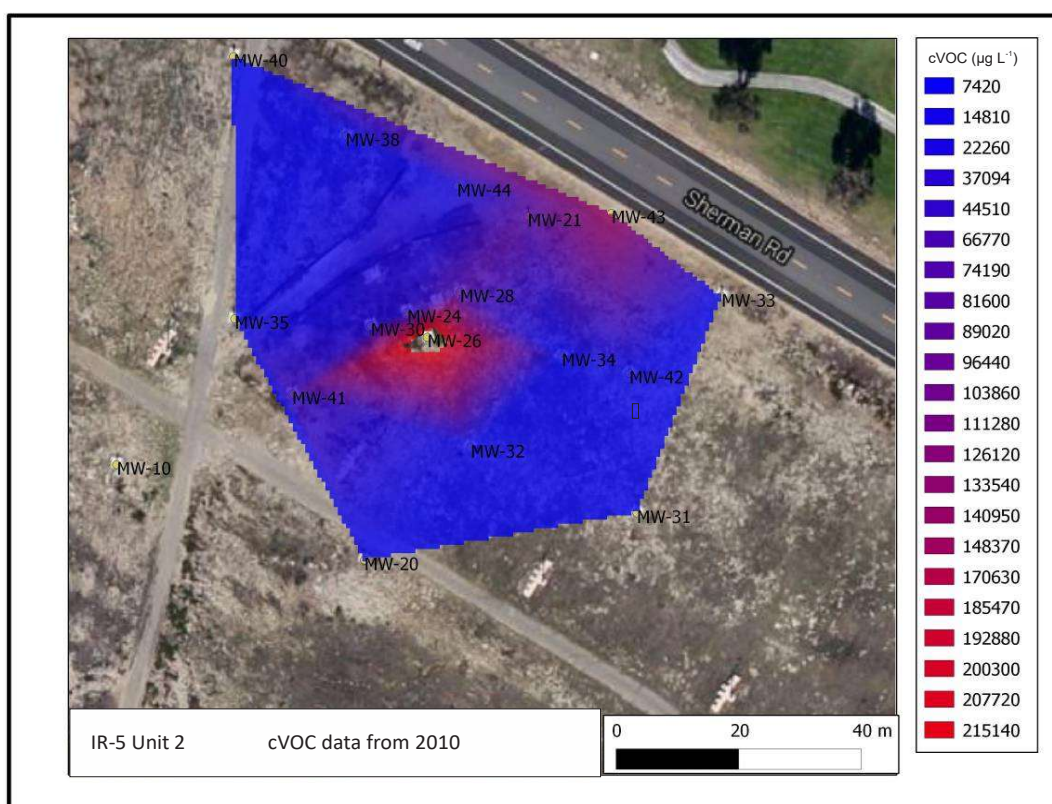


Figure 14. Historical cVOC contamination IR-5 U2

concentrations – or perhaps that all necessary co-metabolites are too limiting (*e.g.* used up) and reductive dichlorination is stalled.

Conversion from radiocarbon and respiration to cVOC degradation. Background radiocarbon content (MW-01) was used for each time-point to calculate the fraction CO₂ derived at each well from fossil source(s) – *e.g.* cVOC. See Equation (1). The fraction derived from petroleum sources (f_{pet}) was multiplied by the respiration in order to determine the amount of CO₂ produced per unit time and volume from cVOCs. This was converted to TCE equivalents by molar fraction and

molecular weight. Thus, the amount of TCE degraded over the site was calculated ($\text{mg TCE C m}^{-3} \text{ d}^{-1}$). This calculation ranged from 0 to $400 \text{ mg C m}^{-3} \text{ d}^{-1}$ with the highest values at fringe wells (MW-21, MW-34, MW-35, MW-38 and MW42). Within the central well cluster, the only significant TCE degradation occurred at MW-26.

TCE degradation was interpolated over the site using the Matlab® scatteredInterpolant function. The relatively regularly-spaced wells justified using the 'natural' interpolation method and no extrapolation was used as wells having clogged lines or otherwise compromised were left out of the final spatial calculations. Interpolant outputs contained spatial area sampled (m^2 gridded between sampled wells), and an interpolated degradation rate. A uniform 3 m plume depth (31) was used to estimate the total degradation over the site in terms of the plume volume. TCE (carbon basis) degradation interpolated over the site for each collection period is shown in Figs. 16-34 (images courtesy of the U.S. Geological Survey).

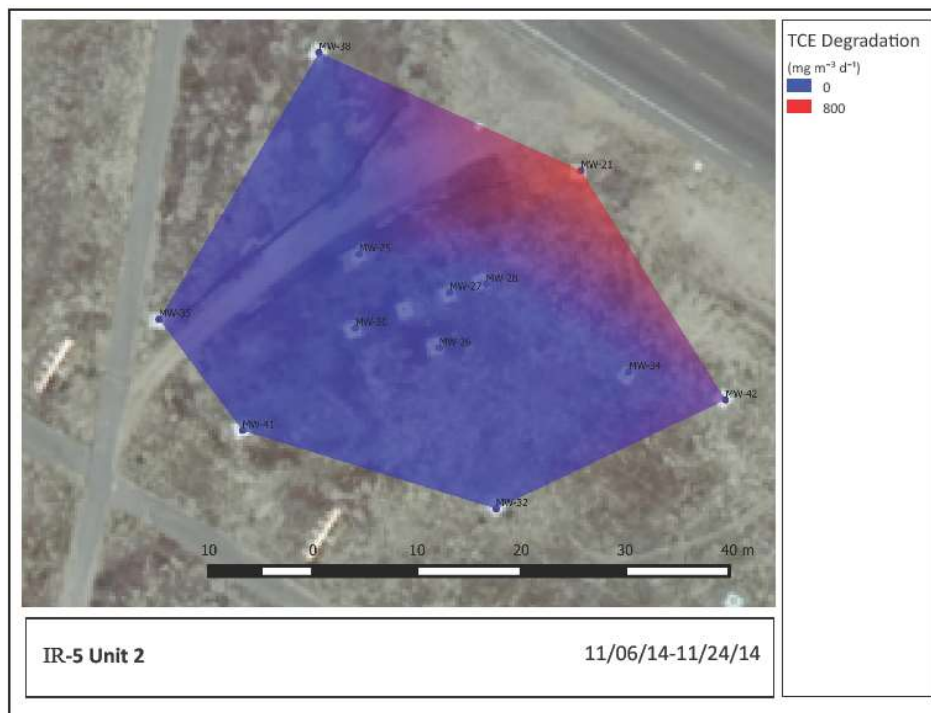


Figure 15. TCE degradation 11/06/14-11/24/14

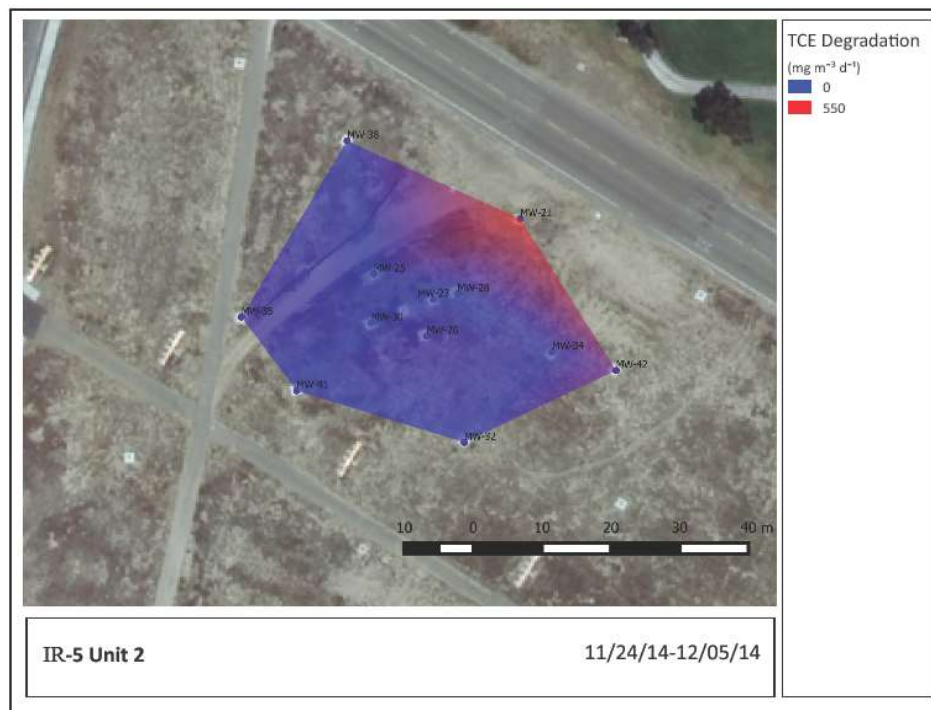


Figure 16. TCE degradation 11/24/14-12/05/14

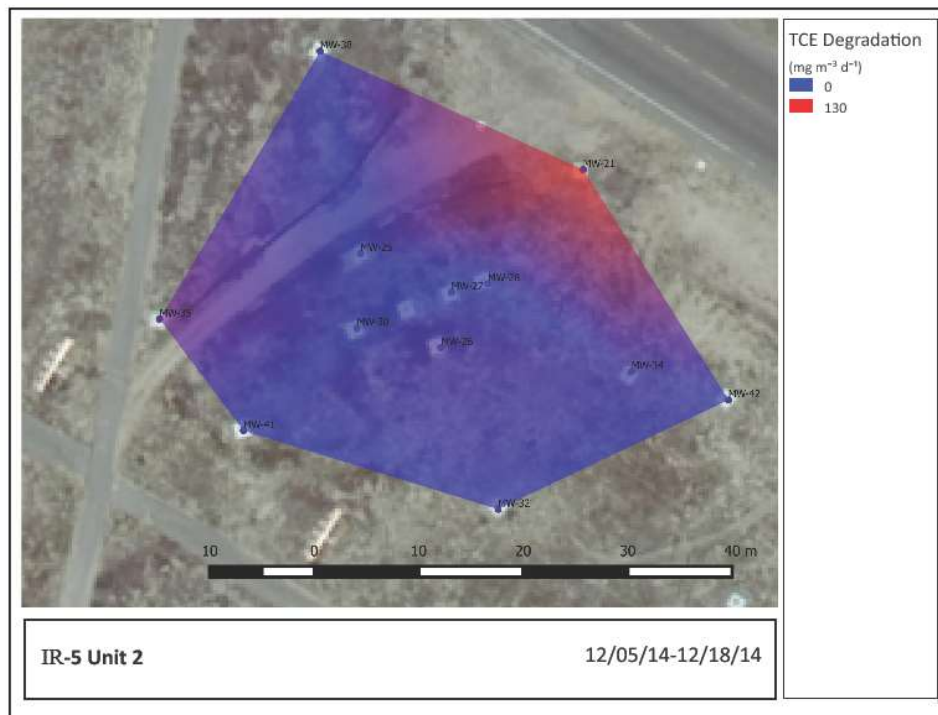


Figure 17. TCE degradation 12/05/14-12/18/14

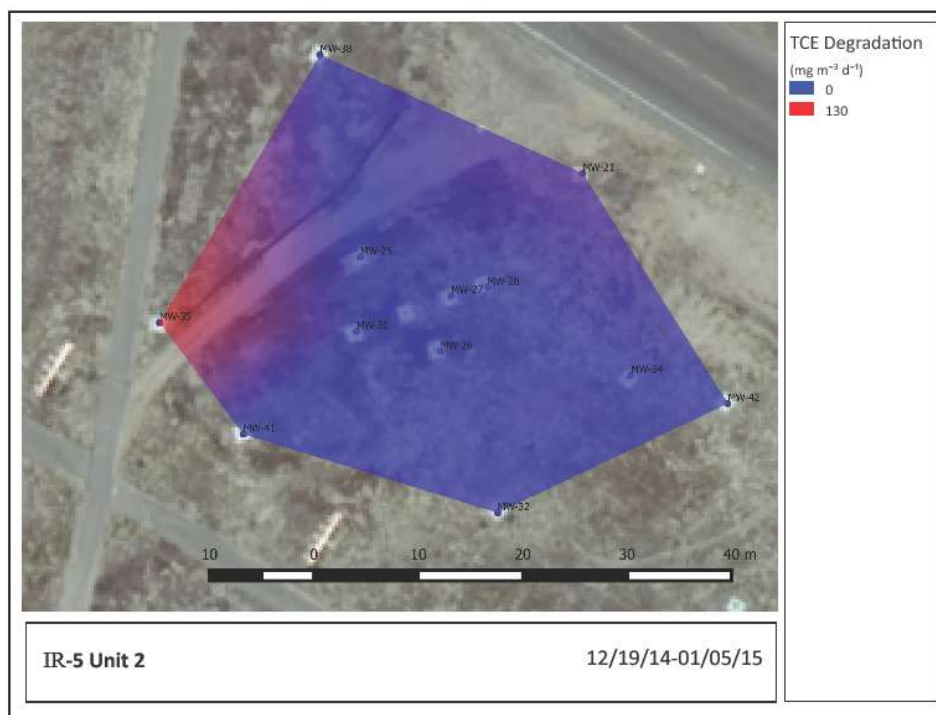


Figure 18. TCE degradation 12/19/14-01/05/15

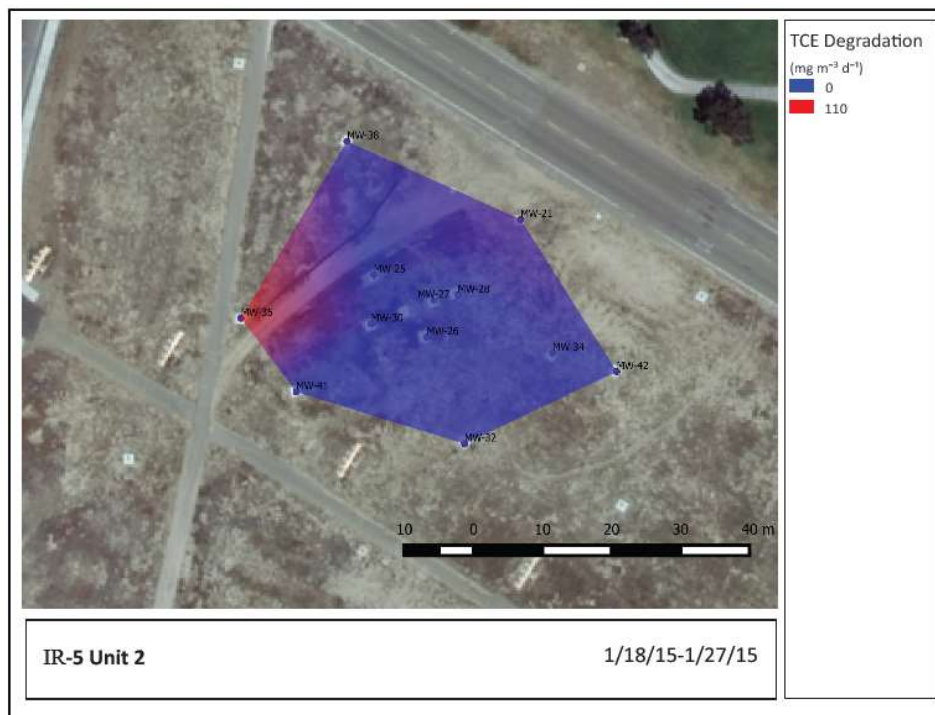


Figure 19. TCE degradation 01/18/15-01/27/15

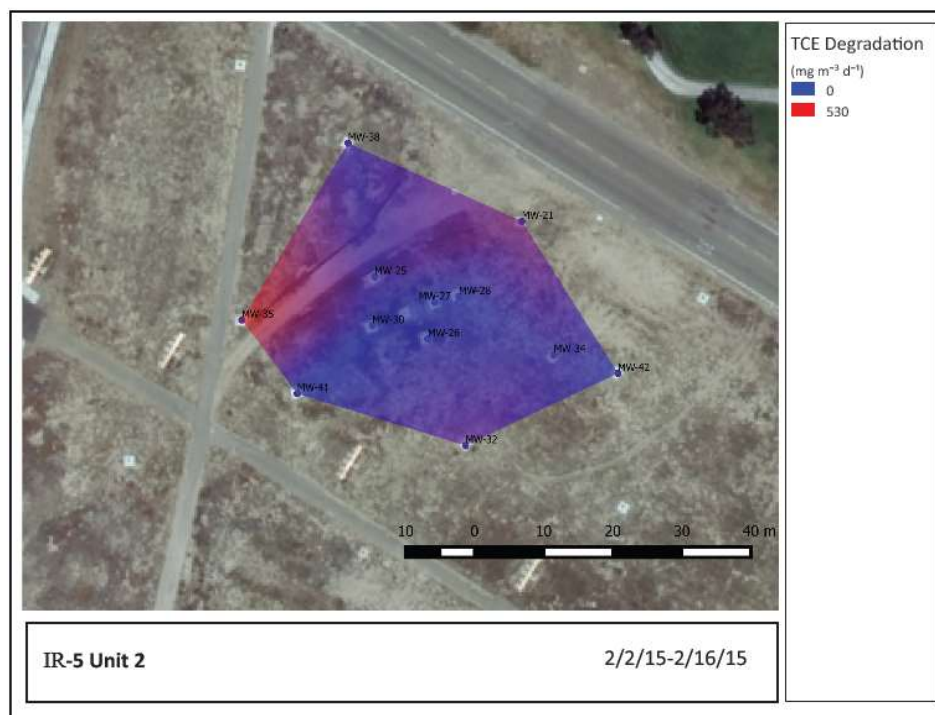


Figure 20. TCE degradation 02/02/15-02/16/15



Figure 21. TCE degradation 02/16/15-03/09/15



Figure 22. TCE degradation 03/10/15-04/10/15

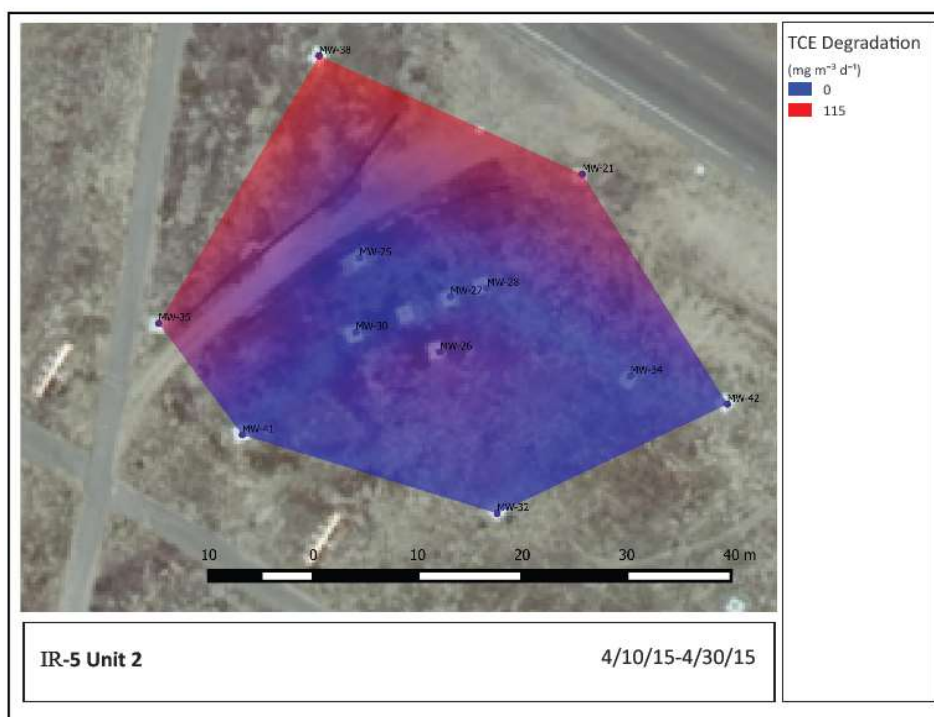


Figure 23. TCE degradation 04/10/15-04/30/15

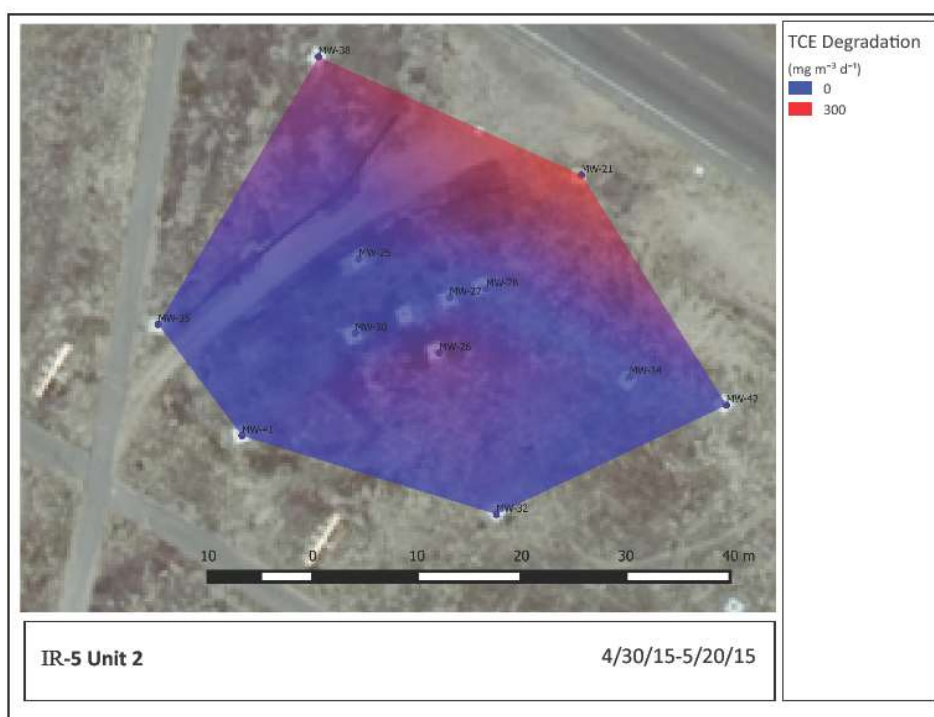


Figure 24. TCE degradation 04/30/15-05/20/15

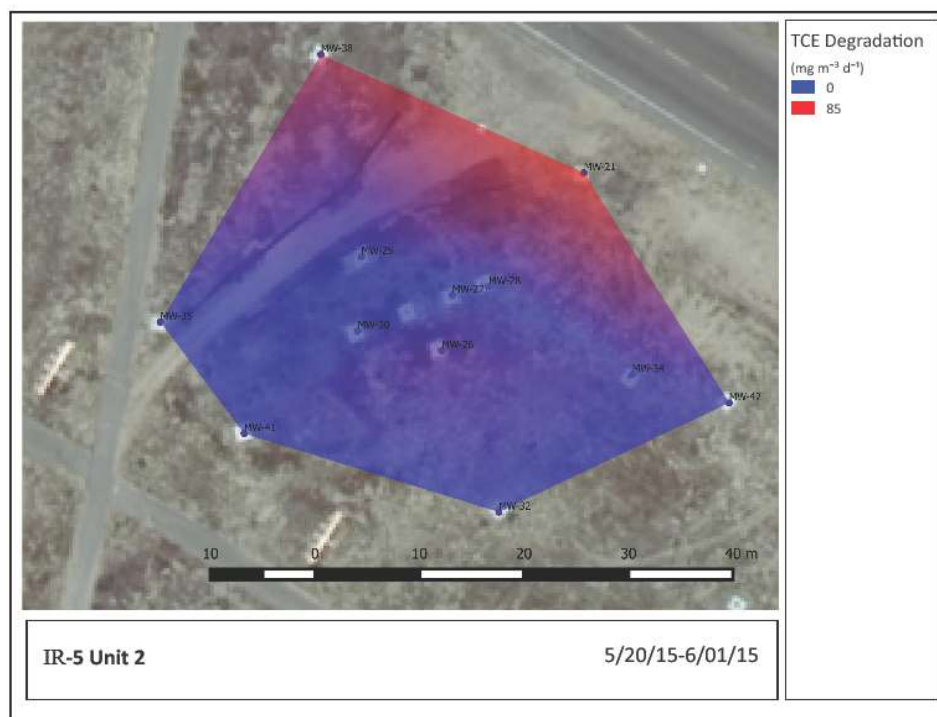


Figure 25. TCE degradation 05/20/15-06/01/15

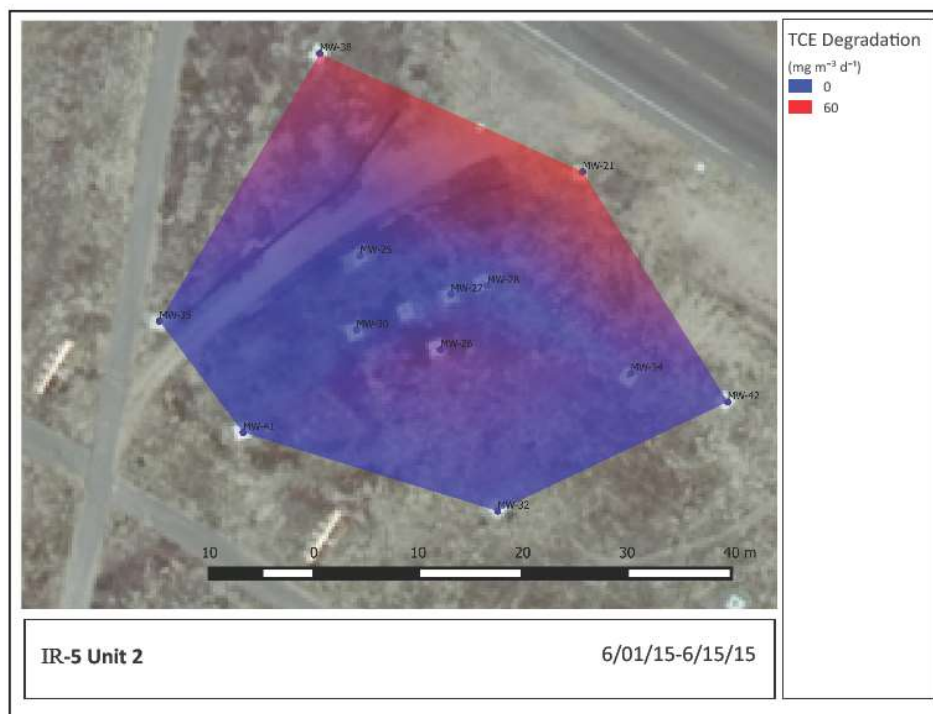


Figure 26. TCE degradation 06/01/15-06/15/15

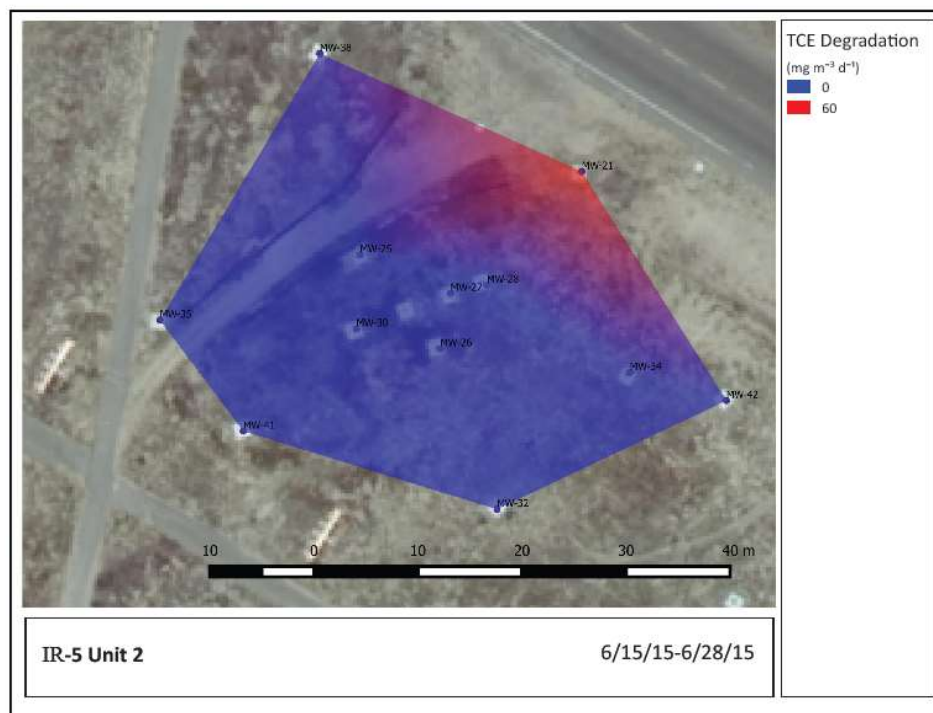


Figure 27. TCE degradation 06/15/15-06/28/15

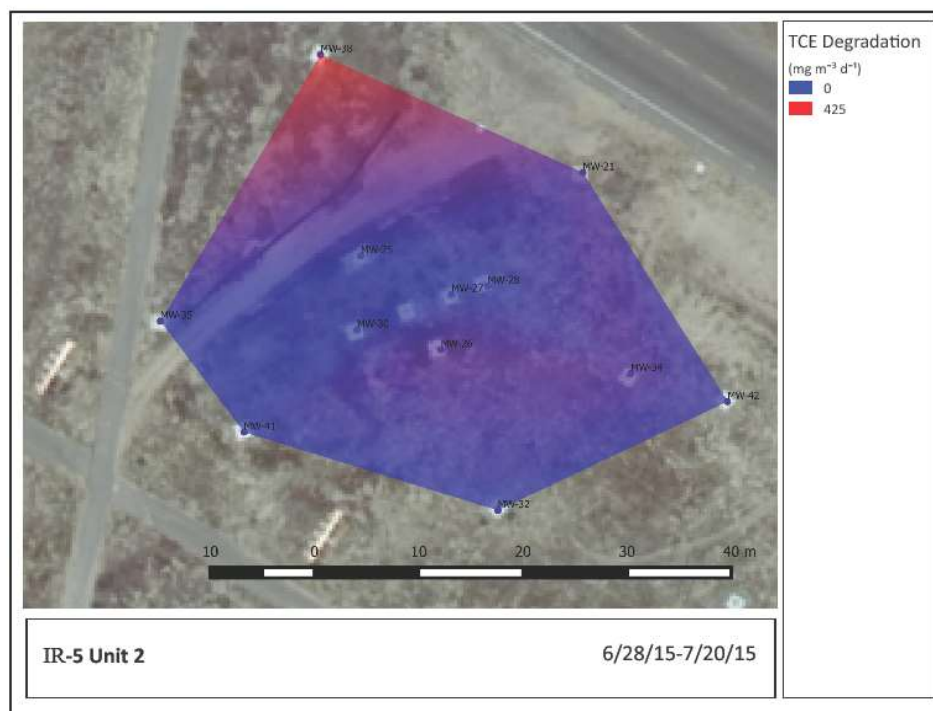


Figure 28. TCE degradation 06/28/15-07/20/15

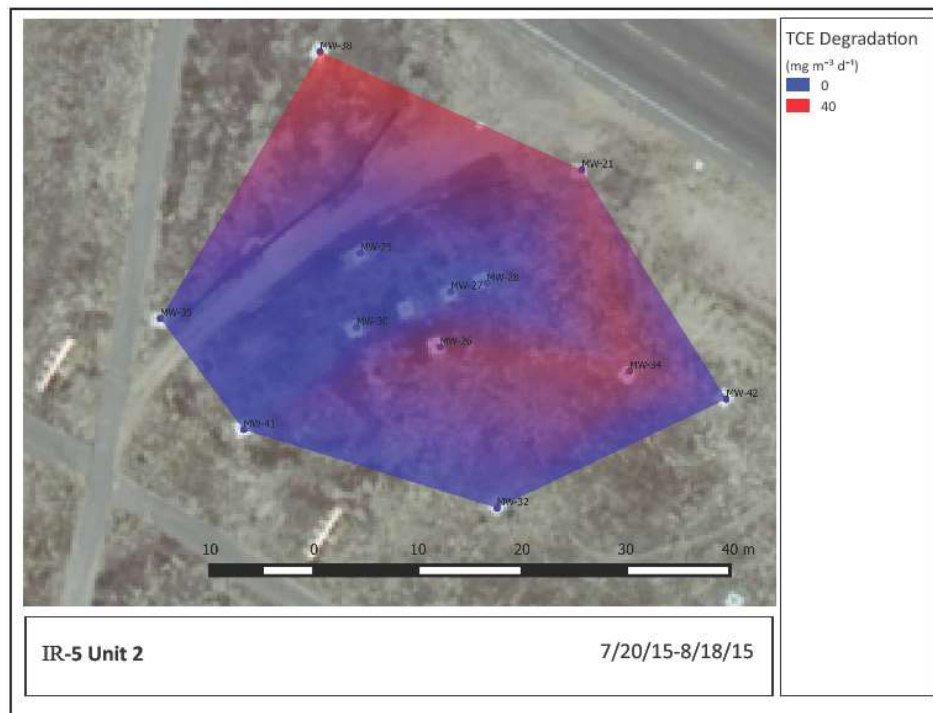


Figure 29. TCE degradation 07/20/15-08/18/15

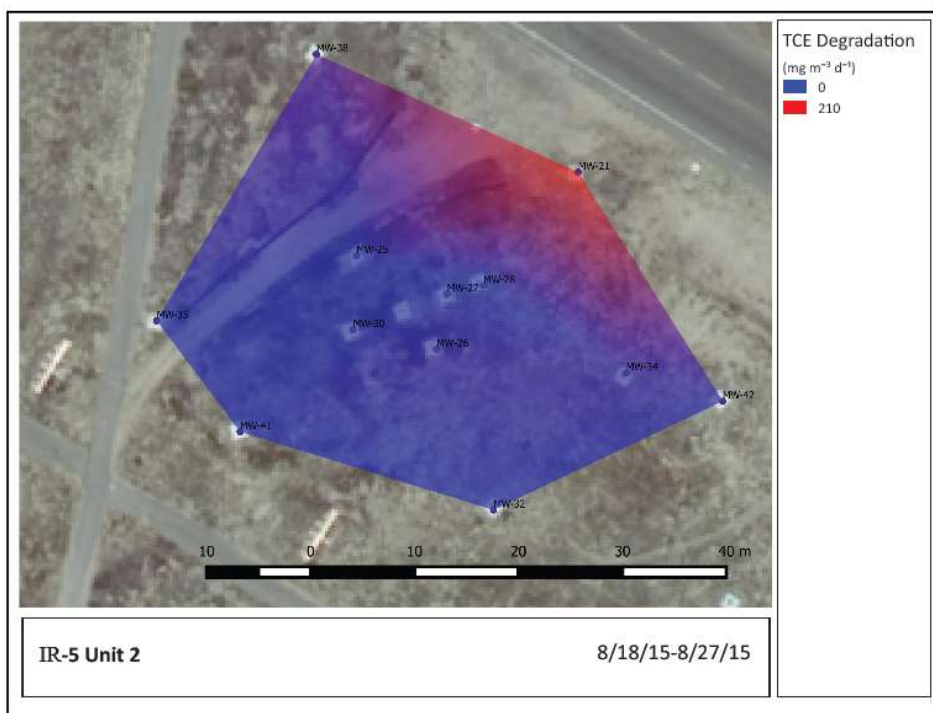


Figure 30. TCE degradation 08/18/15-08/27/15

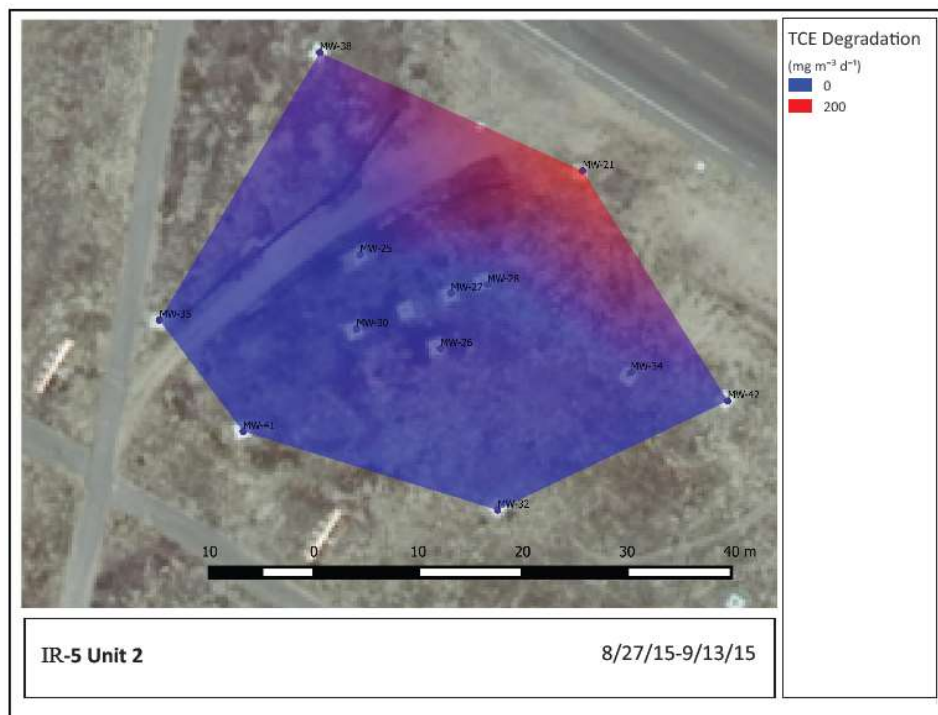


Figure 31. TCE degradation 08/27/15-09/13/15

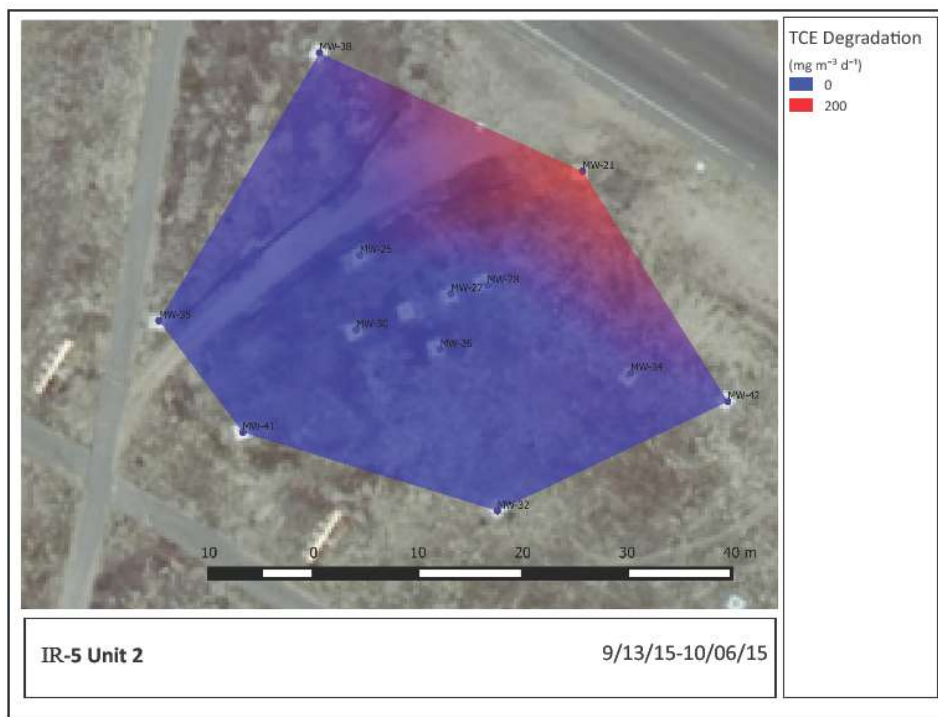


Figure 32. TCE degradation 09/13/15-10/06/15

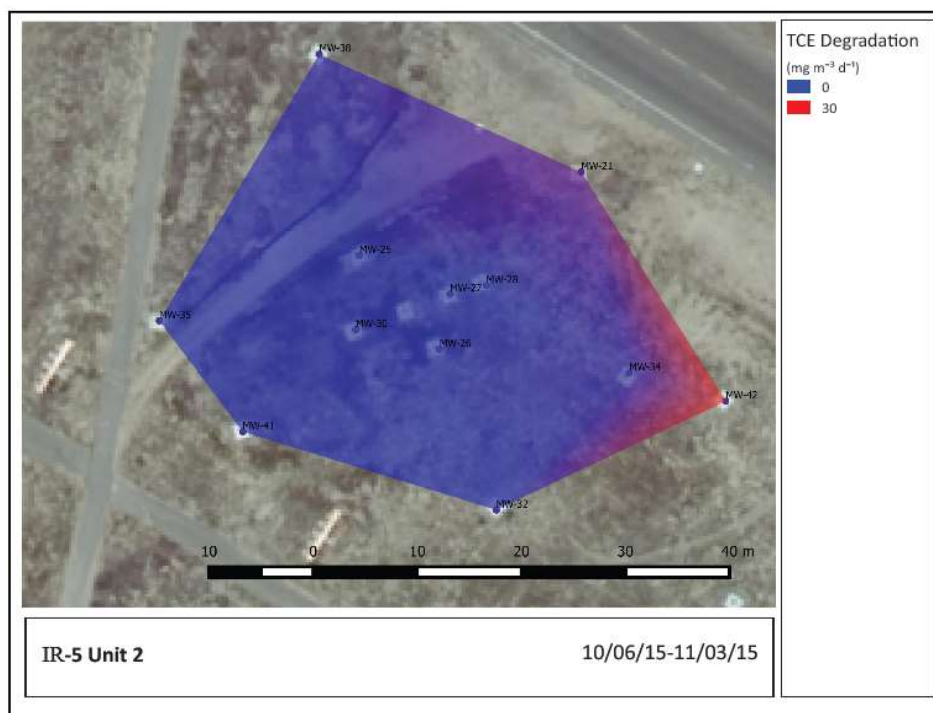


Figure 33. TCE degradation 10/06/15-11/03/15

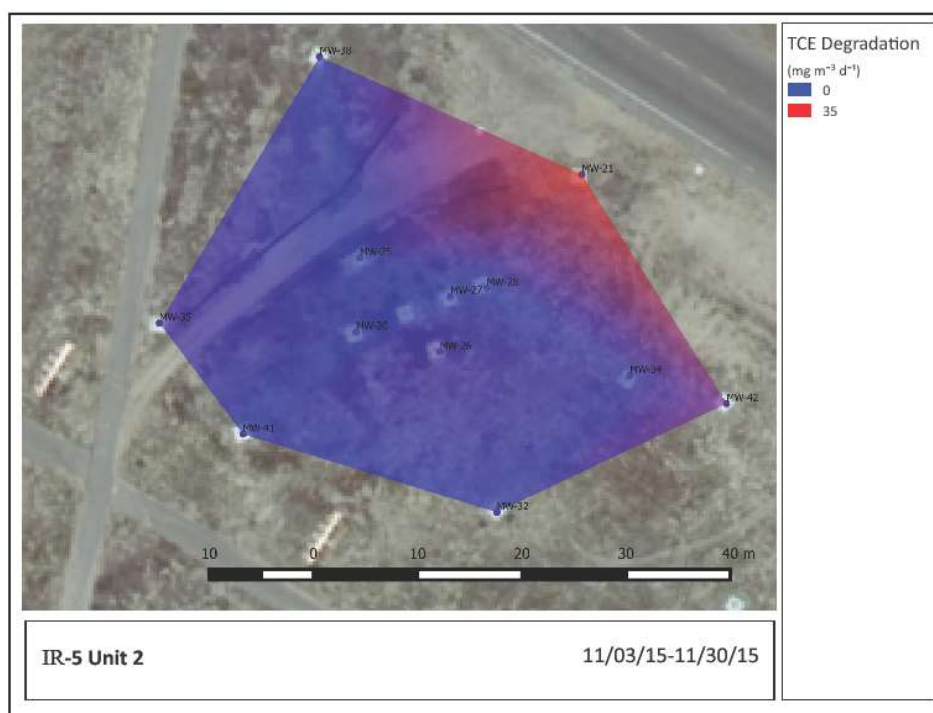


Figure 34. TCE degradation 11/03/15-11/30/15

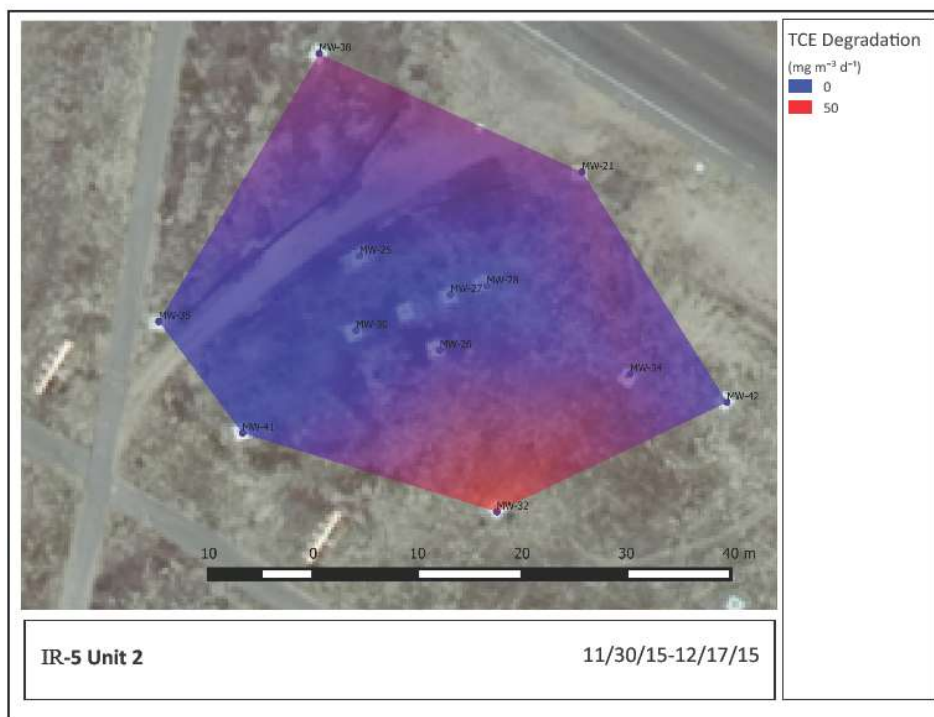


Figure 35. TCE degradation 11/30/15-12/17/15

Site-Wide TCE degradation and long-term remediation. Interpolated data for IR-5 U2 was processed by summing the degradation rate over the site so that total TCE degraded over the entire plume volume was estimated for each collection period. The total area varied based on successful sample collection. Instances where clogging or leaks occurred, respective wells were

Table 3. TCE degradation over IR-5 U2 by time bin

Date in (Date)	Date out (Date)	Total area (m ²)	Maximum TCE degradation (mg TCE C m ⁻³ d ⁻³)	Site TCE degradation (g TCE C d ⁻¹)
11/6/2014	11/24/2014	717	403	103
11/24/2014	12/5/2014	1240	283	45.7
12/5/2014	12/18/2014	1240	64.3	17.4
12/18/2014	1/5/2015	1429	183	112
1/9/2015	1/26/2015	1072	102	33.6
2/2/2015	2/16/2015	1072	265	69.8
2/15/2015	3/9/2015	1072	62.0	22.3
4/10/2015	4/30/2015	1213	45.2	18.8
4/30/2015	5/20/2015	1072	57.0	23.3
5/20/2015	6/1/2015	1217	148	34.2
6/1/2015	6/15/2015	751	41.3	18.7
6/15/2015	6/28/2015	1217	30.4	8.14
6/28/2015	7/20/2015	1217	29.6	7.63
7/21/2015	8/18/2015	865	211	44.8
8/18/2015	8/27/2015	1011	18.9	10.1
8/28/2015	9/13/2015	1429	103	23.5
9/13/2015	10/6/2015	943	95.6	19.2
10/6/2015	11/3/2015	1217	97.2	12.8
11/4/2015	11/30/2015	1429	14.0	4.27
11/30/2015	12/17/2015	1099	16.4	5.94

not included in the interpolation. Site-wide TCE degradation ranged from ~5 to 112 g per day over the year (Table 3). Due to the shallow groundwater and relatively high conductivity (sandy soils), rainfall – which is sporadic in San Diego – may have an impact on degradation kinetics, possibly replenishing limiting nutrients or other metabolic resources. Previous work attempting to validate natural attenuation highlighted the change in dissolved TCE associated with rainfall (31). Although not tightly correlated, dissolved TCE concentrations spiked within weeks of significant rainfall.

Total site-wide TCE degradation was plotted alongside rainfall (taken from CIMIS San Diego station (Station ID 184)) in order to assess the impact (Fig. 36). Although a tight correlation was elusive (we attempted 1-3-week delay in the degradation data for correlation tests), it appears degradation spikes after significant rainfall (over 1.2”) probably indicating short but strong rain events are more disruptive to static on-site conditions than shorter, less severe events (c.f. Nov15-Jan16; Fig. 36).

Finally, the site-wide TCE degradation was summed for the entire year sampling period. As only a few days were “un-sampled” during the year, we summed the TCE degraded for each time-slice time the days within each respective time-slice. These data were then summed to determine the cumulative degradation for the year. This estimates the entire site year-wide TCE degradation as 11.1 kg. In some ways, the estimate may be conservative because the lowest measurement is assumed to be due to equilibrium kinetics alone, the ZOI simulations assume site conditions are homogeneous, and only a portion of the entire site was sampled during the year-long event. Additionally, significant CH₄ concentrations (not reported here for brevity and lack of a ZOI model

specific to CH₄ to allow estimating groundwater concentration(s)) were observed in well headspace gas indicating CO₂ collection alone may underestimate total contaminant conversion. However, the estimate could be seen as too high given any metabolite in the degradation pathway could be assigned to TCE degradation. For instance, vinyl chloride degradation will produce CO₂ that is radiocarbon depleted. Its degradation will be “counted” as TCE degradation. cVOC concentrations have been estimated for modeling based on soil and groundwater

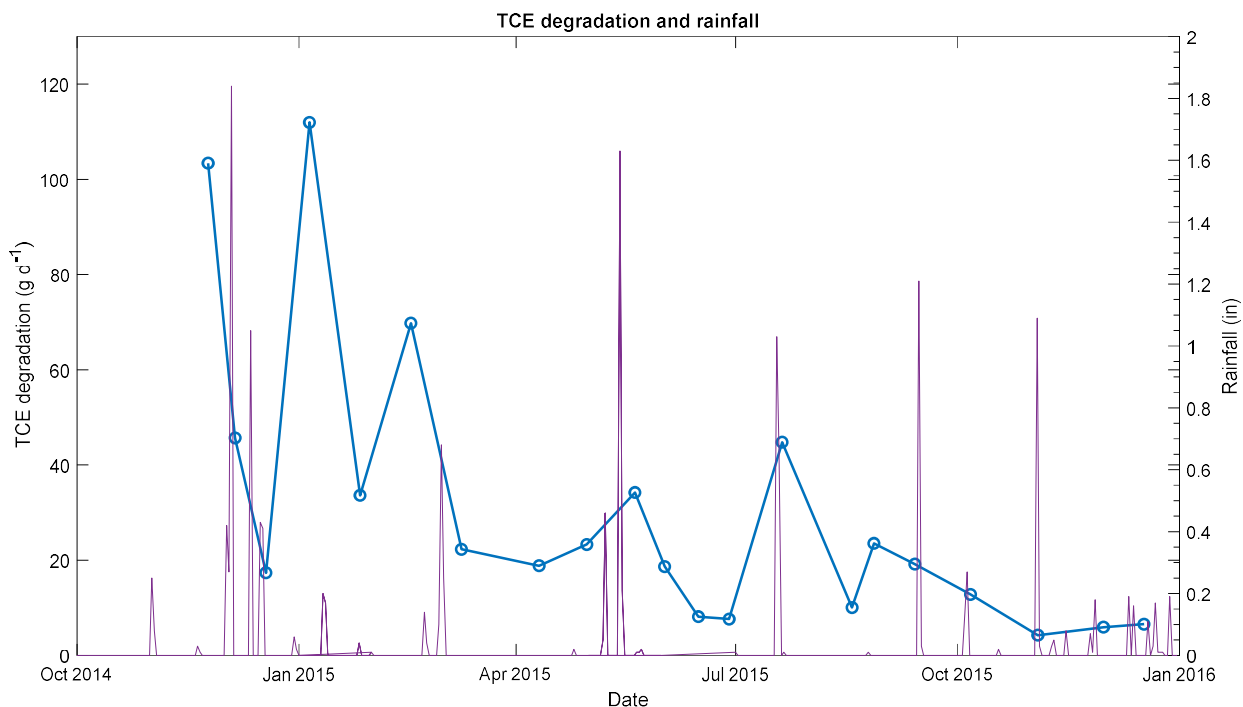


Figure 36. Total site-wide TCE degradation and rainfall over the entire sampling period

concentrations (31). Mass was estimated at ~1,000 kg in 2008. Because our data are not time-averaged (similar to a first order decay rate), the estimate for ~100 years to remediate is longer than the 40 years predicted by first order attenuation models (31).

OU-19/20 NASNI. A limited number of traps were deployed starting in August 2015 in order to obtain some pre-EVO injection data. The full suite sampling (OU-19 and OU-20) began in November 2015. Trap cycling was expanded to ~30-62 days for the OU-19/20 deployments due to logistical and travel constraints. Trap material was analyzed for CO₂ concentration and combined radiocarbon. Selected samples obtained and analyzed for cations by Noreas, Inc were used to assess possible CaCO₃ interference. Well casing CH₄ concentrations were also analyzed. Results are summarized by analysis.

ZOI simulations. Groundwater hydraulic and CO₂ solute properties for the study site were obtained from Noreas, Inc (Table 4). ZOI models were developed exactly as with IR-5 U2 using the CO₂ flux rates from OU-19/20 – which were lower based on passive traps vs the active trapping at IR-5 U2. ZOI values are reported for each well and sample period in Appendix A. ZOI estimates ranged from 0.0030 to 0.0040 m⁻³. These were two orders of magnitude less than ZOI estimates for IR-5 U2. The mechanics for generating the ZOI models for each well and time-point are discussed in detail under the IR-5 U2

Table 4. Hydrogeologic parameters used for OU-19/20 ZOI models

Parameter	Units	Value
Hydrology		
Hydraulic Conductivity	(m hr ⁻¹)	0.07
Porosity (aquifer)		0.40
Bulk Density	(g cm ⁻³)	1.59
Specific Yield	(cm ³ cm ⁻³)	0.10
Hydraulic Gradient	(m m ⁻¹)	0.0295
CO₂ Solute Transport		
Diffusion Coefficient (CO ₂)	(m ² hr ⁻¹)	6.77 X 10 ⁻⁶
Longitudinal Dispersivity	(m)	15
Horizontal Transverse Dispersivity	(m)	3
Vertical Transverse Dispersivity	(m)	0.3

Table 5. Selected cation and pH measurements for OU-19/20

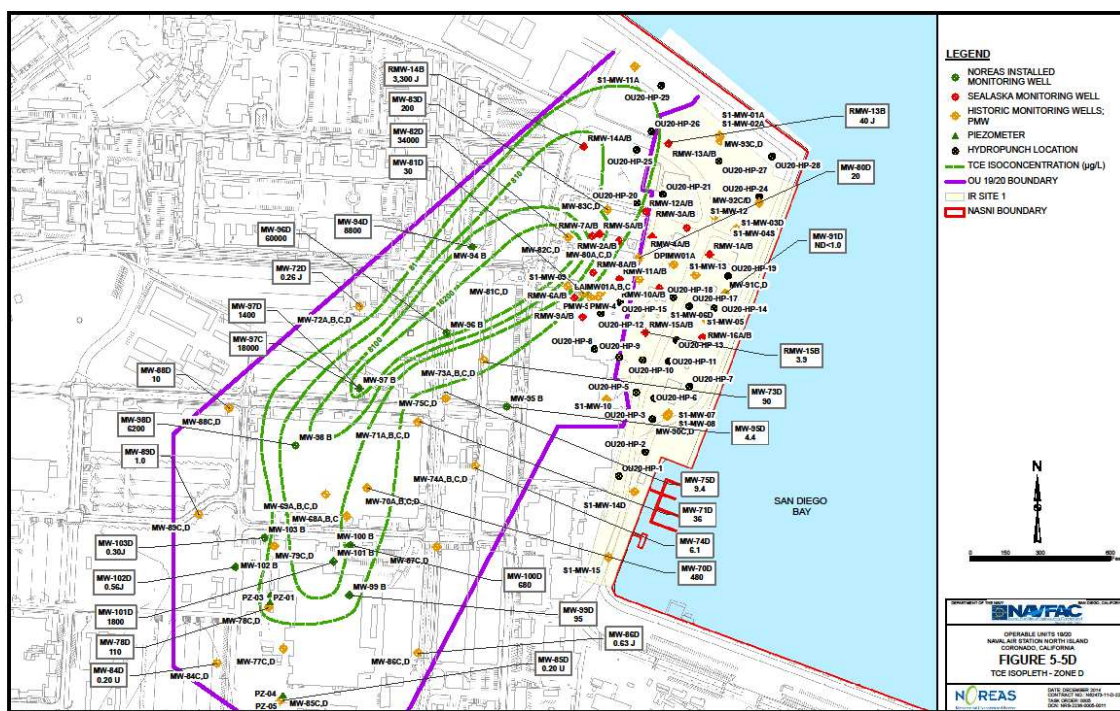
Well	Na ⁺ (mg L ⁻¹)	Ca ²⁺ (mg L ⁻¹)	pH
MW81C	871	62.2	7.16
MW82C	455	17.7	7.74
PEW-4	577	54.3	7.86
RMW-5A	165	27.3	7.97
RMW-5B	114	53	7.75
RMW-7A	218	22.2	8.82
RMW-7B	3100	411	8.56
RMW-8A	217	9.19	7.71
RMW-8B	2540	246	7.69
RMW-9A	2440	137	7.98
RMW-9B	719	71.5	7.6

results section. The same methods and general sequences were followed for ZOI models at OU-19/20. Because ZOI model outputs were so vastly different than those for IR-5 U2 (and IR-17, IR-57 at Indian Head), there is concern that some unusual values in conductivity and other parameters are biasing the simulations. Discussions with Noreas, Inc. lead us to believe that severe channeling and diking at portions of OU-20 led to values which may be nonrepresentative to OU-19/20 (for our analysis). At present, an average ZOI estimate from IR-5 U2 has been used (0.173 m⁻³) in order to place our data in context. We are continuing to evaluate the ZOI models and they will be re-simulated with additional site hydrogeologic parameters (being collected) before any final publication.

Water quality measurements. Samples for cation and pH were analyzed in 2015 as part of on-going investigations by Noreas, Inc. A small sampling from the Noreas data repository spanning the OU-19/20 area was used to assess cations and pH. Near the quay wall along San Diego Bay, Na⁺ and

Ca⁺⁺ levels were elevated (tidal recharge) but pH variability was relatively narrow (7.6 to 8.82) and never low enough to be responsible for CaCO₃ dissociation (Table 5). It seems highly unlikely that any small amounts of on-site CaCO₃ could influence respiration radiocarbon measurements.

Respiration. Respiration was measured during each time period as the amount of CO₂ collected per unit time per unit volume (using ZOI simulations). The lowest CO₂ collection rate (2.47 μmol CO₂ d⁻¹) during the year-long collection period was assigned as equilibrium flux only and used to adjust all other values by subtraction. The adjusted flux ranged from 0 to 3.56 mg CO₂ hr⁻¹ (85.5 mg CO₂ d⁻¹) across the site and across all time-slices. While the respiration measurements were on the same order of magnitude as those seen at IR-5 U2, the very small ZOI simulations made



as background within the two end-member mixing model (eq. 1) for each well and time-bin. Radiocarbon values ranged from 4.71 pmc to modern (100 pmc) (-953 to 0 ‰). The most ^{14}C -depleted CO_2 was found in the OU-19 sub-region, above a steam pipe (MW04, MW-08, MW-11). TCE degradation ranged from 0 to 63 $\text{mg TCE C m}^{-3} \text{ d}^{-1}$ at OU-19 and 0 to 31 $\text{mg TCE C m}^{-3} \text{ d}^{-1}$ at OU-20. Overall, OU-19 had a higher cVOC degradation average ($36 \pm 2.3 \text{ S.E.}$) than OU-20 ($1.7 \pm 0.59 \text{ S.E.}$). TCE mineralization (carbon basis) is shown for each time bin (and by sub-site, *e.g.* OU-19 and OU-20) in Figures 38-54.

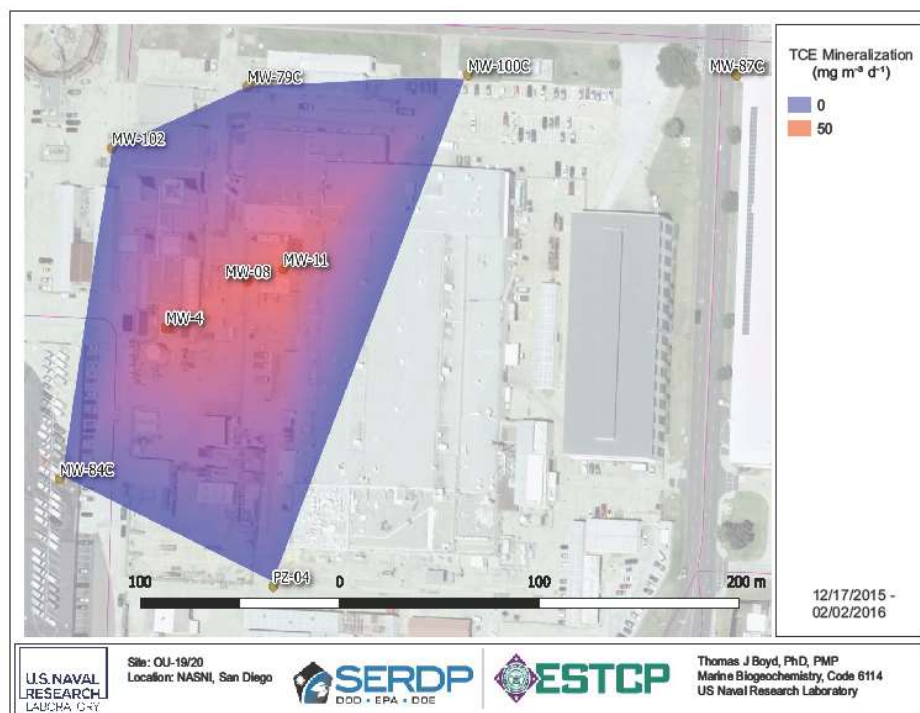


Figure 38. OU-19 TCE degradation 12/17/15-02/02/16

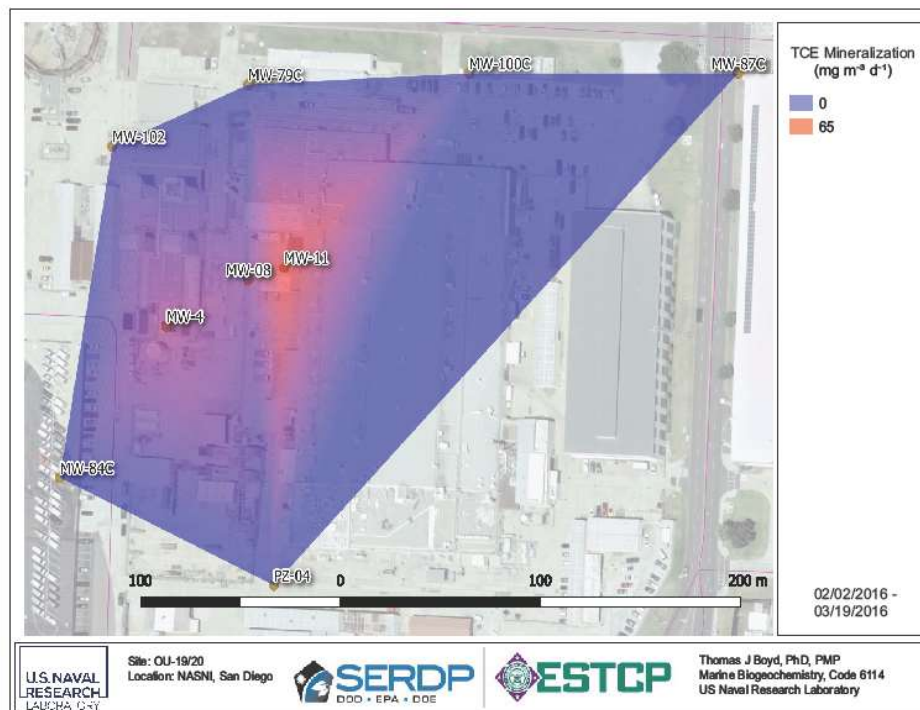


Figure 39. OU-19 TCE degradation 02/02/16-03/19/16

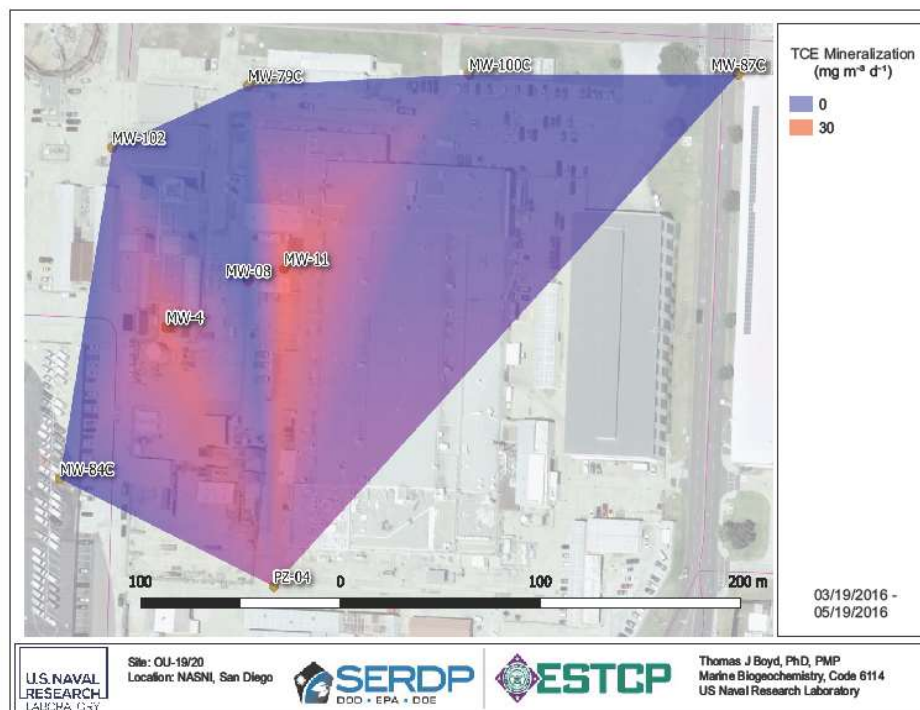


Figure 40. OU-19 TCE degradation 03/19/16-05/19/16

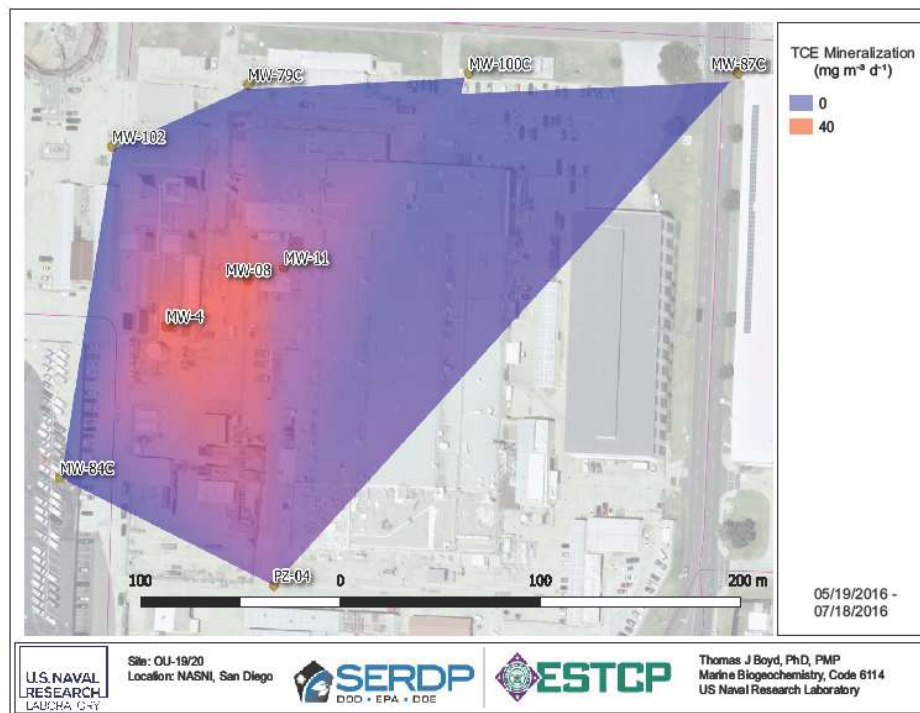


Figure 41. OU-19 TCE degradation 05/19/16-07/18/16

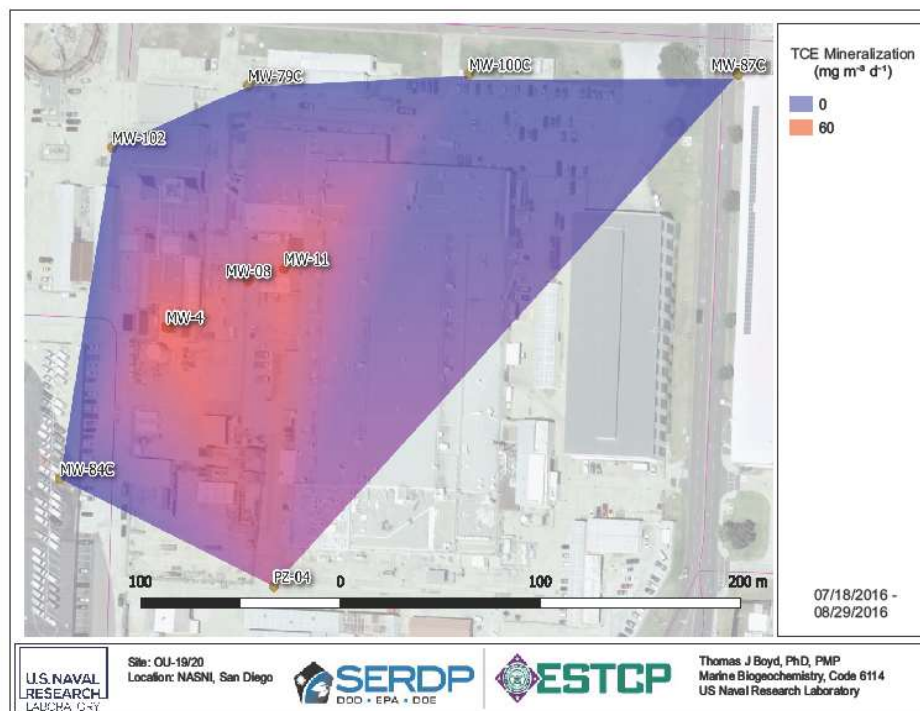


Figure 42. OU-19 TCE degradation 07/18/16-08/29/16

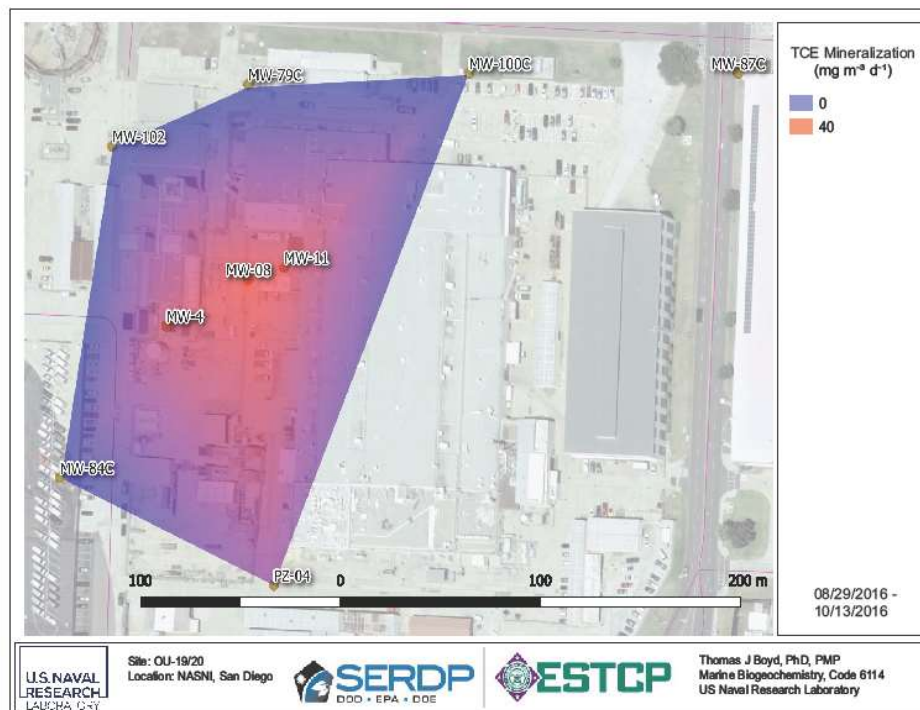


Figure 43. OU-19 TCE degradation 08/29/16-10/13/16

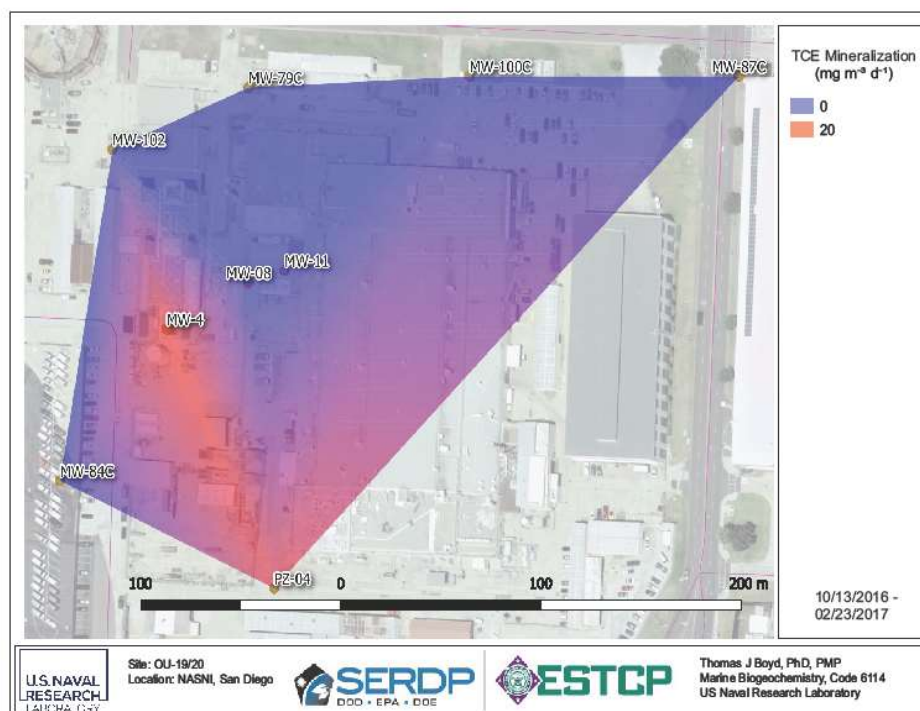


Figure 44. OU-19 TCE degradation 10/13/16-02/23/17

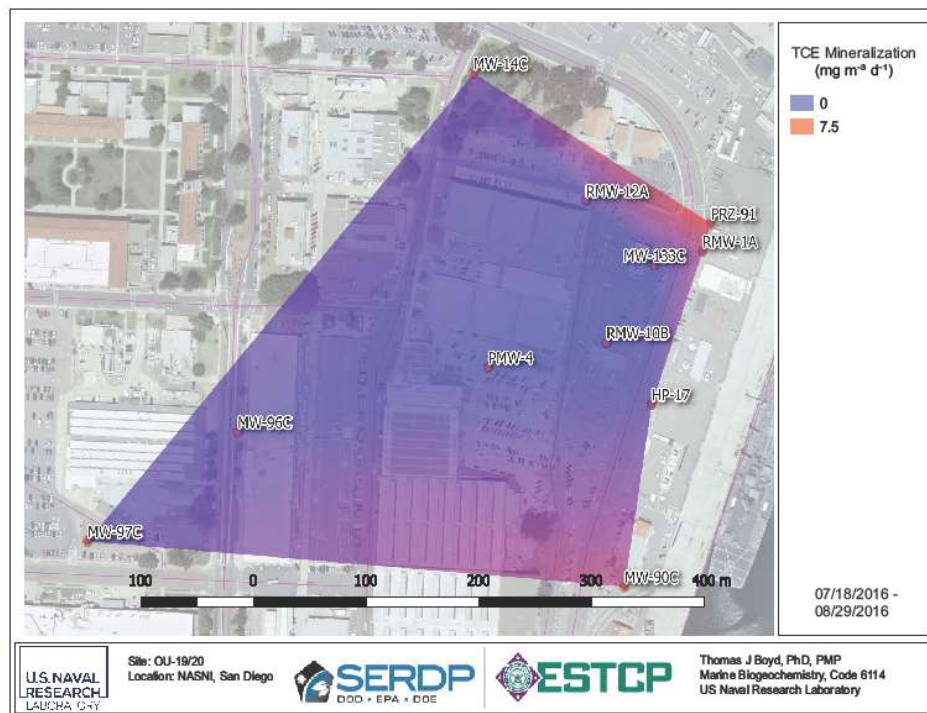


Figure 45. OU-20 TCE degradation 07/21/15-08/29/15

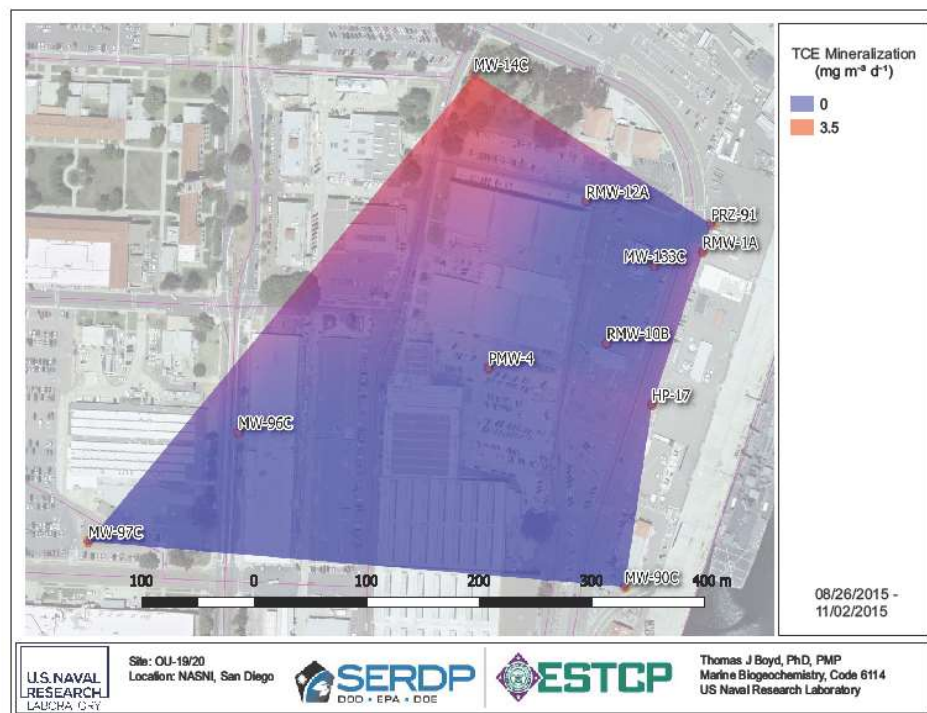


Figure 46. OU-20 TCE degradation 08/29/15-11/02/15

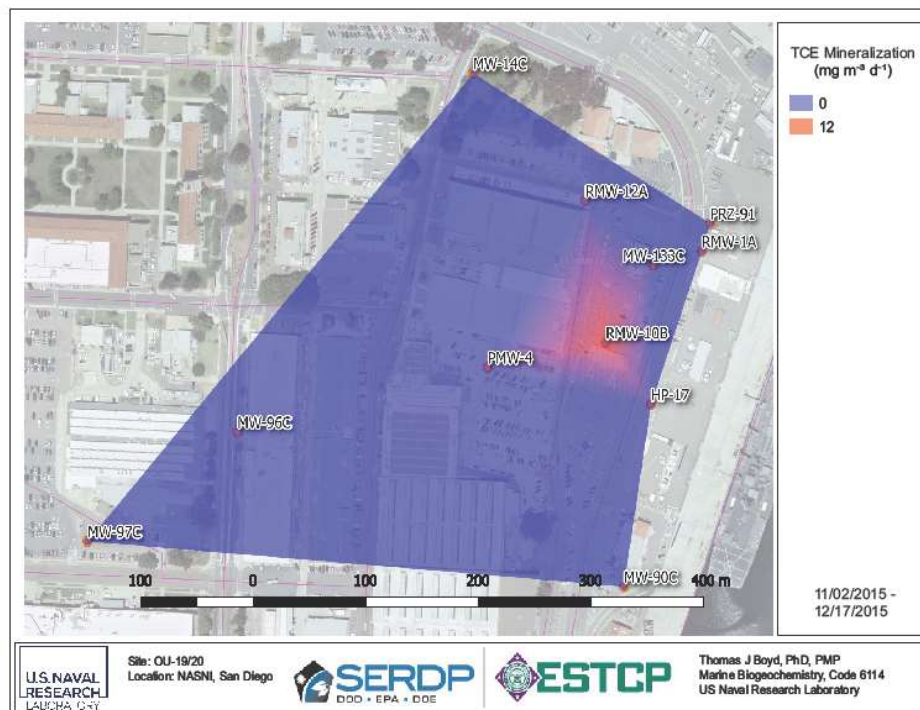


Figure 47. OU-20 TCE degradation 11/02/15-12/17/15

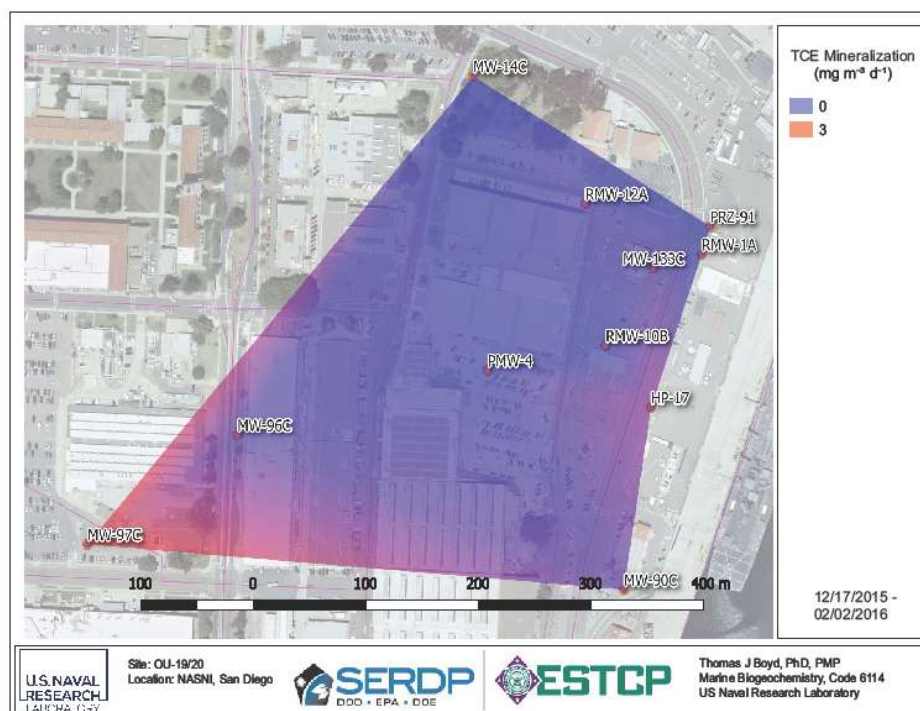


Figure 48. OU-20 TCE degradation 12/17/15-02/02/16



Figure 49. OU-20 TCE degradation 02/02/16-03/18/16

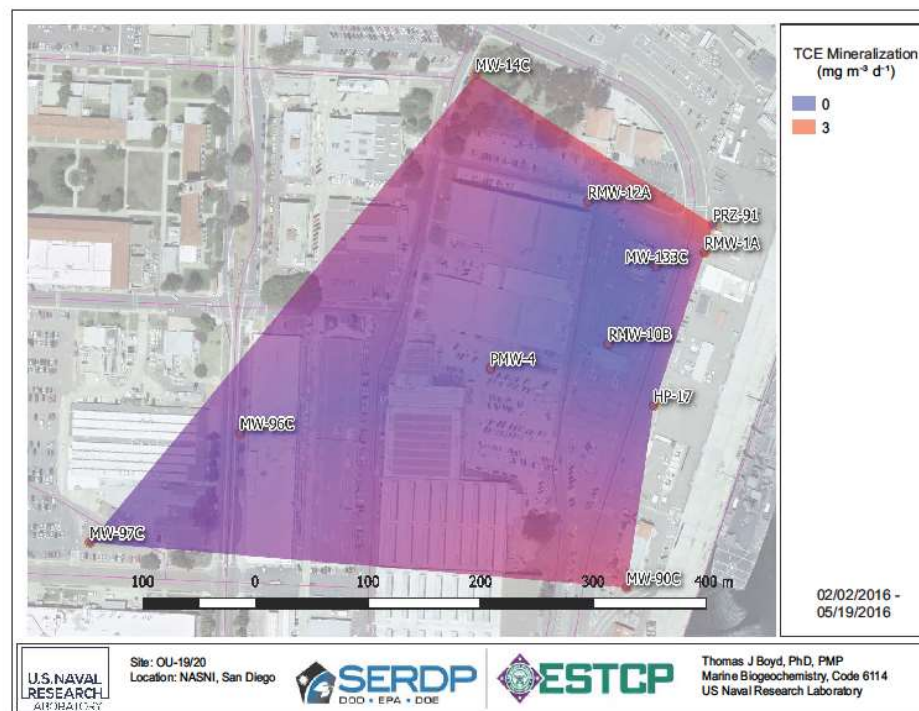


Figure 50. OU-20 TCE degradation 03/19/16-05/19/16

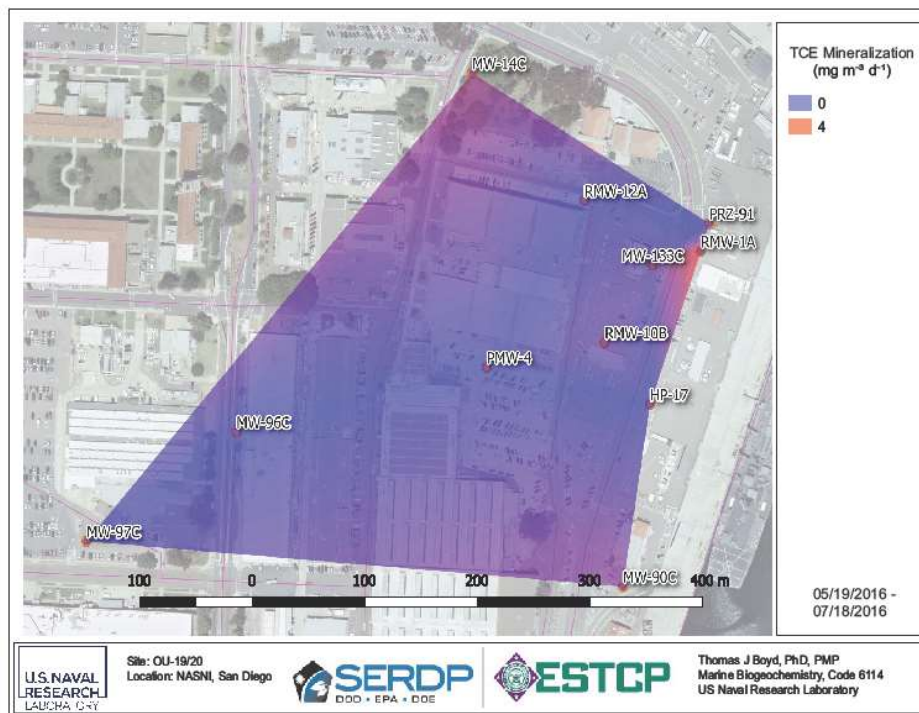


Figure 51. OU-20 TCE degradation 05/19/16-07/18/16

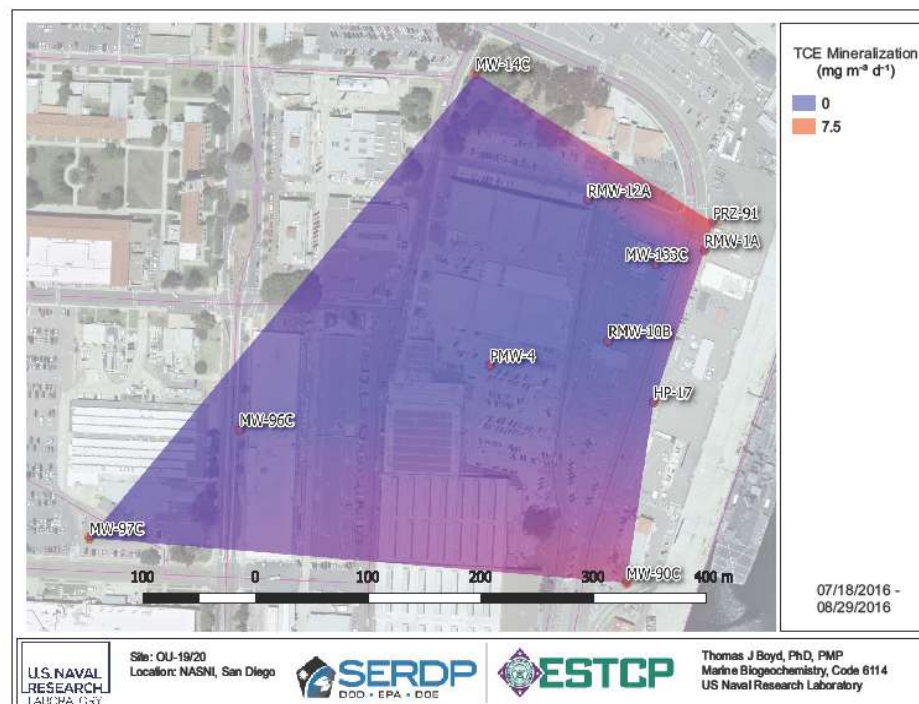


Figure 52. OU-20 TCE degradation 07/18/16-08/29/16

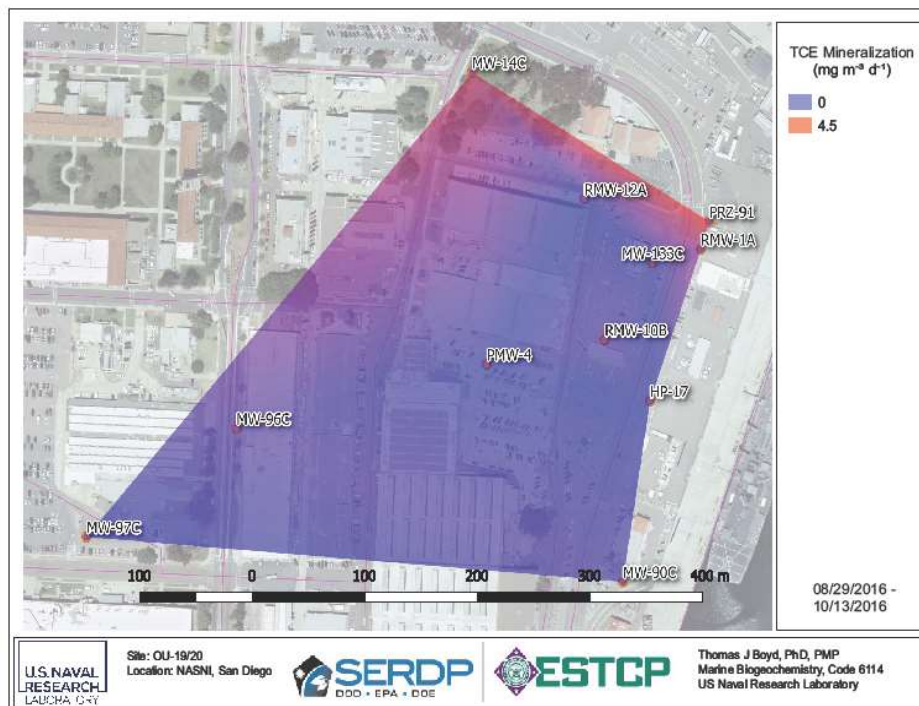


Figure 53. OU-20 TCE degradation 08/29/16-10/13/16

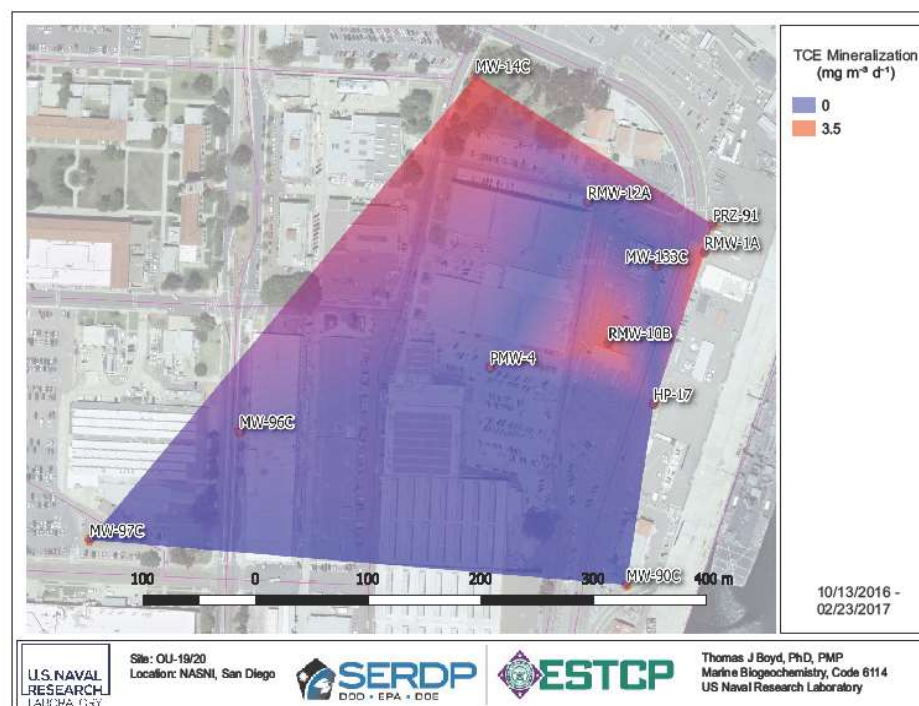


Figure 54. OU-20 TCE degradation 10/13/16-02/23/17

Site-Wide TCE degradation and long-term remediation. Interpolated data for both OU-19 and OU-20 were processed as with IR-5 U2 by summing degradation rate over the site. Because the “middle ground” area between OU-19 and the quay are at OU-20 was generally inactive relative

Table 6. TCE degradation over OU-19 by time bin

Date in (Date)	Date out (Date)	Total area (m ²)	Average TCE degradation (mg TCE C m ⁻³ d ⁻³)	Site TCE degradation (kg TCE C d ⁻¹)
12/2/2015	2/2/2016	3657	44.8	1.64
2/2/2016	3/19/2016	22997	13.9	3.19
3/19/2016	5/19/2016	34981	18.2	6.35
5/19/2016	7/18/2016	54111	8.2	4.42
7/18/2016	8/29/2016	38288	29.2	11.19
8/29/2016	10/13/2016	21996	18.2	4.00
10/13/2016	2/23/2017	38288	9.8	3.74

to the upper (OU-19) plume and OU-20 plume, those subregions were processed separately. The total area varied based on successful sample collection (some samples were compromised – mostly by rain events that brought the water table to the trap level). Compromised wells were not included in the interpolation and are

identified by color on the master sheets (Appendix A). At OU-19, site-wide TCE degradation ranged from 1.64 to 11.2 kg per day over the year’s sampling (Table 6). The average TCE degradation was in-line with IR-5 U2 (Table 3), but due to the larger area sampled, cumulative TCE degradation was higher.

Daily rainfall during the sampling period was obtained from the NOAA National Centers for Environmental Information (<https://www.ncdc.noaa.gov/>).

At OU-19/20, depth to groundwater was generally great than at IR-5 U2 (10-30 ft). Additionally, most of OU-19/20 is covered in asphalt with many wells in building areas, parking lots and adjacent to quay walls. As with IR-5 U2, it was difficult to correlate TCE degradation with rainfall, but it seems plausible that after a relatively

Table 7. TCE degradation over OU-20 by time bin

Date in (Date)	Date out (Date)	Total area (m ²)	Average TCE degradation (mg TCE C m ⁻³ d ⁻³)	Site TCE degradation (g TCE C d ⁻¹)
7/21/2015	8/26/2015	20434	0.50	0.10
8/26/2015	11/2/2015	115990	0.80	0.93
11/2/2015	12/17/2015	94516	0.51	0.49
12/17/2015	2/2/2016	73663	0.97	0.72
2/2/2016	3/19/2016	81972	3.89	3.19
3/19/2016	5/19/2016	98471	1.48	1.45
5/19/2016	7/18/2016	98825	1.25	1.24
7/18/2016	8/29/2016	98471	2.33	2.29
8/29/2016	10/13/2016	98471	1.48	1.46
10/13/2016	2/23/2017	98471	1.22	1.21

long period of sustained and occasionally heavy rainfall (January through early February 2016), there was a spike in cVOC degradation rates at both sites (into May). Another spike in rates occurred in August however, with no heavy antecedent rainfall (Fig. 55).

The OU-19 region displayed higher average TCE degradation than the OU-20 region. Most of the higher CO₂ flux with most ¹⁴C-depleted signature was found in the area around wells MW-04, MW-08 and MW-11. In this sub-region, a steam pipe underlays the paved surface. During sampling events, there was visible steam seeping up through cracks in the pavement. It is likely

that increased temperature(s) in the groundwater and vadose zone leads to increased respiration in this area. One unresolved issue is the vastly different ZOI simulations for OU-19/20. We will be

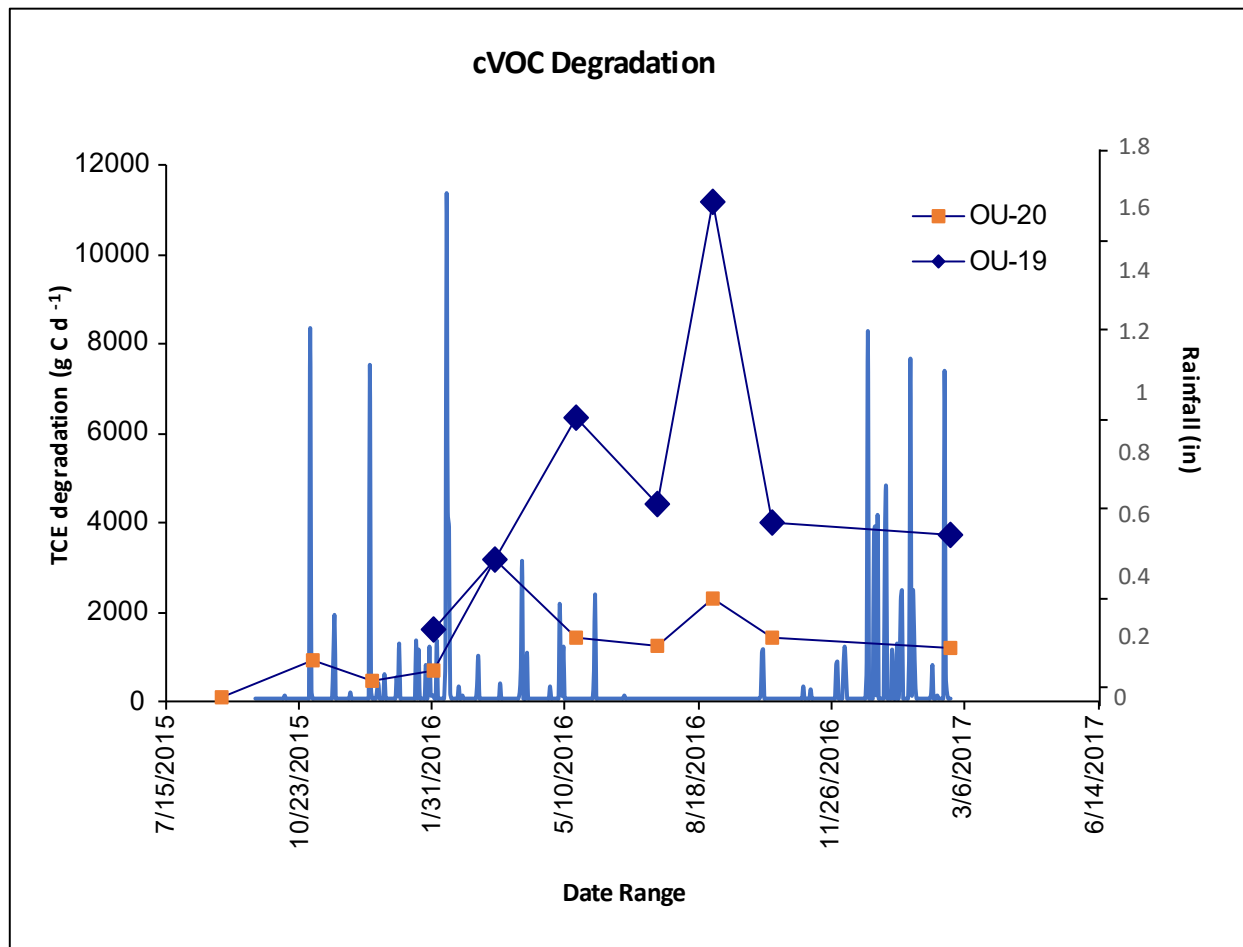


Figure 55. cVOC degradation and rainfall at OU-19/20

updating the simulations based on field data collected in 2019-2020 which may bring the models closer in-line to IR-5 U2 simulations. We believe that buried aquitards (old pier system) and channeling (un-annotated stormwater pipes) may have led to nonrepresentative hydrogeologic data from slug and other tests on site.

IR-17 Indian Head. Traps were deployed starting in February 2017 at IR-17. Ten total wells were

Table 8. IR-17 analyses by sample time bins

Date in (Date)	Date out (Date)	CH ₄ sampling and analysis	Dissolved CO ₂ quantified	ZOI simulation completed
02/14/17	03/17/17		✓	✓
04/20/17	05/19/17		✓	✓
05/19/17	07/14/2017	✓	✓	✓
07/14/2017	10/03/17	✓		
10/03/17	11/16/2017	✓	✓	✓
11/16/2017	01/08/2018	✓	✓	✓
01/25/2018	02/20/2018	✓	✓	✓
02/20/2018	03/29/2018	✓	✓	✓
03/29/2018	05/21/2018		✓	
05/21/2018	07/10/2018	✓	✓	
07/10/2018	09/26/2018	✓	✓	
09/26/2018	11/05/2018		✓	

outfitted with passive traps. These wells covered the North and South Plume areas as well as a background location (MW-18) (Fig. 6). Wells fitted with traps were: MW-01, MW-06, MW-07, MW-08, MW-11, MW-12, MW-13, MW-14, MW-16, MW-17, and MW-18. After given collection times, traps were recovered, trap material dissolved and CO₂ quantified (Table 8). Sub-samples were reserved for radiocarbon analysis.

Additionally, continuously-monitoring pressure transducers were deployed in selected wells (MW-01, MW-14, and MW-17) to assist in ZOI modeling. Before selected trap collections and redeployments, well headspace CH₄ was sampled using 60 mL syringes.

ZOI simulations. ZOI simulations were made from hydrogeologic data obtained from the remedial project manager. Hydrogeologic data for four wells (MW-12, MW-13, MW-16, MW-18) and results from pressure transducer deployments over one year were used to develop the simulations (Table 9). ZOIs ranged from 0.0077 m⁻³ to 0.112 m⁻³ with the largest values found in the

Table 9. Hydrogeologic parameters used for IR-17 ZOI models

Parameter	Units	Value
Hydrology		
Hydraulic Conductivity	(m hr ⁻¹)	0.10
Porosity (aquifer)		0.51
Bulk Density	(g cm ⁻³)	2.09
Specific Yield	(cm ³ cm ⁻³)	0.18
Hydraulic Gradient	(m m ⁻¹)	0.0295
CO ₂ Solute Transport		
Diffusion Coefficient (CO ₂)	(m ² hr ⁻¹)	6.77 X 10 ⁻⁶
Longitudinal Dispersivity	(m)	15
Horizontal Transverse Dispersivity	(m)	3
Vertical Transverse Dispersivity	(m)	0.3

North Plume region (Fig. 6). The largest ZOIs tended to be at wells closest to Mattawoman Creek (MW-13, MW-14, MW-01, MW-07, MW-08). These wells have the highest tidal influence and thus are likely to be more channelized with greater hydraulic conductivity (even though average values were used for simulations). All ZOI simulations are reported in Appendix A.

Water quality measurements. As with OU-19/20, previous long-term monitoring data were used to assess possible limestone interference with $^{14}\text{CO}_2$ measurements. At present, the data on-hand do not include pH measurements (sample log sheets should be available by the time any data from IR-17 are published). Long-term monitoring records from 2010-2016 were screened for calcium (as precipitated CaCO_3) and various low molecular weight organic acids (as a proxy for pH). We analyzed > 75 individual measurements of acetic, lactic, propanoic, pyruvic and butyric acid with precipitated CaCO_3 over the course of 6 years monitoring with no significant correlation observed (Fig. 56).

Respiration. Respiration was measured as the amount of CO_2 collected during each time point – minus the lowest value collected during the entire field deployment (assuming the lowest value is equilibrium capture only). CO_2 respiration values were converted volumetric estimates by dividing the amount collected per hour by the ZOI estimate for each well and time period (Appendix A). Respiration ranged from $\sim 70 \mu\text{g CO}_2 \text{ m}^{-3} \text{ h}^{-1}$ to $12 \text{ mg CO}_2 \text{ m}^{-3} \text{ h}^{-1}$ with highest values generally coincident with lower elevation wells - perhaps more influenced by tidal recharge (MW-01, MW-08, MW-12, and MW-14).

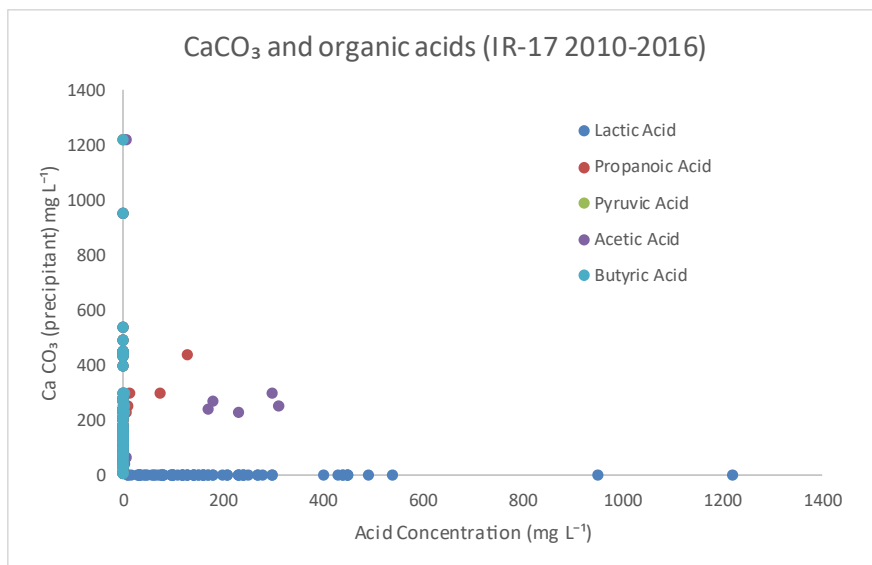


Figure 56. CaCO_3 and organic acid concentrations, IR-17

IR-57 Indian Head. At the RPM's request, traps were also deployed starting in February 2017 at IR-57. Twelve total wells were outfitted with passive traps. One well (MW-48) was consistently flooded and after several failed attempts, was abandoned for the study. The wells covered the entire plume area (Fig. 7) and a potential background well (Site X, MW-29). The background well is upgradient of the TCE plume but may historically have shown contamination. Wells in the TCE source area include MW-38, and MW-11. Downgradient wells include MW-09 and MW-10 (with TCE concentrations routinely $\sim 100 \mu\text{g L}^{-1}$), MW-05, MW-06, MW-28 and MW-29 (with a mix of TCE and daughter products), MW-31 and MW-22 – which usually have only VC above regulatory limits. MW-22 is closest to Mattawoman Creek (Fig. 7).

In April 2018, an EVO injection event commenced at IR-57. Traps were removed from the site after the 29 March 2018 collection. Traps were re-installed in late May 2018 (5/21/18) to capture impacts from EVO injection(s). Results from November 2018 samplings by Terra Systems, Inc. indicated reductions in TCE concentrations with concomitant rise(s) in ethene and ethane at wells

Table 10. IR-57 analyses by sample time bins

Date in (Date)	Date out (Date)	CH ₄ sampling and analysis	Dissolved CO ₂ quantified	ZOI simulation completed
02/14/17	03/17/17		✓	✓
04/20/17	05/19/17		✓	✓
05/19/17	07/14/2017	✓	✓	✓
07/14/2017	10/03/17	✓	✓	
10/03/17	11/16/2017	✓	✓	✓
11/16/2017	01/08/2018	✓	✓	✓
01/25/2018	02/20/2018	✓	✓	✓
02/20/2018	03/29/2018	✓	✓	✓
03/29/2018	05/21/2018*			
05/21/2018	07/10/2018	✓	✓	
07/10/2018	09/26/2018	✓	✓	
09/26/2018	11/05/2018	✓	✓	
11/20/2018	07/25/2019		✓	

*EVO injection(s)

around the injection location(s) (see source area in Fig. 7). Ethene and ethane are readily oxidized by microorganisms under non-reducing conditions so long-term CO₂ collections after the event (samples were collected through 07/25/2018) should demonstrate ¹⁴C-depleted signatures. Samples have been taken and reserved for this purpose.

The overall completed sampling and analyses are presented in Table 10.

ZOI simulations. ZOI

simulations were created for IR-57 wells using CO₂ collection rate information and hydrogeologic parameters obtained from site records and Meadows CMPG, Inc. (*personal communications*). Parameters were identified for 10 separate wells spanning the site relief (upland to water edge). Most variable were porosity, bulk density and hydraulic gradient. Mean parameters are presented in Table 11. ZOIs ranged from 0.0001 to 0.379 m⁻³ over IR-57 with mid-gradient wells usually showing the largest collection volume (MW-09, MW-10, MW-28, MW-29). Larger collection volumes seemed to also be coincident with colder months (Appendix A).

Water quality measurements.

Water quality measurements from IR-57 long-term monitoring activities were provided by Meadows CMPG, Inc. (*personal communication*) spanning 2004 to the present. As with IR-17, selected data were pulled from the archive to assess limestone dissociation impact on values obtained from eventual radiocarbon analyses. Along with pH,

Table 11. Mean hydrogeologic parameters used for IR-57 ZOI models

Parameter	Units	Value
Hydrology		
Hydraulic Conductivity	(m hr ⁻¹)	0.03
Porosity (aquifer)		0.38
Bulk Density	(g cm ⁻³)	1.64
Specific Yield	(cm ³ cm ⁻³)	0.22
Hydraulic Gradient	(m m ⁻¹)	0.020
CO ₂ Solute Transport		
Diffusion Coefficient (CO ₂)	(m ² hr ⁻¹)	6.77 X 10 ⁻⁶
Longitudinal Dispersivity	(m)	15
Horizontal Transverse Dispersivity	(m)	3
Vertical Transverse Dispersivity	(m)	0.3

organic acids were correlated with CaCO₃ (precipitated) from groundwater samples over 2004-2016 (where all measurements co-occurred). We found no significant correlation between pH or

organic acids and CaCO_3 over the 12-year dataset indicating CaCO_3 dissolution under site

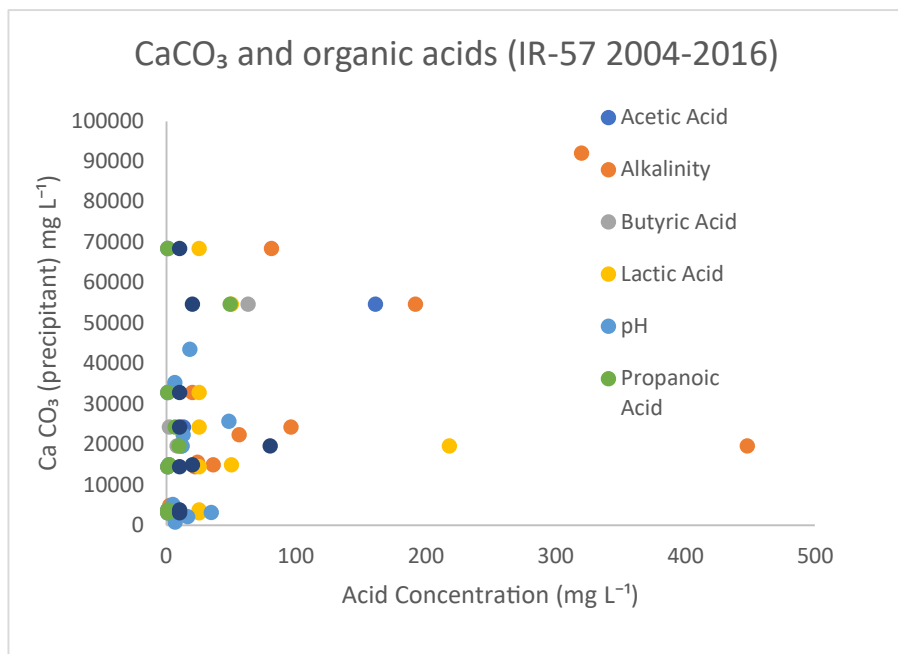


Figure 57. CaCO_3 relation to pH, alkalinity and organic acids, IR-57

conditions should have no impact on $^{14}\text{CO}_2$ fluxes assumed to arise from respiration (Fig. 57).

Respiration. As with IR-17, respiration was calculated from CO_2 collected during each time point – less the lowest value from the entire field deployment (assumes the lowest value is equilibrium capture only). CO_2 respiration values are included for each well and time-point are

contained in Appendix A. Respiration ranged from $\sim 50 \mu\text{g CO}_2 \text{ m}^{-3} \text{ h}^{-1}$ to $4.8 \text{ kg CO}_2 \text{ m}^{-3} \text{ h}^{-1}$ (MW-22, October 17) with all other values below $1 \text{ kg CO}_2 \text{ m}^{-3} \text{ h}^{-1}$. The anomalously high respiration value was the result of high CO_2 collection and very small (0.0012 m^{-3}) ZOI model for MW-22. While inconsistent, the upgradient background well (Site X, MW-29), mid-gradient (MW-05, MW-06, MW-28, MW-29, MW-31 and MW-22) usually had the highest respiration values. Source are wells (MW-11 and MW-46) were generally the lowest in respiration (Appendix A).

Radiocarbon – IR-17 and IR-57. When asked to sample these sites at Indian Head by the RPM, the workload and costs seemed manageable by reviving a CO_2 distillation line which we used at NRL while the Lab's AMS was still up and running (for carbon dating measurements). Recent instrument upgrade(s) at The National Ocean Sciences Accelerator Mass Spectrometry (NOSAMS) facility (Woods Hole) allow direct source inlet for CO_2 gas with dramatically reduced cost per sample (\$60 vs \$400). The precision is worse than traditional graphite target-based AMS, but for ER2338 purposes where we are differentiating highly radiocarbon-depleted end members (e.g. the petroleum-sourced contaminant carbon) from modern organic matter carbon, this newer option offers both higher resolution results and significant cost-savings. To this end, parts of the old distillation and graphitization line were removed from storage and set up to make cryogenically-distilled CO_2 targets. This process was begun in 2018 and cobbling together the system took almost into 2019 to field a “working” system. Rough and turbomolecular pumps had been stored for > 5 years and needed servicing and refurbishment. In early 2019, CO_2 targets were created and sent to NOSAMS for testing. Unfortunately, the targets did not contain sufficient nor adequately purified CO_2 .

After system tests, it was determined that the main vacuum gauge (2007 manufacture) was well out of calibration and vacuum estimates for CO₂ purification had not been met. After replacement and leak checking, it was finally determined that two welds from the initial line had cracked and caused leaking. In addition, valves were found to have small leaks. Rather than continue to try piecemeal fixes, a new line (simplified) with new valves was commissioned and



Figure 58. New distillation line (early 2019)

assembled by a local pressure and vacuum specialist company. The new system was brought online in 2019 (Fig. 58) but was found to not hold adequate vacuum. A field engineer from Swagelok was summoned to service all the valves (all were brand new). Still, the vacuum issues persisted (to the writing of this report). A wide-ranging vacuum gauge was purchased in 2019 to consolidate measurements (replacing both a rough and high vacuum gauge). Very recently, this gauge was found to contain an internal leak and is being replaced by the manufacturer.

Obviously, these issues have led to considerable frustration and delay in obtaining radiocarbon numbers for IR-17 and IR-57 which we hoped would be possible as two added sites above the three-site original plan. We have worked out a means of having the samples analyzed for radiocarbon by gas-source inlet and will have well over 100 high-resolution temporal and spatial measurements for Indian Head. It is not difficult to make ~10 CO₂ targets a day by cryogenic distillation, so once the vacuum issues are finally resolved, radiocarbon measurements should be possible

within about 6 months. We have manuscript outlines for IR-17 and IR-57 and at this point are mostly awaiting the radiocarbon data so that conclusions can be drawn.

Conclusions and Implications for Future Research / Implementation

In this project, we combined time-averaged and spatial respiration and radiocarbon measurements to determine site cVOC degradation (TCE carbon equivalents) at IR-5 U2 (Naval Air Station North Island), OU-19 (NASNI), OU-20 (NASNI) and partially completed the analysis at two sites (IR-17 and IR-57) at Indian Head Naval Surface Warfare Center (MD). These measurements were combined with a zone of influence (ZOI) model to estimate the volume sampled at each well. Plume characteristics (volume) and volumetric TCE degradation values were used to determine the annual cVOC degradation occurring over the sites studied. cVOC respiration measurements are likely conservative because we assumed the lowest rate was due to equilibrium CO₂ capture only which is unlikely unless there were timepoints when no actual respiration occurred. ZOIs were calculated using site-specific hydrological data and represent a refined estimate of the sampled area compared to a single groundwater sample (representing the well only at the time of sampling). The ultimate goal was to determine the contaminant to CO₂ conversion rate per unit area (m⁻³) per unit time (d⁻¹). With this successful effort, we completed the following:

- Assessed sites for potential complicating factors (limestone deposits)
- Measured well head-space methane which could be a contaminant repository not evaluated as such (but planned in eventual publications)
- Measured respiration rate(s) as CO₂ collected over 1-3 month time periods at 5 sites
- Measured radiocarbon content for CO₂ respired at three sites
- Created ZOI models for each well and time-point sampled to determine volume sampled
- Determined respiration from contaminants by calculating the fraction CO₂ derived from petroleum sources
- Determined well-specific cVOC degradation based on volumetric ZOI models and contaminant respiration
- Determined site-wide cVOC degradation using interpolation between sampled wells
- Used estimated plume dimensions to calculate site-wide degradation over relevant time-scales
- Presented results to regulators (IR-5 U2) for validation.
- Published results from IR-5 U2 in peer-reviewed literature
- Published methods and validation in peer-reviewed literature
- Performed a small comparative study (outlined in ESTCP ER19-5106) using different methods for time-averaged CO₂ radiocarbon collection and calculation for cross validation.

At IR-5 U2, the lowest apparent cVOC utilization was coincident with regions of highest historical contamination. There was no direct correlation ($r^2 < 0.50$) between contaminant concentrations and cVOC utilization. CO₂ collected above the high historical contamination region had the most modern carbon indicating less relative contribution from cVOC than natural organic matter.

At OU-19/20, cVOC degradation rates were highest at the OU-19 sub-region associated with steam pipes under the pavement. At the OU-20 sub-region, cVOC degradation rates were highest at the plume fringes (as with IR-5 U2). An EVO injection event did not appear to stimulate cVOC degradation based on this method. However, this event would stimulate releasing massive quantities of modern CO₂ (from vegetable oil biodegradation). It is unclear if that could mask the signal from cVOC CO₂ (¹⁴C-depleted).

Future goals will be to transition the technology with different means for measuring CO₂ flux:

- In-well passive CO₂ traps
- Soil:atmosphere CO₂ flux traps
- Short-term groundwater incubations to determine respiration rates

These techniques performed at the same site at the same time(s) and coupled with radiocarbon analysis would allow cross-validation and give RPMs an arsenal of techniques to answer the fundamental question whether on-site processes stimulate the conversion of cVOCs to harmless degradation end products in a time-frame that suits site management strategies.

Literature Cited

1. N. R. Council, *In situ bioremediation: When does it work?* C. o. i. s. bioremediation, Ed., (National Academy of Sciences, Washington, DC, 1993), pp. 1-207.
2. K. M. Vangelas, "Summary Document of Workshops for Hanford, Oak Ridge and Savannah River Site as part of the Monitored Natural Attenuation and Enhanced Passive Remediation for Chlorinated Solvents - DOE Alternative Project for Technology Acceleration," (U.S. Department of Energy, Westinghouse Savannah River Company, Aiken, SC, 2003).
3. T. H. Wiedemeier *et al.*, "Technical Protocol for Evaluating Natural Attenuation of Chlorinated Solvents in Ground Water," (USEPA Office of Research and Development, Washington, DC, 1998).
4. J. Šimůnek, D. L. Suarez, M. Sejna, "The UNSATCHEM Software Package for Simulating One-Dimensional Variably Saturated Water Flow, Heat Transport, Carbon Dioxide Production and Transport, and Solute Transport with Major Ion Equilibrium and Kinetic Chemistry, Version 2.0," (USDA-ARS U.S. Salinity Laboratory, Riverside, CA, 1996).
5. A. Leeson, H. F. Stroo, "SERDP and ESTCP workshop on investment strategies to optimize research and demonstration impacts in support of DoD restoration goals," (SERDP/ESTCP, Arlington, VA, 2011).
6. SERDP/ESTCP, "SERDP/ESTCP Expert Panel Workshop on Research and Development Needs for Cleanup of Chlorinated Solvent Sites," (2002).
7. J. V. Weiss, I. M. Cozzarelli, Biodegradation in contaminated aquifers: Incorporating microbial/molecular methods. *Ground water* **46**, 305-322 (2008).
8. W. A. Illman, P. J. Alvarez, Performance assessment of bioremediation and natural attenuation. *Critical Reviews in Environmental Science and Technology* **39**, 209-270 (2009).
9. P. Bombach, H. H. Richnow, M. Kästner, A. Fischer, Current approaches for the assessment of in situ biodegradation. *Applied Microbiology and Biotechnology* **86**, 839-852 (2010).
10. H. B. Kerfoot, C. L. Mayer, P. B. Durgin, J. J. D'Lugosz, Measurement of Carbon Dioxide in Soil Gases for Indication of Subsurface Hydrocarbon Contamination. *Ground Water Monitoring & Remediation* **8**, 67-71 (1988).
11. K. H. Suchomel, D. K. Creamer, A. Long, Production and transport of carbon-dioxide in a contaminated vadose zone - a stable and radioactive carbon isotope study. *Environmental Science and Technology* **24**, 1824-1831 (1990).
12. C. M. Aelion, C. M. Swindoll, F. K. Pfaender, Adaptation to and Biodegradation of Xenobiotic Compounds by Microbial Communities from a Pristine Aquifer. *Applied and Environmental Microbiology* **53**, 2212-2217 (1987).
13. B. C. Kirtland, C. M. Aelion, P. A. Stone, D. Hunkeler, Isotopic and Geochemical Assessment of in Situ Biodegradation of Chlorinated Hydrocarbons. *Environmental Science and Technology* **37**, 4205-4212 (2003).
14. B. C. Kirtland, C. M. Aelion, P. A. Stone, Assessing *in situ* mineralization of recalcitrant organic compounds in vadose zone sediments using $\delta^{13}\text{C}$ and $\Delta^{14}\text{C}$ measurements. *Journal of Contaminant Hydrology* **76**, 1-18 (2005).
15. R. B. Coffin *et al.*, Radiocarbon and Stable Carbon Isotope Analysis to Confirm Petroleum Natural Attenuation in the Vadose Zone. *Environmental Forensics* **9**, 75-84 (2008).

16. T. J. Boyd, M. T. Montgomery, R. H. Cuenca, Y. Hagimoto, Measuring Carbon-based Contaminant Mineralization Using Combined CO₂ Flux and Radiocarbon Analyses. *Journal of Visualized Experiments*, e53233 (2016).
17. T. J. Boyd, M. T. Montgomery, R. H. Cuenca, Y. Hagimoto, Combined radiocarbon and CO₂ flux measurements used to determine *in situ* chlorinated solvent mineralization rate. *Environmental Science: Processes & Impacts* **17**, 683 - 692 (2015).
18. T. J. Boyd, M. J. Pound, R. H. Cuenca, Y. Hagimoto, M. T. Montgomery, "Radiocarbon Allows Direct Determination of Fuel and Industrial Chemical Degradation at ER Sites," *ER News* (US Naval Facilities, Port Hueneme, CA, 2014).
19. T. J. Boyd, M. J. Pound, D. Lohr, R. B. Coffin, Radiocarbon-depleted CO₂ evidence for fuel biodegradation at the Naval Air Station North Island (USA) fuel farm site. *Environmental Science: Processes & Impacts* **15**, 912-918 (2013).
20. G. C. Bugna, J. P. Chanton, T. B. Stauffer, W. G. Macintyre, E. L. Libelo, Partitioning microbial respiration between jet fuel and native organic matter in an organic-rich long time-contaminated aquifer. *Chemosphere* **60**, 177-187 (2005).
21. T. J. Boyd, J. Gryzenia, D. Ramquist, G. M. Wyatt, "Short-term respiration measurements coupled with CO₂ radiocarbon analysis provide fuel degradation rates at an underground fuel storage tank leak site," (US Naval Research Laboratory, Washington, DC, 2018).
22. K. McCoy, J. A. Zimbron, T. Sale, M. Lyverse, Measurement of Natural Losses of LNAPL Using CO₂ Traps. *Groundwater* **53**, 658-667 (2015).
23. N. J. Sihota, K. Ulrich Mayer, Characterizing vadose zone hydrocarbon biodegradation using carbon dioxide effluxes, isotopes, and reactive transport modeling. *Vadose Zone Journal* **11**, (2012).
24. E. Warren, N. J. Sihota, F. D. Hostettler, B. A. Bekins, Comparison of surficial CO₂ efflux to other measures of subsurface crude oil degradation. *Journal of Contaminant Hydrology* **164**, 275-284 (2014).
25. S. M. Carroll, A. D. Peacock, J. Zimbron, K. N. Alepidis, J. A. Clock, Demonstrating Contaminant Degradation at an MGP Site With Metabolic Gas Flux and Radio Carbon Dating. *Remediation Journal* **27**, 51-64 (2017).
26. C. M. Aelion, B. C. Kirtland, P. A. Stone, Radiocarbon assessment of aerobic petroleum bioremediation in the vadose zone and groundwater at an AS/SVE site. *Environmental Science and Technology* **31**, 3363-3370 (1997).
27. U. EPA, "BIOCHLOR Natural attenuation decision support system, User's Manual," (US EPA, Washington, DC, 2000).
28. R. U. Meckenstock, C. Griebler, B. Morasch, H. H. Richnow, Stable isotope fractionation analysis as a tool to monitor biodegradation in contaminated aquifers. *Journal of Contaminant Hydrology* **75**, 215-255 (2004).
29. C. Vogt, C. Dorer, F. Musat, H.-H. Richnow, Multi-element isotope fractionation concepts to characterize the biodegradation of hydrocarbons — from enzymes to the environment. *Current Opinion in Biotechnology* **41**, 90-98 (2016).
30. API, "Quantification of Vapor Phase-related Natural Source Zone Depletion Processes," (American Petroleum Institute (API), 2017).
31. S. I. Inc., "Draft Feasibility Study, Installation Restoration Site 5, Unit 2, Naval Air Station North Island, San Diego, California," (Shaw Infrastructure, Inc, Concord, CA, 2013).
32. V. Hosangadi, "Draft Appendix B Site Conceptual Model Technical Memorandum Operable Units 19/20," (Noreas, Inc, San Diego, CA, 2013).
33. M. Stuiver, H. A. Polach, Discussion: Reporting of ¹⁴C Data. *Radiocarbon* **19**, 355-363 (1977).

34. K. M. Johnson, J. M. Sieburth, P. J. I. B. Williams, L. Brändström, Coulometric total carbon dioxide analysis for marine studies: Automation and Calibration. *Mar.Chem.* **21**, 117-133 (1987).
35. A. G. Dickson, Standards for ocean measurements. *Oceanography* **23**, 34-47 (2010).
36. C. Zheng, P. P. Wang, "MT3DMS: A modular three-dimensional multispecies transport model for simulation of advection, dispersion, and chemical reactions of contaminants in groundwater systems; documentation and user's guide," (DTIC Document, 1999).
37. A. W. Harbaugh, *MODFLOW-2005, the US Geological Survey modular ground-water model: The ground-water flow process*. (US Department of the Interior, US Geological Survey, 2005).
38. H. Prommer, D. A. Barry, C. Zheng, MODFLOW/MT3DMS-based reactive multicomponent transport modeling. *Ground Water* **41**, 247-257 (2003).
39. R. B. Winston, in *Ground Water - Book 6*. (U.S. Geological Survey, Reston, VA, 2009), vol. Techniques and Methods 6-A29, chap. 29.
40. Accord Engineering Inc., "Semi-Annual Post-Closure Maintenance Report for Calendar Year 2011 Installation Restoration (IR) Program Site 2 (Old Spanish Bight Landfill), Site 4 (Public Works Salvage Yard), and Site 5, Unit 1 (Golf Course Landfill)," (San Diego, CA, 2011).
41. Geosyntec Consultants, "Annual Progress Report October 2010 to December 2011, Operable Unit 24," (Columbia, MD, 2012).

Appendix A. Supporting Data

Compiled data files for IR-5 U2, OU-19/20, IR-17, and IR-57



IR-5 U2 compiled
data.xlsx



IR-5 U2
interpolation.xlsx



OU-19-20 compiled
data.xlsx

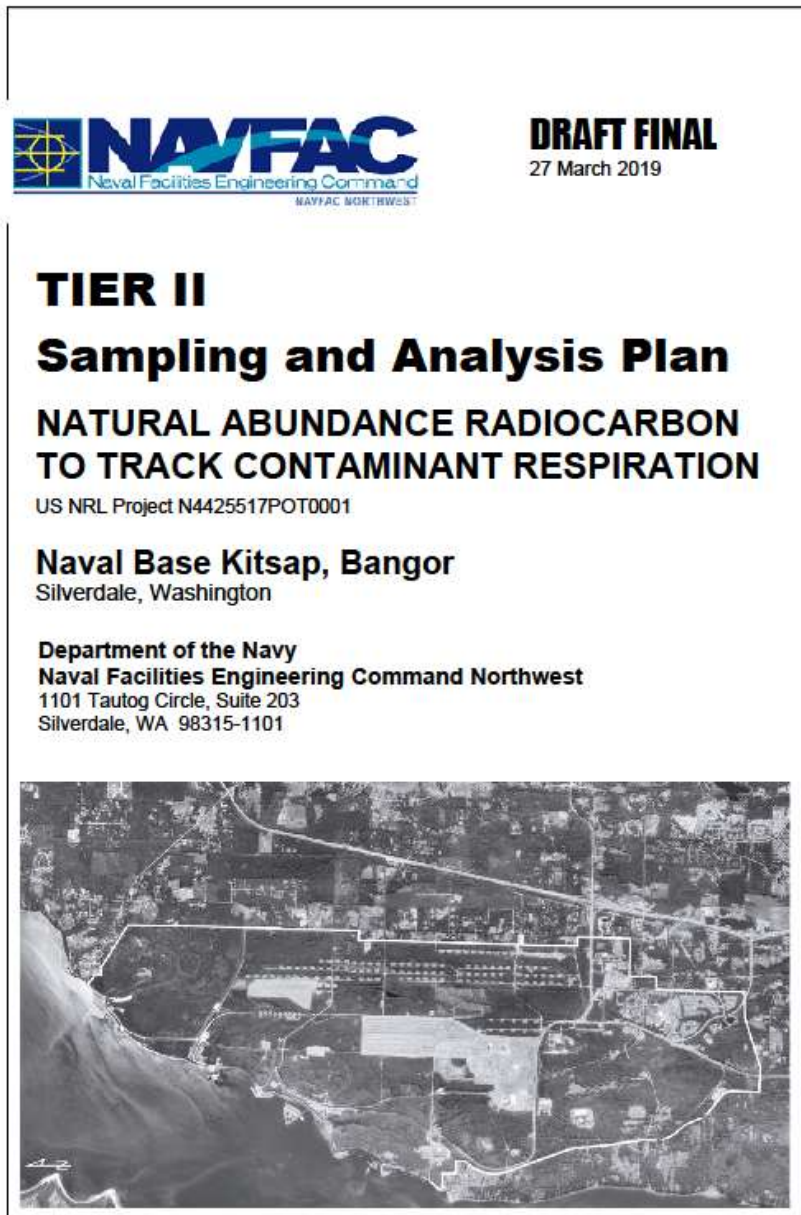


OU-19-20
interpolation.xlsx



IR-17 - IR-57
compiled data.xlsx

Clickable link to a Tier II SAP template amenable to new sites (with regulatory approval)



Appendix B. List of Scientific / Technical Publications

Boyd, T. J., M. J. Pound, D. Lohr and R. B. Coffin (2013). "Radiocarbon-depleted CO₂ evidence for fuel biodegradation at the Naval Air Station North Island (USA) fuel farm site." Environmental Science: Processes & Impacts **15**(5): 912-918.

Boyd, T. J., M. T. Montgomery, R. H. Cuenca and Y. Hagimoto (2014). CO₂ Radiocarbon Analysis to Quantify Organic Contaminant Degradation, MNA, and Engineered Remediation Approaches, United States Naval Research Laboratory: 59.

Boyd, T. J., M. J. Pound, R. H. Cuenca, Y. Hagimoto and M. T. Montgomery (2014). Radiocarbon Allows Direct Determination of Fuel and Industrial Chemical Degradation at ER Sites. ER News. A. W. Ortiz. Port Hueneme, CA, US Naval Facilities. **14**: 13-14.

Boyd, T. J., M. T. Montgomery, R. H. Cuenca and Y. Hagimoto (2015). "Combined radiocarbon and CO₂ flux measurements used to determine *in situ* chlorinated solvent mineralization rate." Environmental Science: Processes & Impacts **17**(3): 683 - 692.

Boyd, T. J., M. T. Montgomery, R. H. Cuenca and Y. Hagimoto (2016). "Measuring Carbon-based Contaminant Mineralization Using Combined CO₂ Flux and Radiocarbon Analyses." Journal of Visualized Experiments(116): e53233.

Boyd, T. J., J. Gryzenia, D. Ramquist and G. M. Wyatt (2018). Short-term respiration measurements coupled with CO₂ radiocarbon analysis provide fuel degradation rates at an underground fuel storage tank leak site. Washington, DC, US Naval Research Laboratory.

Boyd, T. J., J. A. Zimbron, R. H. Cuenca, Y. Hagimoto, C. J. Newell, J. T. Wilson and K. J. Johnson "Evaluating CO₂ radiocarbon flux measurement techniques for assessing organic contaminant remediation in groundwater and vadose horizons " In Preparation.